

Understanding the impact of the scavenging capacity on associated costs to use UV/Cl and UV/H₂O₂ for drinking water treatment.

By:

Reece Lima-Thompson

A thesis submitted in conformity with the requirements for the degree of Master of Applied Science

Department of Civil Engineering

York University

© Copyright by Reece Lima-Thompson 2024

Understanding the impact of the scavenging capacity on associated costs to use UV/Cl and UV/H₂O₂ for drinking water treatment.

Reece Lima-Thompson

Master of Applied Science

Department of Civil Engineering

York University

2024

Abstract

UV-driven advanced oxidation processes (e.g. UV/H₂O₂, UV/Cl) that couple UV irradiation with oxidizing chemicals to generate highly reactive species such as ·OH radicals and reactive chlorine species are increasingly being recommended for the removal of recalcitrant organic contaminants in drinking water and wastewater. Establishing the doses of UV and oxidant required to achieve treatment objectives is challenging because many species besides the contaminant(s) of interest exert a scavenging capacity for the highly reactive species generated in advanced oxidation processes. Overall, the aim of this research was to establish whether a colour-based test developed to measure the hydroxyl radical scavenging capacity of water samples could be adapted to measure the scavenging capacity of reactive chlorine species in addition to hydroxyl radicals. The results were used to estimate the cost implications of installing a UV/H₂O₂ or UV/Cl reactor in a drinking water treatment plant. Initial capital and ongoing operational and maintenance cost curves were developed to characterize the potential cost savings of utilizing the method to treat a well-known contaminant of concern.

Acknowledgments

I'd like to first and foremost acknowledge my mom, Maria Lima, who has been my greatest supporter, not only during my years as a graduate student, but for my entire life. I would not have been able to achieve what I have in my life without her love and support. This thesis is dedicated to her.

I'd also like to acknowledge the Safe and Sustainable Water Research Group in which all members have at some point provided me with great advice, assistance, and guidance over the past two and a half years. I'd especially like to acknowledge my supervisor, Dr. Stephanie Gora, who is a huge role model for myself and someone who I dearly respect. She has been so supportive of me and my success as a graduate student and engineer. I could not have asked for a better supervisor and I'm so glad that I met her. I'd also to thank my committee members Dr. Audrey Murray and Dr. Satinder Brar who have provided me with great feedback for this project. I'd like to thank Jason Wade and Allan Gomes, two undergraduate students who assisted me in the lab and provided me with great and much needed company.

This research was made possible through the Natural Sciences and Engineering Research Council of Canada (NSERC), One Water, and Lassonde School of Engineering.

Table of Contents

Abstract.....	ii
List of Tables.....	vii
List of Figures	ix
1.0. Introduction	1
1.1. Background.....	1
1.1.1. Advanced Oxidation Processes (AOPs)	1
1.1.2. Scavenging Capacity.....	1
1.1.3. Cost Estimates for Water Treatment Processes	2
1.2. Research Objectives.....	3
1.3. Organization of the Thesis	4
2.0. Literature Review	5
2.1. AOPs for the Removal of Recalcitrant Contaminants	5
2.2. Radical Scavenging Effects of the Water Matrix and Impacts on UV/AOPs	6
2.3. Determining the RSC of Water Matrices for Radical Species Generated by AOPs	11
2.4. Impact of Wavelength on UV/AOPs.....	15
2.5. Characterizing UV Apparatus.....	16
2.6. Previous AOP Cost Analyses	20
2.6.1. Sharma et al. 2013	21
2.6.2. Plumlee et al. 2013	21
2.6.3. Tian et al. 2020.....	22
2.6.4. Lima-Thompson and Gora 2023.....	23
2.6.5. Mackey et al., 2022	23
2.7. Optimum UV and Oxidant Dose	24
2.8. Summary of Literature Review	25
3.0. Methods and Materials.....	26
3.1. Objective 1: Adapting the External Calibration Method to UV/Cl.....	26
3.1.1. Characterizing the UV Apparatus.....	26
3.1.2. Replicating the Results of Wang et al. 2020.....	26
3.1.3. Adapting the External Calibration Method to UV/Cl	27
3.1.4. Materials	30
3.2. Objective 2: Modelling Required and Optimum UV and Oxidant Doses to Degrade Contaminants of Concern Based on the Radical Scavenging Capacity of the Water Matrix	30

3.3.	Objective 3: Conceptualizing the Capital and O&M Costs of UV/H ₂ O ₂ and UV/Cl through the Development of Cost Curves.....	37
4.0.	Results and Discussion	39
4.1.	Objective 1: Adapting the External Calibration Method to UV/Cl.....	39
4.1.1.	Replicating Wang et al. 2020.....	39
4.1.2.	Methylene Blue Degradation	40
4.1.3.	Summarizing Log Reduction Results	50
4.1.4.	UV/Cl External Calibration Curves.....	51
4.1.5.	Comparing Similar Real Water Matrices Radical Scavenging Capacity Values Determined with the External Calibration Method.	56
4.1.6.	Summarizing Results of Applying the External Calibration Method to UV/Cl	59
4.1.7.	Future Research Steps	60
4.2.	Objective 2: Modelling Optimum Dosing Requirements to Degrade Contaminants of Concern Based on the Radical Scavenging Capacity of the Water Matrix	62
4.2.1.	Future Research Steps.....	66
4.3.	Objective 3: Conceptualize the Capital and O&M Costs of UV/H ₂ O ₂ and UV/Cl Through the Development of Cost Curves.....	67
4.3.1.	Capital Costs of UV/H ₂ O ₂	67
4.3.2.	Capital Costs for UV/Cl	71
4.3.3.	Comparison of Capital Costs	74
4.3.4.	O&M Costs for UV/H ₂ O ₂	74
4.3.5.	O&M Costs for UV/Cl	77
4.3.6.	Comparison of O&M Costs	82
4.3.7.	Seasonality Analysis	82
4.3.8.	Comparison of Previous Cost Curves	85
4.3.9.	Future Research Steps	87
5.0.	Conclusions and Future Research Implications	88
5.1.	Future Research Implications	88
5.2.	Conclusions.....	88
	References.....	91
	Appendix A: UV Characterization Figures	101
	Appendix B: Fraction of HOCl/OCl ⁻ Present in the Water Matrix.....	103
	Appendix C: Methylene Blue Absorbance vs Concentration Calibration Curve.....	104
	Appendix D: Residual Free Chlorine Concentration of Treated Water Samples	105

Appendix E: Replicating Kwon et al., 2019.....	106
Appendix F: Objective 1 RStudio Code.....	107
Appendix G: Objective 2 RStudio Code.....	132
Appendix H: Objective 3 RStudio Code.....	141

List of Tables

Table 1: Water matrix impacts on treatment with UV/H ₂ O ₂	7
Table 2: Water matrix impacts on treatment with UV/Cl.....	8
Table 3: Plumlee et al. 2013 summary of conceptual cost curve regression equations for various treatment processes	22
Table 4: Materials utilized for external calibration method experiments.....	30
Table 5: Model inputs for replication of Kwon et al., 2019 results. All inputs used were the same as Kwon et al., 2019.	31
Table 6: Model inputs for required doses for UV/H ₂ O ₂ treatment.	32
Table 7: Model inputs for optimum dosing of UV/H ₂ O ₂ treatment.....	33
Table 8: Model inputs for required doses for UV/Cl treatment.	34
Table 9: Model inputs for optimum dosing of UV/Cl treatment.	36
Table 10: Model inputs for required UV and oxidant doses for UV/Cl treatment at a pH of 5.....	36
Table 11: Statistical significance of wavelength and pH on the degradation of methylene blue at a free chlorine dose of 5 mg L ⁻¹	43
Table 12: Statistical significance of wavelength and pH on the degradation of methylene blue at a free chlorine dose of 5 mg L ⁻¹ and a TBA dose of 460 µM.....	43
Table 13: Statistical significance of wavelength and pH on the degradation of methylene blue at a free chlorine dose of 7 mg L ⁻¹	45
Table 14: Statistical significance of wavelength and pH on the degradation of methylene blue at a free chlorine dose of 7 mg L ⁻¹ and a TBA concentration of 460 µM.....	46
Table 15: Statistical significance of free chlorine dose on the degradation of methylene blue with and without added scavenging capacity.	46
Table 16: Statistical significance of free chlorine dose and pH on the degradation of methylene blue with free chlorine only (no UV light/dark experiments).....	47
Table 17: Statistical significance of pH and wavelength on the colour decay rate with experimental conditions 5 mg L ⁻¹ free chlorine and 500 mJ cm ⁻² UV dose.....	53
Table 18: Statistical significance of pH and wavelength on the colour decay rate with experimental conditions 5 mg L ⁻¹ free chlorine and 1000 mJ cm ⁻² UV dose.....	54
Table 19: Statistical significance of pH and wavelength on the colour decay rate with experimental conditions 7 mg L ⁻¹ free chlorine and 500 mJ cm ⁻² UV dose.....	55
Table 20: Statistical significance of pH and wavelength on the colour decay rate with experimental conditions 7 mg L ⁻¹ free chlorine and 1000 mJ cm ⁻² UV dose.....	56
Table 21: Summarizing the average determined radical scavenging capacity (RSC) values of a similar water matrix to compare external calibration curves at the studied experimental conditions. Highlighted values indicate a negative RSC value which is a result of residual chlorine being present in the treated water. The concentration of free chlorine was greater than 7 mg L ⁻¹ in the treated water samples which was the free chlorine dose used to develop the external calibration curves. Statistical significance of pH and Wavelength on the determined RSC value is also presented in the table. A p-value of 0.05 or less is considered statistically significant.	58
Table 22: Statistical significance of free chlorine dose and UV dose on the application of the external calibration method to UV/Cl at pH 7 and a wavelength of 255 nm.....	59
Table 23: Statistical significance of free chlorine dose and UV dose on the application of the external calibration method to UV/Cl at pH 5 and a wavelength of 255 nm.....	60

Table 24: Statistical significance of free chlorine dose and UV dose on the application of the external calibration method to UV/Cl at pH 7 and a wavelength of 280 nm. 60

Table 25: Statistical significance of free chlorine dose and UV dose on the application of the external calibration method to UV/Cl at pH 5 and a wavelength of 280 nm. 60

Table 26: Water quality and treatment objectives that were used to build cost curves for UV/H₂O₂. 67

Table 27: Water quality and treatment objectives that were used to build cost curves for UV/H₂O₂. 72

List of Figures

Figure 1: External calibration method schematic (adapted from Wang et al., 2020).....	15
Figure 2: Molar absorbance ($M^{-1} cm^{-1}$) vs wavelength (nm) for H_2O_2 and free chlorine (Morris, 1966; Morgan et al., 1988).....	16
Figure 3: A photo of a quasi-collimated beam bench scale apparatus.	17
Figure 4: Illustration of the concept irradiance (adapted from Bolton and Stefan, 2002).....	17
Figure 5: Illustration of the concept of fluence rate (adapted from Bolton and Stefan, 2002).	18
Figure 6: Replicating Wang et al., 2020 results.	40
Figure 7: Expected primary radicals in UV/Cl at acidic and neutral pH.....	41
Figure 8: MB log reduction with UV/Cl with a free chlorine dose of $5 mg L^{-1}$	43
Figure 9: MB log reduction with UV/Cl with a free chlorine dose of $5 mg L^{-1}$ and a TBA concentration of $460 \mu M$	43
Figure 10: MB log reduction with UV/Cl with a free chlorine dose of $7 mg L^{-1}$	45
Figure 11: MB log reduction with UV/Cl with a free chlorine dose of $7 mg L^{-1}$ and a TBA concentration of $460 \mu M$	46
Figure 12: Degradation of methylene blue with only free chlorine (no UV light/dark experiments).....	47
Figure 13: Methylene blue log reduction in real water matrices (free chlorine dose of $7 mg L^{-1}$ and UV dose of $500 mJ cm^{-2}$).....	49
Figure 14: Statistical significance of wavelength and pH on methylene blue log reduction in treated water (free chlorine dose of $7 mg L^{-1}$ and UV dose of $500 mJ cm^{-2}$).....	49
Figure 15: UV/Cl external calibration curves at free chlorine dose of $5 mg L^{-1}$ and UV dose of $500 mJ cm^{-2}$	53
Figure 16: UV/Cl external calibration curves at free chlorine dose of $5 mg L^{-1}$ and UV dose of $1000 mJ cm^{-2}$	54
Figure 17: UV/Cl external calibration curves at free chlorine dose of $7 mg L^{-1}$ and UV dose of $500 mJ cm^{-2}$	55
Figure 18: UV/Cl external calibration curves at free chlorine dose of $7 mg L^{-1}$ and UV dose of $1000 mJ cm^{-2}$	56
Figure 19: UV/Cl external calibration curves at free chlorine dose of $7 mg L^{-1}$ and UV dose of $500 mJ cm^{-2}$ with results of radical scavenging capacities of real water samples from a source water source in Southern Ontario. The black points are the external calibration curve for the mentioned chlorine and UV dose presented in Figure 17.....	58
Figure 20: Schematic of how the external calibration method could be utilized to determine real time measurements of the radical scavenging capacity (RSC) to optimize the reactor's operating conditions.	61
Figure 21: Required and optimum doses for 2-log reduction of MC-LR with UV/ H_2O_2 . Optimum doses are based on minimum energy requirement to treat MC-LR. The high RSC corresponds to a value of 8×10^4 and the low RSC corresponds to a value of $3 \times 10^4 s^{-1}$	63
Figure 22: Required and optimum doses for 2-log reduction of MC-LR with UV/Cl at neutral pH. Optimum doses are based on minimum energy requirement to treat MC-LR. The high RSC corresponds to a value of 9.14×10^4 and the low RSC corresponds to a value of $4.14 \times 10^4 s^{-1}$	64
Figure 23: Required and optimum doses for 2-log reduction of MC-LR with UV/Cl at acidic pH. Optimum doses are based on minimum energy requirement to treat MC-LR. The high RSC corresponds to a value of 9.14×10^4 and the low RSC corresponds to a value of $4.14 \times 10^4 s^{-1}$	65

Figure 24: Capital cost curves for UV/H₂O₂ to achieve 2-log reduction of MC-LR. The dotted red and green lines indicate error bounds of +50% and -30%, respectively. 68

Figure 25: Percent contribution of UV equipment and H₂O₂ storage and dosing to overall capital costs. . 69

Figure 26: Comparison of capital costs calculated for high RSC to reported full-scale installations of UV/H₂O₂ listed in industry magazines, conference proceedings, and other online sources (red points), and conceptual estimates conducted by researchers through the consultation of equipment vendors (black points). The dotted red and green lines indicate +50% and -30% of the calculated cost, respectively. 70

Figure 27: Comparison of capital costs calculated for low RSC to reported full-scale installations of UV/H₂O₂ listed in industry magazines and conference proceedings (red points) and conceptual estimates conducted by researchers through the consultation of equipment vendors (black points). The dotted red and green lines indicate +50% and -30% of the calculated cost, respectively. 71

Figure 28: Capital cost curves for UV/Cl to achieve 2-log reduction of MC-LR. The dotted red and green lines indicate error bounds of +50% and -30%, respectively. 73

Figure 29: Percent contribution of UV equipment and NaOCl storage and dosing to overall capital costs. 73

Figure 30: Process flow diagram of conventional drinking water treatment retrofitted with a UV/H₂O₂ reactor. 75

Figure 31: O&M cost curves for UV/H₂O₂ to achieve 2-log reduction of MC-LR. The dotted red and green lines indicate error bounds of +50% and -30%, respectively. 76

Figure 32: Percent contribution of H₂O₂ costs, quenching costs, maintenance, energy, and labour costs to overall O&M costs. 76

Figure 33: O&M cost curves for UV/Cl to achieve 2-log reduction of MC-LR with no pH adjustment. The dotted red and green lines indicate error bounds of +50% and -30%, respectively. 78

Figure 34: Percent contribution of NaOCl costs, quenching costs, maintenance, energy, and labour costs to overall O&M costs. 79

Figure 35: Process flow diagram of conventional drinking water treatment retrofitted with a UV/Cl reactor. 80

Figure 36: O&M cost curves for UV/Cl to achieve 2-log reduction of MC-LR with pH adjustment. The dotted red and green lines indicate error bounds of +50% and -30%, respectively. 81

Figure 37: Percent contribution of NaOCl costs, quenching costs, maintenance, energy, pH adjustment and labour costs to overall O&M costs. 82

Figure 38: Seasonal O&M cost curves for UV/H₂O₂ to achieve 2-log reduction of MC-LR. The dotted red and green lines indicate error bounds of +50% and -30%, respectively. 83

Figure 39: Seasonal O&M cost curves for UV/Cl to achieve 2-log reduction of MC-LR with no pH adjustment. The dotted red and green lines indicate error bounds of +50% and -30%, respectively. 84

Figure 40: Seasonal O&M cost curves for UV/Cl to achieve 2-log reduction of MC-LR with pH adjustment. The dotted red and green lines indicate error bounds of +50% and -30%, respectively. 85

Figure 41: Comparison of previous capital cost curves versus current cost curves developed for UV/H₂O₂. 86

Figure 42: Comparison of previous capital cost curves versus current cost curves developed for UV/H₂O₂. 86

Figure S. 1: Intensity profile of the 255 nm wavelength used in experiments.	101
Figure S. 2: Intensity profile of the 280 nm wavelength used in experiments.	102
Figure S. 3: Relative emission spectra of UV LED wavelengths utilized in this study.	102
Figure S. 4: Illustration of the fraction of HOCl and OCl ⁻ at various pH.	103
Figure S. 5: Methylene blue calibration curve.	104
Figure S. 6: Residual concentration of free chlorine in treated water samples vs time.	105
Figure S. 7: Replicating results of Kwon et al. 2019 with the exact same inputs in Equation 22. Results show the required UV and H ₂ O ₂ doses to achieve 1-log reduction of MC-LR in a water matrix with a OH demand of $3 \times 10^4 \text{ s}^{-1}$.	106

Nomenclature

AOPs – Advanced oxidation processes.

ANCOVA – Analysis of covariances.

ANOVA - Analysis of variances.

CCI - Construction Cost Index.

EE/O – Electrical energy per order.

ENR - Engineering News-Record.

HOCl – Hypochlorous acid.

H₂O₂ – Hydrogen peroxide.

LEDs – light emitting diodes.

MB – Methylene blue.

OCl⁻ Hypochlorite.

O&M – Operation and maintenance.

ROS – Reactive oxygen species.

RSC - Radical scavenging capacity.

TBA – Tert-butanol.

USEPA - United States Environmental Protection Agency.

UV – ultraviolet light.

·OH – Hydroxyl radicals.

1.0. Introduction

1.1. Background

1.1.1. Advanced Oxidation Processes (AOPs)

The levels of many contaminants of concern have been increasing in drinking water supplies in recent years due to human activities and climate change (Fang et al. 2014; Boehlert et al. 2015). Contaminants such as taste and odour compounds, toxin producing cyanobacteria, and endocrine disrupting compounds like 1-4 dioxane, are not easily removed by conventional treatment processes (Vlad et al. 2014; Zhang et al. 2019). In the future, water utilities will need to consider implementing advanced treatment technologies to ensure that they are achieving targeted removal goals.

Advanced oxidation processes (AOPs) produce highly reactive compounds like reactive oxygen species or reactive chlorine species that are capable of degrading recalcitrant micropollutants that conventional treatment processes struggle to remove. Ultraviolet light (UV) induced AOPs like UV/H₂O₂ and UV/Cl have been researched extensively through bench, pilot, and some full-scale studies, for the removal of recalcitrant micropollutants in drinking water and wastewater. However, currently there are very few full-scale adaptations of UV induced AOPs due to their large capital and operation and maintenance (O&M) costs relative to conventional treatment infrastructure (Sgroi et al. 2021).

There are several potential economic benefits of UV/Cl compared to UV/H₂O₂. One potential benefit that UV/Cl has is that most water utilities in North America already use HOCl for primary and/or secondary disinfection, meaning most water utilities already have infrastructure in place for monitoring and dosing HOCl. This could be a key factor when considering retrofitting a UV/AOP into a treatment train.

1.1.2. Scavenging Capacity

UV AOPs are highly dependent on the water quality conditions in the reactor, particularly the presence of non-targeted water matrix constituents (carbonates and NOM) that scavenge the radical species formed, reducing the amount available to degrade the target contaminants (Wang et al. 2020; Lado Riberio et al. 2019). Non-target water matrix constituents can also absorb the UV light meant for the photolysis of the oxidant (H₂O₂/HOCl) reducing the yield of radicals formed. This can impact full-scale designs of these systems as they can be over designed to ensure that no matter the water quality coming

into the reactor, the system is still achieving its targeted log reduction values, which further inflates associated capital and O&M costs (Mackey et al. 2022). Conventional methods of measuring the radical scavenging capacity of water matrices are laborious and time consuming (Wang et al. 2020), by the time a measurement is obtained, the radical scavenging capacity in the water matrix in the reactor has more than likely changed. The radical scavenging capacity is an important input when designing UV/AOPs (Mackey et al. 2022).

A potential solution to this problem would be to have a rapid online radical scavenging capacity monitoring system that can adjust the operating parameters of an AOP treatment system based on the scavenging capacity of the water in the reactor, reducing projected costs, which could increase the viability of UV AOPs at the full-scale. An external calibration method was developed by Wang et al. 2020 which can be used to quickly determine the radical scavenging capacity of water matrices. A new portable device was developed using the external calibration method and can measure the radical scavenging capacity of water matrices for the UV/H₂O₂ AOP, quickly. However, there are several economic advantages that UV/Cl has compared to UV/H₂O₂, which will be discussed in detail in Chapter 4.3, which could make it a more viable option compared to UV/H₂O₂ and applying the external calibration method to UV/Cl could increase the feasibility of applying UV/Cl to the full-scale.

1.1.3. Cost Estimates for Water Treatment Processes

Cost estimates are normally developed by obtaining and comparing quotes from multiple vendors for the design of a system that meets the targeted treatment goals at the specified plant capacity (Sharma et al. 2013). Estimates can also be developed through combining individual costs of each component of the treatment system or can be based on total costs of similar projects completed in the past (United States Protection Agency, 2015). The best cost estimates are site specific and include all relevant local considerations (e.g. treatment guidelines, source water quality, labor rates, etc.)

Cost estimates can also be used to develop generalizable cost curves and costing functions. Cost curves plot the estimated cost to construct or operate a unit process against the capacity of the water treatment plant. These cost curves can be useful in the early stages of the engineering process to determine whether a treatment system is feasible. This approach has been used by the United States Environmental Protection Agency (USEPA) to develop cost curves for a variety of water treatment processes including UV disinfection and free chlorine disinfection. A costing function is an equation that relates the plant capacity to the total cost and is a mathematical expression of the cost curve.

Cost estimates can quickly become out of date and must be updated to accommodate for inflation and other cost increases. The Construction Cost Index (CCI) is published in the Engineering News-Record (ENR) and is a popular tool for updating cost estimates developed in a previous year into a more contemporary value. Equation 1 below illustrates how a cost estimate prepared in 1990 can be converted to a value relevant in 2023 using the CCI.

$$Cost_{2023} = \frac{CCI_{2023}}{CCI_{1990}} \times Cost_{1990} \quad [1]$$

1.2. Research Objectives

The research objectives of this project are listed and described in the subsections below.

1. *Evaluate the application of the external calibration method to UV/Cl.*

Conventional methods to determine the radical scavenging capacity are laborious and time consuming. If this parameter is measured quickly, it could potentially be used to update the operating conditions of the UV/Cl reactor, optimizing the system based on the influent water quality present, potentially minimizing costs. A simple colorimetric test to quantify the hydroxyl radical scavenging capacity of water matrices has been developed for UV/H₂O₂ systems. This method is known as the external calibration method. The external calibration method is explained in more detail in Chapter 2.3. To date, the applicability of this method for quantifying other reactive radical species that are generated in other UV/AOPs has not been tested.

2. *Model optimum dosing requirements for UV/Cl to degrade MC-LR based on radical scavenging capacity of the water matrix.*

The second objective of this project was to develop a mathematical model to predict optimum UV/Cl conditions (UV dose, free Cl dose) to degrade microcystin-LR, a commonly detected cyanotoxin, based on the radical scavenging capacity of the water matrix. Microcystin-LR was chosen as the target contaminant because cyanotoxins are a class of recalcitrant pollutants that conventional water treatment trains struggle to remove. Additionally, the effects of climate change, population growth, and intensification of agriculture, may increase the presence of cyanotoxins in drinking water in the future, which could force water utilities into retrofitting advanced treatment processes such as UV/AOPs into existing water treatment plants (Vlad et al. 2014).

- 3. Conceptualize the capital and O&M costs of UV/H₂O₂ and UV/Cl through the development of cost curves.*

This last objective was to generalize initial capital costs and ongoing operation and maintenance costs based on the optimum operating parameters provided by the mathematical model from the second objective. The goal of this objective is to provide a preliminary feasibility analysis for water utilities to retrofit UV/Cl with the objective of treating microcystin-LR in drinking water. Additionally, the significance of the external calibration method on cost savings could be measured and presented.

1.3. Organization of the Thesis

The thesis is organized according to the guidelines outlined by the faculty of graduate studies at York University which describe the general, organizational, and technical requirements to complete a master's thesis.

Chapter 1.0 introduces key aspects of the project and the main research objectives. Chapter 2.0 provides in-depth background information about UV AOPs drawn from the scientific literature and government literature. Chapter 3.0 describes the methodology used to complete research objectives. Chapter 4.0 presents the results and findings. Chapter 5.0 discusses major conclusions and suggests future research implications.

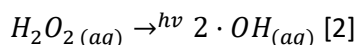
2.0. Literature Review

2.1. AOPs for the Removal of Recalcitrant Contaminants

Advanced oxidation processes (AOPs) use radical species with high oxidative potential to degrade contaminants in drinking water or wastewater (Mackey et al. 2022; Wang et al. 2019; Tian et al. 2020). The use of advanced oxidation processes has increased in municipal applications as more recalcitrant contaminants are detected in water supplies that are more susceptible to advanced oxidation than to conventional treatment processes.

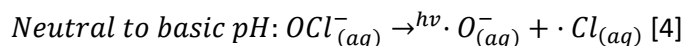
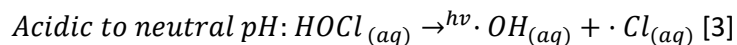
A radical is a chemical species that has one or more unpaired electrons. The radical species formed in an AOP can degrade contaminants that conventional drinking water treatment trains (coagulation/flocculation, filtration, and disinfection) or conventional wastewater treatment trains (primary secondary, and tertiary) are not well equipped to remove. Examples of recalcitrant contaminants that drinking water treatment trains perform poorly in removal are toxic producing cyanobacteria, which are more prevalent in the summer months, and more persistent contaminants like 1-4 dioxane, an endocrine disrupting compound (Tian et al. 2020; Vlad et al. 2014; Zhang et al. 2019). The most common radical species used in AOPs are hydroxyl radicals ($\cdot\text{OH}$) which have a very high oxidative potential of 2.8 V (Guo et al. 2017). This means that hydroxyl radicals are extremely reactive and normally exist in water for less than one millionth of a second (Mackey et al. 2022).

Ultraviolet advanced oxidation processes (UV/AOPs) utilize ultraviolet radiation to generate radical species like $\cdot\text{OH}$. UV/H₂O₂ is the most implemented UV/AOP at the full scale for water treatment because its fundamental chemistry is better understood compared with others (Wang et al. 2019; Mackey et al. 2022). However, for most water utilities UV/AOPs are too expensive to consider retrofitting into their treatment trains. Equation 2 shows how UV/H₂O₂ generates its primary radical species, when H₂O₂ is exposed to UV light.



Combining UV and free chlorine is another means to generate radical species. UV light decomposes free chlorine to generate $\cdot\text{OH}$ and reactive chlorine species (Hoang et al. 2022; Guo et al. 2019). Equation 3 and Equation 4 show how the primary radicals are formed in the UV/Cl AOP. In general, free chlorine can generate a higher quantum yield (more radical species formed per photon of light absorbed) of radical

species compared to UV/H₂O₂, due to its strong UV absorbance at most pH generally experienced in water treatment. This makes UV/Cl a more effective UV/AOP at the degradation of a broad range of contaminants. However, the fundamental chemistry is much more complex than UV/H₂O₂ and is not as well understood. Thus, UV/Cl is not as widely adopted at the full scale as UV/H₂O₂ (Mackey et al. 2022).



Secondary radicals are produced in UV/H₂O₂ and UV/Cl that can also contribute to the degradation of some contaminants. However, these secondary radicals have a smaller oxidative potential relative to the primary radicals and are therefore theoretically more selective towards the degradation of contaminants. Secondary radical chlorine species such as $\cdot ClO_{(aq)}$ and $\cdot Cl_2_{(aq)}$ are formed in UV/Cl (Guo et al. 2017). Secondary reactive oxygen species like $\cdot HO_2_{(aq)}$ are also formed in UV/H₂O₂ (Lado Ribeiro et al. 2019). When $NO^-_{3(aq)}$ is present in the water matrix, $\cdot OH_{(aq)}$ and $\cdot NO_2_{(aq)}$ are formed in both UV/H₂O₂, and UV/Cl. When $HCO^-_{3(aq)}$ is present in the water matrix $\cdot CO^-_{3(aq)}$ is formed in both UV/H₂O₂, and UV/Cl (Lado Ribeiro et al. 2019).

In the degradation of pharmaceutical drugs ronidazole and nalidixic acid with UV/Cl, primary radicals $\cdot OH$ and $\cdot Cl$ were to be the most contributive (Guo et al., 2017). However, some studies did find that some secondary radicals were more contributive in the degradation of contaminants. Specifically, Kong et al., 2018 found that the secondary radicals of $\cdot Cl_2$ and $\cdot ClO$ were responsible for the degradation of iopamidol. Therefore, the effectiveness of the contribution of primary and secondary radicals is specific to the target contaminant but in general primary radicals, due to the higher oxidative potential, contribute more to the degradation of contaminants.

2.2. Radical Scavenging Effects of the Water Matrix and Impacts on UV/AOPs

The water matrix can have large impacts on the efficiency and effectiveness of UV/AOP treatment. Radical scavenging and light attenuation from constituents in the water matrix other than the targeted contaminant, decrease the radical species available for the degradation of the targeted contaminant. The water matrix has such a large impact on UV/AOPs that they are usually retrofitted at the end of the treatment train where UVT is highest and radical scavenging capacity is lowest (Mackey et al., 2022).

Table 1 and

Table 2 explain important water matrix components and their impact on treatment with UV/H₂O₂ and UV/Cl.

Table 1: Water matrix impacts on treatment with UV/H₂O₂

Parameter	Known effects	References
pH	UV/H ₂ O ₂ has a high pKa value (11.7) so pH is not a major driver of its activity. However, if pH were to increase significantly above neutral (>8) treatment efficiency may decrease due to a change in bicarbonate to carbonate which is a stronger radical scavenger.	Wang et al., 2019; Mackey et al., 2022
Natural organic matter (NOM)	<p>Reduces the efficiency of degradation of micropollutants by absorbing UV light meant for the photolysis of H₂O₂ and reacting with hydroxyl radicals.</p> <p>Can be broken down into more biodegradable compounds or DBP precursors such as aldehydes and organic acids.</p> <p>Depending on the composition of NOM, reactions with hydroxyl radicals may produce other reactive species that can contribute to the degradation of micropollutants. However, these reactive species are more selective and may not contribute to the degradation of the target contaminant.</p>	Metz et al., 2011; Lee et al., 2020; Martijn et al., 2018; Lado Ribeiro et al., 2019
Carbonates	<p>Reacts with hydroxyl radicals meant for the degradation of targeted micropollutants reducing efficiency of performance.</p> <p>Forms carbonate radicals when reacting with hydroxyl radicals which are a more selective oxidant than hydroxyl radicals.</p> <p>Attenuates light meant for the photolysis of oxidants leading to reduced yield of hydroxyl radicals.</p>	Yang et al., 2016; Lado Ribeiro et al., 2019
Chloride and Bromide	<p>Reacts with hydroxyl radicals meant to degrade targeted micropollutants reducing efficiency of performance.</p> <p>Attenuates light meant for the photolysis of oxidants leading to reduced yield of hydroxyl radicals.</p> <p>Likely have little impact on performance.</p>	Lado Ribeiro et al., 2019; Yang et al., 2016; Mackey et al., 2022

Parameter	Known effects	References
Nitrogen species	<p>Photolysis of nitrate results in nitrite formation which is a potential carcinogen. Nitrite also has a high radical scavenging capacity.</p> <p>Reduces the efficiency of degradation by absorbing UV light meant for the photolysis of oxidants and reacting with hydroxyl radicals.</p> <p>Photolysis of nitrate produces hydroxyl radicals which could benefit efficiency.</p>	Martijn et al., 2015; Lado Ribeiro et al., 2019
Other	Residual H ₂ O ₂ will scavenge hydroxyl radicals meant for the degradation of targeted pollutants.	Yang et al., 2016

Table 2: Water matrix impacts on treatment with UV/Cl

Parameter	Known effects	References
pH	<p>Determines the chlorine species present in the water matrix (OCl⁻/HOCl) which impacts the radical species formed and their quantum yield at the wavelength of UV irradiation.</p> <p>Optimal pH will depend on the reactivity of the target contaminant with reactive chlorine species, however in general, acidic pH will be more efficient as HOCl is the dominant chlorine species which photolyzes into hydroxyl radicals.</p>	Yin et al., 2018; Mackey et al., 2022

Parameter	Known effects	References
Natural organic matter (NOM)	<p>Reacts with hydroxyl radicals and reactive chlorine species meant for the degradation of targeted micropollutants reducing efficiency of treatment.</p> <p>Attenuates light meant for the photolysis of oxidants leading to reduced yield of reactive species.</p> <p>Reacts with free chlorine to form haloacetic acids and trihalomethanes two regulated chlorine disinfection byproducts.</p>	Lado Ribeiro et al., 2019; Tian et al., 2020; Mackey et al., 2022
Carbonates	<p>Reacts with hydroxyl radicals meant for the degradation of targeted micropollutants reducing efficiency of performance.</p> <p>Forms carbonate radicals when reacting with hydroxyl radicals which are a more selective oxidant than hydroxyl radicals.</p> <p>Attenuates light meant for the photolysis of oxidants leading to reduced yield of hydroxyl radicals.</p>	Lado Rebeiro et al., 2019; Mackey et al., 2022
Chloride and bromide	<p>Reacts with hydroxyl radicals meant to degrade targeted micropollutants reducing efficiency of performance.</p> <p>Attenuates light meant for the photolysis of oxidants leading to reduced yield of hydroxyl radicals.</p> <p>Likely have little impact on performance, however, elevated concentrations of bromide can result in the formation of bromate, a regulated disinfection byproduct.</p>	Lado Rebeiro et al., 2019; Mackey et al., 2022

Parameter	Known effects	References
Nitrogen species	<p>Nitrate is not a big concern as free chlorine quickly reacts with nitrite to turn it back into nitrate.</p> <p>Ammonium quickly reacts with free chlorine to form chloramines. If ammonium is present in the water matrix, the free chlorine concentration in the reactor will likely be overestimated. Chloramines are heavy radical scavengers and attenuate light meant for the photolysis of free chlorine.</p> <p>If ammonium is not controlled in the water matrix, it is advised to use a different UV/AOP.</p>	Mackey et al., 2022; Weil and Morris 1949
Other	<p>Residual free chlorine will scavenge hydroxyl radicals and reactive chlorine species meant for the degradation of targeted pollutants.</p> <p>The temperature of the water impacts the chlorine species present at the current pH and should be considered when dosing free chlorine.</p>	Fang et al, 2014; Guo et al., 2017; Mackey et al., 2022

To summarize the results of Table 1 and

Table 2, the more constituents that are present in the water matrix the greater the radical scavenging capacity of the water matrix and the more light attenuated by non-target constituents. Basically, the efficiency and efficacy of the degradation of target contaminants in a UV/AOP is largely dependent on the concentration of non-target contaminants. This highlights the importance of retrofitting a UV/AOP towards the end of the treatment train.

In typical drinking water sources, the pH is around 6.5 – 8.5. Natural waters pH can be lower because of acid rain intrusion and higher due to the source water being in limestone regions, for example (World Health Organization, 2007). Natural organic matter (NOM) is present in all water bodies which originates from natural sources like biological activity and excretions from aquatic organisms. The concentration of NOM varies throughout the course of the year and is typically highest during the summer months and the lowest during the winter months (Crittenden et al., 2012). Carbonates and bicarbonates provide the buffer capacity in typical natural water sources and typically range from 1 – 1000 mg L⁻¹ (Crittenden et al., 2012). Chloride is present in water almost exclusively as the chloride ion and is typically found in concentrations less than 10 mg L⁻¹ (Crittenden et al., 2012). Nitrogen species are often found in water sources as organics and are typically in the form of ammonia, ammonium, nitrite and/or nitrate. Nitrogen species make up around 1% of the NOM content. Nitrogen species are often in greater concentrations when the source water has an influx of domestic and agricultural waste (Crittenden et al., 2012). Bromide is typically found in drinking water sources but usually at very low concentrations. The highest levels of bromide in drinking water sources are found in ground water sources where saltwater intrusion has occurred (World Health Organization, 2009).

2.3. Determining the RSC of Water Matrices for Radical Species Generated by AOPs

UV/AOPs are designed by developing reactor-specific deterministic models which predict the performance of treatment based on in-situ water quality. These models often include the radical scavenging capacity (RSC) as an input. However, because conventional methods of measuring the RSC of water matrices are time consuming, and there can be a large variation of RSC depending on influent

water quality in the reactor, the input of the RSC is usually assumed to be higher than it may be, which can lead to UV/AOPs being oversized, inflating already large O&M and capital costs. If the RSC could be determined quickly, the input could be used to adjust and optimize the reactor in real time which could reduce expected costs, making UV/AOPs a more viable option for water utilities (Mackey et al. 2022).

The RSC of real water matrices can be determined using Equation 5 if the water matrix constituents' concentrations and $\cdot\text{OH}$ reaction rates are known (Wang et al. 2020). However, water that needs to be treated contains many unknown constituents, like heterogenous organic matter, thus the concentrations of all water matrix constituents and their corresponding $\cdot\text{OH}$ reaction rates are likely not known. Therefore, the RSC is typically measured as a bulk parameter with two components:

1. The $\cdot\text{OH}$ generated by the system at steady state.
2. A probe compound with known $\cdot\text{OH}$ reaction rate constant.

Note that conventional methods of determining the scavenging capacity of UV AOPs were developed for UV/H₂O₂ and only consider the scavenging rate of hydroxyl radicals ($\cdot\text{OH}$).

These methods depend on the decay rate of a probe compound which is then used to mathematically determine the RSC using Equation 6, Equation 7, Equation 8, and Equation 9.

$$RSC (M^{-1}s^{-1}) = \sum k_{si}[S]_i \quad [5]$$

Where $[S]_i$ is the i th scavenger's concentration, and k_{si} is the second order rate constant.

Type 1 method, measures the primary production rate of $\cdot\text{OH}$:

$$\sum k_{si}[S]_i = k_p * r_{OH} * \frac{1}{(\ln \frac{[P]_0}{[P]})/t} - k_{Oxidant} * [Oxidant]_0 - k_p * [P]_0 \quad [6]$$

Where k_p is the second order rate constant of the probe compound with $\cdot\text{OH}$ radicals; r_{OH} is the primary production rate of $\cdot\text{OH}$ radicals; $(\ln \frac{[P]_0}{[P]})/t$ is the decay rate of the probe compound; $k_{Oxidant}$ is the second order rate constant of the oxidant with $\cdot\text{OH}$ radicals; $[Oxidant]_0$ is the initial concentration of the oxidant; $[P]_0$ is the initial concentration of the probe compound; $[P]$ is the molar concentration of the probe after the reaction time of t .

Type 2 method, monitor probe decay at different $[P]_0$ but constant $[Oxidant]$:

$$\sum k_{si}[S]_i = k_p * \frac{b}{m} - k_{Oxidant} * [Oxidant]_0 \quad [7]$$

Where m and b are the slope and intercept of $\left(\frac{1}{(\ln\frac{[P]_0}{[P]})/t}\right)$ vs $* [P]_0$, respectively; k_p is the second order rate constant of the probe compound with $\cdot\text{OH}$ radicals; k_{oxidant} is the second order rate constant of the oxidant with $\cdot\text{OH}$ radicals.

Type 2 method, add a second probe R, and monitor probe's decay at different $[R]_0$ but constant $[\text{H}_2\text{O}_2]_0$ and $[P]_0$.

$$\Sigma k_{si}[S]_i = k_R * \frac{b}{m} - k_p * [P]_0 - k_{\text{oxidant}} * [\text{Oxidant}]_0 \quad [8]$$

Where m and b are the slope and intercept of $\left(\frac{1}{(\ln\frac{[P]_0}{[P]})/t}\right)$ vs $* [R]_0$, respectively; k_p is the second order rate constant of the first probe compound with $\cdot\text{OH}$ radicals; k_R is the second order rate constant of the second probe compound with $\cdot\text{OH}$ radicals; $[P]_0$ is the initial concentration of the probe compound; $[R]_0$ is the initial concentration of the probe compound; ; k_{oxidant} is the second order rate constant of the oxidant with $\cdot\text{OH}$ radicals.

Type 2 method, monitor probe decay at different $[\text{Oxidant}]_0$ but constant $[P]_0$:

$$\Sigma k_{si}[S]_i = k_{\text{oxidant}} * \frac{m}{b} - k_p * [P]_0 \quad [9]$$

Where m and b are the slope and intercept of $\left(\frac{1}{(\ln\frac{[P]_0}{[P]})/t}\right)$ vs $1/[\text{Oxidant}]_0$, respectively; $[P]_0$ is the initial concentration of the probe compound; k_p is the second order rate constant of the probe compound with $\cdot\text{OH}$ radicals; k_{oxidant} is the second order rate constant of the oxidant with $\cdot\text{OH}$ radicals.

The external calibration method was developed by Wang et al. 2020 and is used to quickly determine the radical scavenging capacity of the UV/H₂O₂ AOP. It is a variation of a type 1 method because it incorporates the primary production rate of $\cdot\text{OH}$. The external calibration method can be performed as follows:

1. Spike the same concentration of a dye into a series of standard solutions in which the scavenging capacity are already known, determined from equation [1].
2. Subject the standard solutions to the same treatment conditions (same oxidant and UV dose).

3. Create a calibration curve of the colour decay rate vs the radical scavenging capacity.
4. Spike a real water sample with the same concentration of the dye and subject it to the same treatment conditions.
5. Use the calibration curve to determine the radical scavenging capacity of the water sample.

Figure 1 illustrates the schematic of the external calibration method with tert-butanol (TBA) as the standard solution, and Equation 10 shows the corresponding mathematical expression, respectively.

Where $\frac{1}{(\ln \frac{[a]_0}{[a]})/t}$ is the color decay rate; a_0 and a are the absorption coefficients at the dye's signature wavelength at the beginning and the end of the reaction, respectively; k_{colour} is the second order rate constant for the colour decay; $[\text{Dye}]_0$ is the initial concentration of the dye; k_{Dye} is the second order reaction rate constant with $\cdot\text{OH}$.

Another major factor of the external calibration method that impacts its accuracy is the light path length. A long light path (the distance between the edge of the UV collimator and the surface of the sample) will lead to different $\cdot\text{OH}$ primary production rates in the real water samples vs the standard solutions. Therefore, a small light path length is preferred to minimize error when utilizing the external calibration method. An optimal light path length is $< 5\text{cm}$ when the real water sample has a small absorption coefficient ($< 0.07\text{ cm}^{-1}$), with a difference in $\cdot\text{OH}$ primary production rates of $< 3\%$, and $< 0.2\text{ cm}$ when the real water sample has a large absorption coefficient ($> 0.07\text{ cm}^{-1}$), with a difference in $\cdot\text{OH}$ primary production rates of $< 1\%$, when MB is dosed at $5\mu\text{M}$.

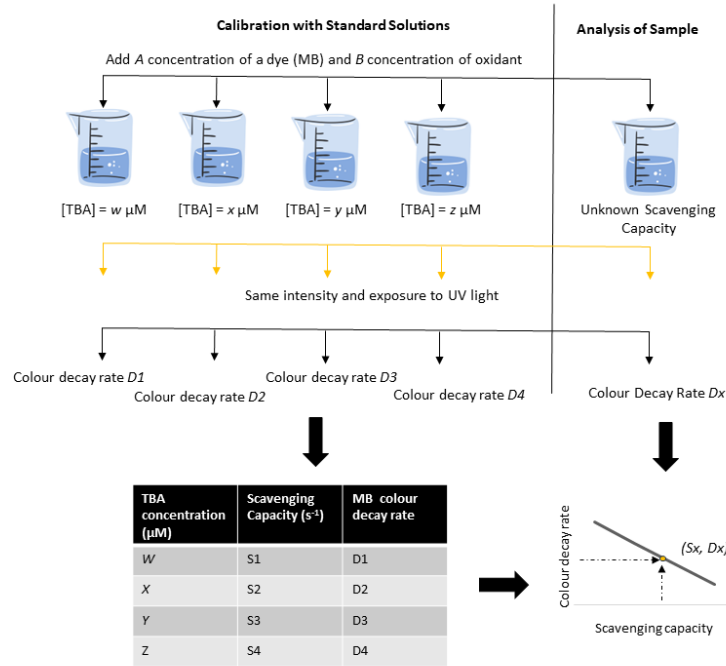


Figure 1: External calibration method schematic (adapted from Wang et al., 2020).

$$\sum k_{si}[S]_i = k_{colour} * r_{OH} * \frac{1}{(\ln \frac{[a]_0}{[a]})/t} - k_{oxidant} * [Oxidant]_0 - k_{Dye} * [Dye]_0 \quad [10]$$

The amount that the RSC will vary in a water matrix will be dependent of the site. Data of the in-situ variation of the water quality over the course of a year would be required to design a full-scale UV/AOP.

2.4. Impact of Wavelength on UV/AOPs

The peak wavelength at which the UV device irradiates can have a large impact on the efficiency of different UV/AOPs (Yin et al. 2018). This is due to the different molar absorption coefficients of the oxidant at various wavelengths which dictates the amount of energy an individual molecule of the oxidant can absorb from UV radiation. The greater the molar absorption coefficient of the oxidant is at a certain wavelength, the greater the expected radical yield formation, thus more radicals available for the degradation of the target contaminant. Figure 2 illustrates the relationship between the wavelength and molar absorption coefficients of H₂O₂, HOCl, and OCl⁻. HOCl is the dominant chlorine species found in acidic pH, while OCl⁻ is dominant at basic pH. At neutral pH both HOCl and OCl⁻ are present and the fraction of concentrations of HOCl and OCl⁻ at a given pH can be calculated using Equation 11.

$$\text{fraction of HOCl in a solution} = \frac{1}{1+10^{pH-7.5}} [11]$$

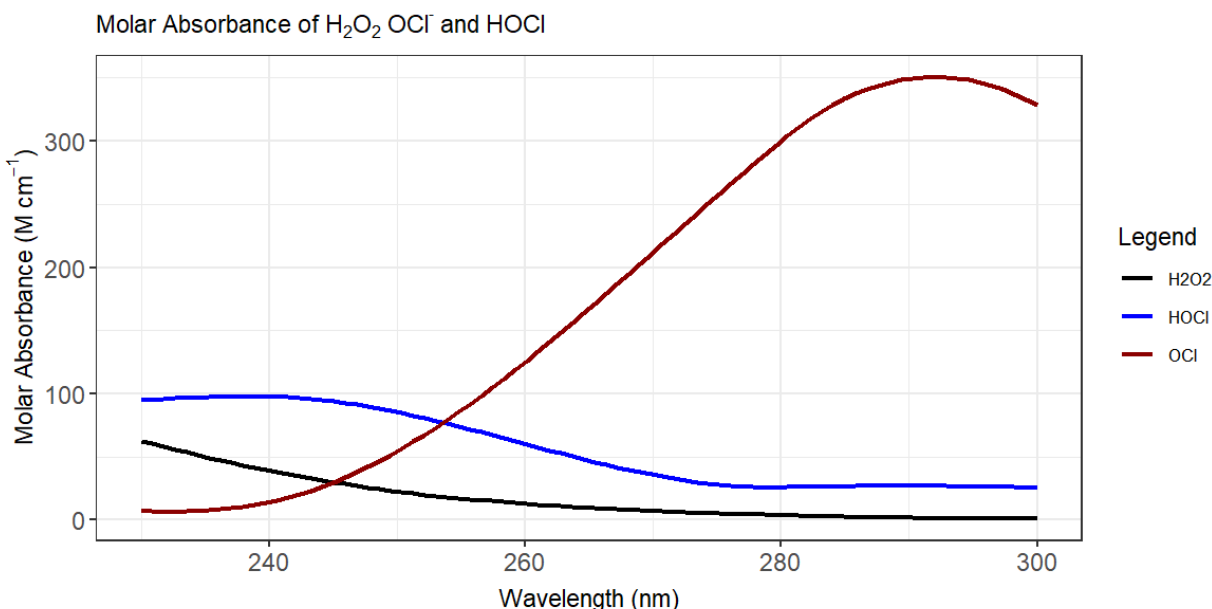


Figure 2: Molar absorbance ($M^{-1} cm^{-1}$) vs wavelength (nm) for H₂O₂ and free chlorine (Morris, 1966; Morgan et al., 1988)

H₂O₂'s molar absorption coefficient decreases with increasing wavelength. Therefore, conventional low-pressure (LP) mercury UV lamps ($\lambda = 255$ nm), which consume less power than MP lamps (Yin et al., 2018), are expected to be the most efficient at radical yield formation. UV/Cl, however, is more complex. This is because of the difference in chlorine species at various pH. At more acidic pH (5-6) conventional LP mercury lamps are expected to be more effective at radical formation but at neutral pH wavelengths between 280-320 nm are expected to be effective at radical formation. LP mercury lamps irradiate at about 255 nm while MP mercury lamps can irradiate at a broad spectrum of UV light, including 280-320 nm (Guo et al., 2019). Additionally, UV LEDs can irradiate at a broad spectrum of UV light including UV-C (200-290 nm), UV-B (290-320 nm) and UV-A (320-400 nm) (Yin et al., 2018).

2.5. Characterizing UV Apparatus

Bolton and Stefan 2002 developed a fundamental approach to determine the fluence (often used interchangeably with the term UV dose despite differences between the two terms) for photochemical degradation reactions. This approach has become a standard method for determining the UV dose applied to samples in photochemical degradation experiments, allowing researchers to reproduce results from another study and/or draw validated comparisons. Photochemical studies are usually conducted

using a quasi-collimated beam of UV light. A quasi-collimated beam bench scale apparatus is illustrated in Figure 3 below.

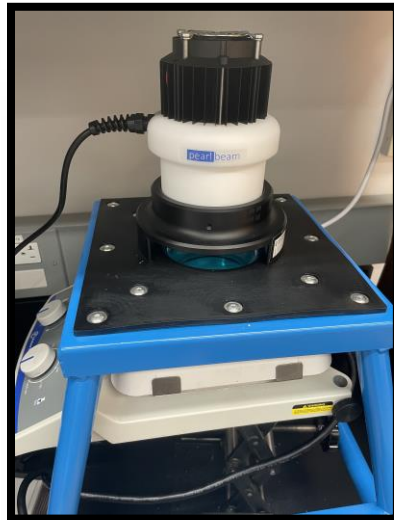


Figure 3: A photo of a quasi-collimated beam bench scale apparatus.

It is important to define certain quantities that are necessary for determining the UV dose. Irradiance, E (W m^{-2}), is the total radiant power incident from all upward directions on an infinitesimal element of surface of area dA containing the point under consideration divided by dA . This concept is illustrated in Figure 4 below.

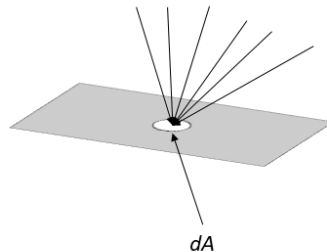


Figure 4: Illustration of the concept irradiance (adapted from Bolton and Stefan, 2002).

Fluence rate, E' (W m^{-2}), is the total radiant power incident from all directions onto an infinitesimally small sphere of cross-sectional area dA , divided by dA . This concept is illustrated in Figure 5 below.

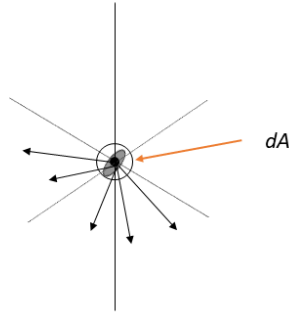


Figure 5: Illustration of the concept of fluence rate (adapted from Bolton and Stefan, 2002).

When the light is a parallel beam, not scattered or reflected and is perpendicularly incident to the measured surface, the irradiance and the fluence are equivalent (Bolton and Stefan, 2002). In quasi collimated bench scale experiments, these conditions will not be met, and two additional quantities must be considered:

Photon irradiance, E_p (einstein $s^{-1} m^{-2}$), is defined as the number of einsteins (moles of photons) incident per second on an infinitesimal element of surface area dA containing the point under consideration divided by dA .

Photon fluence rate, E'_p (einstein $s^{-1} m^{-2}$), is defined as the total number of einsteins incident per second from all directions onto an infinitesimally small sphere of cross-sectional area dA , divided by dA . The photon fluence rate can be calculated using actinometry if ϕ is independent of wavelength over the spectral range that is being considered $E'_p =$ (moles of product generated or reactant remove) $\div \phi * exposure\ time * exposure\ area$ (m²) [12] shows how the photon fluence rate can be calculated where ϕ is the photolysis rate of the targeted product.

$$E'_p = \frac{(\text{moles of product generated or reactant remove})}{\phi * \text{exposure time (s)} * \text{exposure area (m}^2\text{)}} [12]$$

The most common way of measuring the fluence rate in quasi collimated beam experiments is with a calibrated spectrophotometer or radiometer. However, this measured fluence rate must be corrected as the volume averaged fluence rate, E'_{avg} , to account for reflection of light from the solution, non-uniformity of the radiation field across the petri dish being used, the attenuation of light from water absorption, and the fact that the beam is not fully collimated. The volume averaged fluence rate assumes the sample is well stirred and is the UV dose of the experiment. The volume averaged fluence

rate can be calculated using Equation 13, Equation 14, Equation 15, Equation 16, Equation 17, and Equation 18.

$$R = \frac{(n_1 - n_2)^2}{(n_1 + n_2)^2} \quad [13]$$

Where R is the reflectance coefficient of the condensed medium; n_1 and n_2 are the refractive indices of the two media traversed by light.

$$\text{Reflection Factor (RF)} = 1 - R \quad [14]$$

$$\text{Petri Factor (PF)} = \frac{\text{avg. radiometer or spectrophotometer irradiance readings across the petri dish}}{\text{radiometer or spectrophotometer irradiance reading at the centre of the petri dish}} \quad [15]$$

$$\text{Water Factor (WF)} = \frac{1 - 10^{-al}}{al \ln 10} \quad [16]$$

Where a is the absorption coefficient of the solution (m^{-1}) at the wavelength of irradiation and l is the path length (m).

$$\text{Divergence Factor (DF)} = \frac{L}{(L+l)} \quad [17]$$

Where L is the distance from the top of the solution in the irradiation solution to the light source; l is the depth of the dish. This only needs to be considered when L is > 4 times than the aperture width.

$$E'_{avg} = E_0 * PF * RF * WF * DF \quad [18]$$

Where E_0 is the irradiance measurement at the centre of the dish.

Bolton and Stefan 2002 conducted this analysis for monochromatic irradiation at ~ 254 nm. However, UV light emitting diodes (LEDs) and medium pressure mercury lamps irradiate UV light at a larger bandwidth compared to conventional low pressure (LP) mercury UV lights. UV LEDs are considered polychromatic. For example, a UV LED may have a peak wavelength at 257.7 nm but irradiates UV light between 252.6 nm and 262.8 nm, while LP mercury lamps irradiate light at 253.7 nm only. See Figure S. 3 for the relative emission spectra of the UV LED wavelengths utilized in this study. Pousty et al. 2022 undertook a polychromatic and monochromatic approach in determining the incident photon flux of UV LEDs. Their analysis concluded that there was no significant difference between a monochromatic approach or a

polychromatic approach, meaning that the methodology undertaken in Bolton and Stefan 2002 to determine UV dose can be applied to UV LEDs.

In full scale applications of UV/AOPs, calculating the achieved UV dose is much more complex relative to bench scale studies. The UV transmittance (UVT) can fluctuate through the reactor causing some molecules to have reduced UV dose relative to others in the reactor. Engineers use a concept called the reduction equivalent dose which is the predicted smallest UV dose that will be subjected to a molecule in the reactor (Mackey et al. 2022). Detailed discussion on how to report and calculate the reduction equivalent dose is out of scope for this research.

2.6. Previous AOP Cost Analyses

Very few publicly accessible studies have attempted to conceptualize cost estimates for AOPs. Though conceptual cost estimates should not be used in lieu of site-specific calculations, they can be an excellent tool for water utilities as an early-stage evaluation on the feasibility of implementing an AOP. These kinds of analyses can also be used to identify important capital and O&M factors that utilities need to consider when implementing an AOP. To the authors knowledge very few have attempted to conduct this kind of analysis. Sharma et al. 2013 conceptualized cost estimates for ozone. Plumlee et al. 2013 conceptualized cost estimates for ozone and UV/H₂O₂. Usually, studies that attempt to conceptualize costs for UV/Cl do so by equating costs to the calculated electrical energy per order (EE/O), like in Tian et al. 2020. The EE/O is defined as the electrical energy (kWh) required to decompose a specific contaminant by one order magnitude in 1m³ of polluted water. The energy can then be equated to a monetary value by multiplying the governing electricity costs of the studied jurisdiction by the calculated EE/O. The total electrical energy for UV/AOPs is constituted from the UV light (EE/O_{UV}) and from the oxidant (EE/O_{oxidant}). The EE/O can be calculated using Equation 19, Equation 20, and Equation 21 listed below.

$$\frac{EE}{O} = \frac{EE}{O_{UV}} + \frac{EE}{O_{oxidant}} \quad [19]$$

$$\frac{EE}{O_{UV}} = \frac{P*t*1000}{V*log\frac{C_0}{C_t}} \quad [20]$$

$$\frac{EE}{O_{oxidant}} = E q_{oxidant} * \frac{[Oxidant]*1000}{log\frac{C_0}{C_t}} \quad [21]$$

Where P represents power of the electronic energy input of the UV device (kW), V is the volume of the solution (L), t is the photodegradation time (hr), [oxidant] is the oxidant dose (mol L⁻¹), C₀ is the initial concentration of the target contaminant, C_t is the concentration of the contaminant

after t photodegradation time, and $E_{q_{\text{oxidant}}}$ is the electric energy consumption to generated per mole of oxidant.

Lima-Thompson and Gora 2023 conducted a techno economic assessment on AOPs which attempted to characterize the costing factors that need to be accounted for when considering implementing an AOP to remove seasonal contaminants, such as taste and odour compounds and/or cyanotoxins, and year-round contaminants like 1-4 dioxane. The AOPs studied in the assessment was O_3 and UV/ H_2O_2 . Lastly, Mackey et al., 2022 developed a comprehensive analysis to implement UV/Cl for potable water reuse and compared results to UV/ H_2O_2 . The analysis looked at design considerations for UV AOPs, a cost analysis, and developed a decision tree which outlines the optimum conditions for selecting UV/Cl or UV/ H_2O_2 .

2.6.1. Sharma et al. 2013

The purpose of this study was to update historical construction (capital) costs reported for plant construction, and individual unit costs from actual and conceptual designs to develop generalized costs for a wide range of treatment processes, including ozone. Similarly, O&M costs were updated for water treatment units and included costs for energy, labor, and maintenance materials. The cost curves were originally developed by Gumerman et al. 1979 on behalf of the USEPA, and the costs were updated to 2011 USD dollars using various cost indexes, including the ENR CCI cost index, a popular costing index used by engineers for updating old cost estimates published in previous years to a contemporary value. Sharma et al. 2013 validated their costing functions through comparison with real bids prepared by reputable engineering firms. The ozone generation costing function presented in this study is only valid up to an ozone demand of 3,500 lb/day.

2.6.2. Plumlee et al. 2013

The goal of this study was to develop capital and O&M cost curves for advanced water treatment processes, including ozone and UV/ H_2O_2 , for potable wastewater reuse through soliciting conceptual cost estimates from equipment vendors and design engineers. The ozone cost curves presented were based off estimates from a single vendor and assumed the ozone system was located prior to a reverse osmosis membrane filtration system in the treatment train. The O&M cost estimates omitted factors such as labor, maintenance, or costs associated with producing oxygen onsite or shipping it from an offsite location. The UV/ H_2O_2 cost curves were developed through consultation from three vendors, however, only two were presented in the study as one vendor provided estimates which were

significantly higher than the other two. The estimates assumed that the UV/H₂O₂ system was placed after a reverse osmosis unit and the water that was subjected to treatment was assumed to have a UVT of 95%. The target contaminant for the UV/H₂O₂ system was NDMA and 1,4 dioxane with the treatment objectives of 1.2 log removal and 0.5 log removal, respectively. The UV dose and H₂O₂ dose were not disclosed by the vendors. All capital cost estimates in this study included percent-based multipliers, which were derived from McGivney and Kawamura 2008, to include cost factors like yard piping, sitework and landscaping, electrical and instrumentation installation costs, contingency costs, and fees for contractors, engineering, legal, and administration. The O&M cost estimates were exclusively based on the estimates provided by the vendors and included H₂O₂ supply, hypochlorite quenching, energy, and lamp replacement. Labor costs were assumed to be negligible. A summary of a few of the conceptual cost curve regression equations from the study is provided Table 3 below.

Table 3: Plumlee et al. 2013 summary of conceptual cost curve regression equations for various treatment processes

Process	Capital Costs (\$M/MGD)	Annual O&M Costs(\$M/MGD)
Ozone	2.26 * (Plant Capacity, in MGD) ^{-0.54}	0.0068 * (Plant Capacity, in MGD) ^{-0.051}
UV/H ₂ O ₂	0.474 * (Plant Capacity, in MGD) ^{-0.056}	0.038 * (Plant Capacity, in MGD) ^{-0.052}
Ozone/H ₂ O ₂	2.26 * (Plant Capacity, in MGD) ^{-0.54}	0.016* (Plant Capacity, in MGD) ^{-0.020}

2.6.3. Tian et al. 2020

Unlike the other two studies listed in sections 2.6.1 and 2.6.2, this study's purpose was to compare the degradation kinetics and energy requirements of different UV AOPs, including UV/Cl and UV/H₂O₂, to remove iopamidol, a pharmaceutical drug, in water. The study determined the EE/O of the UV AOPs studied using Equation 19, Equation 20, and Equation 21 which used the results of their bench scale results of the degradation of iopamidol. No conceptual estimates were generated in the study, only the energy requirements were measured for 1 log reduction of iopamidol using the various UV AOPs studied. The energy requirements can be used to estimate energy costs for degradation of iopamidol if the EE/O is multiplied by governing electricity costs. However, this kind of analysis is not as comprehensive as the previous two studies as cost factors such as yard piping, sitework and landscaping, installation costs, contingency costs, and fees for contractors, are not included, and are strictly based on bench scale degradation experiments which may not necessarily translate well into full scale results. The study concluded that UV/Cl was the most energy efficient in the removal of iopamidol based on bench scale results.

2.6.4. Lima-Thompson and Gora 2023

In this desktop study, a techno-economic assessment was conducted to conceptualize the cost factors to implement the AOPs UV/H₂O₂ and O₃ to treat seasonal (taste and odour compounds/cyanotoxins) and persistent contaminants (1-4 dioxane). The study mainly focused on UV/H₂O₂ and developed cost curves based on the capacity of the water treatment plant. They developed the cost curves by updating costing information published in the USEPA document: *Technologies and Costs Document for the Final Long term 2 Enhanced Surface Water Treatment Rule and Final Stage 2 Disinfectants and Disinfection Byproducts*, which has costing information on utilizing O₃ and UV as alternatives or add-ons to chlorine disinfection. The document also contains information on H₂O₂ dosing and storage. The cost curves were compared to the analyses conducted by Sharma et al., 2013 and Plumlee et al., 2013. The results indicated that for UV/H₂O₂, UV equipment drives capital costs, while H₂O₂ related costs, particularly quenching, drive operating costs.

2.6.5. Mackey et al., 2022

This study conducted a comprehensive analysis on implementing UV/Cl for potable water reuse and compared the analysis to UV/H₂O₂. The study looked at design considerations for UV/AOPs, the influence of background water quality on UV/AOP efficacy, conducted an economic analysis on UV/Cl vs UV/H₂O₂, and developed a decision tree to decide when UV/Cl or UV/H₂O₂ would be a better option based upon upstream conditions and downstream requirements. The economic analysis of UV/H₂O₂ agreed with the desktop study done by Lima-Thompson and Gora 2023, where quenching was determined to be the major cost implication when implementing UV/H₂O₂. The decision tree was an “in general” approach where site specific conditions or requirements can change the optimum choice of UV/Cl or UV/H₂O₂. The study found that if the pH of the incoming water quality was < 6, or pH suppression was feasible, and the ammonia and bromide concentration in the incoming water are controlled, UV/Cl is the best option. When ammonia is not controlled, the free chlorine dose will need to increase greatly to overcome ammonia’s free chlorine demand, therefore resulting in UV/H₂O₂ being the better economic option. However, high ammonia concentration is more of a wastewater issue than a drinking water issue and this research has a drinking water focus. When bromide is not controlled, its reaction with free chlorine produces bromate, a regulated disinfection byproduct, meaning mitigation strategies will need to be adapted which may cause UV/H₂O₂ to be the better option. Lastly, in acidic pH UV/Cl outperforms UV/H₂O₂ in the degradation of a broad range of contaminants, therefore, if the pH of the water is low, or

pH suppression is feasible, UV/Cl will be the better option. To reiterate, the decision matrix was made as a general approach to determine whether circumstances favor UV/Cl or UV/H₂O₂, but specific situations may not necessarily abide by these general suggestions based on site specific upstream conditions and downstream requirements.

2.7. Optimum UV and Oxidant Dose

Full scale UV AOPs are commonly designed by developing reactor specific deterministic mathematical models that incorporate empirically measured scavenging capacity coupled with bench, pilot and full-scale studies of optimum oxidant and UV doses to achieve targeted treatment goals (Mackey et al. 2022). Unfortunately, the deterministic mathematical models that have been developed to date are proprietary and are not released for public use. However, Kwon et al. 2019 derived a kinetic equation that can predict removal yields of target contaminants when subjected to UV/H₂O₂ treatment. This equation was then used to predict optimum UV doses and H₂O₂ doses to base on a targeted removal objective (geosmin was the target contaminant in study) and the minimum process electrical energy dose, EED_{UV/H_2O_2} . Equation 22 and Equation 23 below are the derived kinetic equation for predicting required UV and H₂O₂ doses for treatment of a target contaminant and determining optimum doses based on associated EED_{UV/H_2O_2} . The difference between required doses and optimum doses are clarified below.

Required dose: Any combination of UV and oxidant doses able to achieve the treatment objectives.

Optimum dose: The specific UV and oxidant dose able to achieve the treatment objectives that has the smallest electrical energy dose of all required doses.

The required doses to meet treatment objectives were modeled using Equation 22 and the optimum doses were modeled using Equation 23.

$$\ln\left(\frac{[M]_0}{[M]_{H'}}\right) = H' * (k'_d + k'_i)$$

$$= H' * \left(\frac{\epsilon_M * \phi_M * \ln(10)}{U_{254}} + k_{\cdot OH, M} * \frac{\epsilon_{H_2O_2} * [H_2O_2] * \phi_{\cdot OH} * \ln(10)}{U_{254} * (\sum k_{S, OH} [S]_i + k_{H_2O_2, OH} [H_2O_2])} \right) [22]$$

Where [M] is the concentration of micropollutant (mole L⁻¹); H' is the UV fluence (mJ cm⁻²); k'_d is the fluence based pseudo-first order rate constant for direct UV photolysis (cm² mJ⁻¹); k'_i is the fluence-based pseudo-first-order rate constant for ·OH induced degradation (cm² mJ⁻¹); k_{·OH, M} is

the second order rate constant for the $\cdot\text{OH}$ reaction with the target compound M; ϵ_M and $\epsilon_{\text{H}_2\text{O}_2}$ are the molar absorption coefficients ($\text{M}^{-1} \text{cm}^{-1}$) of micropollutant M and H_2O_2 , respectively; ϕ_M and ϕ_{OH} are the quantum yields of micropollutant M and $\cdot\text{OH}$ production from H_2O_2 photolysis, respectively; U_{254} is the molar photon energy at 254 nm; $[\text{H}_2\text{O}_2]$ is the concentration of H_2O_2 (M); $\Sigma k_{s,\text{OH}}[\text{S}]_i$ is the $\cdot\text{OH}$ scavenging capacity (s^{-1}); and $k_{\text{H}_2\text{O}_2, \text{OH}}$ is the second order rate constant with $\cdot\text{OH}$ and H_2O_2 .

$$\text{Water Factor (WF)} = \frac{1 - 10^{-a_{254} * l_{\text{avg}}}}{a_{254} * l_{\text{avg}} * \ln 10}$$

$$\text{EED}_{\text{UV}/\text{H}_2\text{O}_2} = \text{EED}_{\text{UV}} + \text{EED}_{\text{H}_2\text{O}_2}$$

$$= \left(\frac{2.78 * 10^{-7} * \left(\frac{10 * H'}{\text{WF}} \right)}{l_{\text{avg}} * \eta_{\text{UV}}} \right) + (X * [\text{H}_2\text{O}_2]_0) \quad [23]$$

Where EED_{UV} is the electrical energy dose associated with the UV reactor power requirements (kWh m^{-3}); $\text{EED}_{\text{H}_2\text{O}_2}$ is the electrical energy dose required for the production of H_2O_2 dosed in the UV/ H_2O_2 process (kWh m^{-3}); WF is the water factor which accounts for the absorbance of the water at 254 nm, a_{254} ; l_{avg} is the average optical pathlength of the reactor; η_{UV} is the UV lamp efficiency; X is the energy requirements to produce 1 kg of H_2O_2 in the studied jurisdiction (kWh/kg); and $[\text{H}_2\text{O}_2]_0$ is the H_2O_2 dose.

2.8. Summary of Literature Review

All literature outlined in this chapter were discussed to build the foundation of the research in this study and highlight its importance. Almost no research has been done to characterize the radical scavenging capacity specific to UV/Cl or attempt to develop comprehensive cost curves of UV/Cl specific to a drinking water context. With the potential increase of contaminants of concern resultant of climate change, it is important that water utilities increase redundancies in their treatment trains to ensure treated water is safe to drink. UV/Cl could be a viable option to help bolster treatment trains, however it is clear more research is required.

3.0. Methods and Materials

3.1. Objective 1: Adapting the External Calibration Method to UV/Cl

3.1.1. Characterizing the UV Apparatus

To conduct experiments with UV light, the measured and achieved volume averaged fluence rate, or UV dose, must be characterized to ensure a standardized approach has been taken and that the results obtained in the experiments are reproducible. An Aquisense Pearl Beam UV LED, shown in Figure 3, was characterized using a FLAME-S-UV-VIS-ES spectrometer calibrated in house by the manufacturer Ocean Insight to measure and quantify light in the UV range (200-400 nm). The spectrometer contains a cosine collector with a fiber diameter of 3900 μm . The UV LED emits two wavelengths with peaks in the UV-C range (257.7 & 280.6 nm) and one wavelength with a peak in the UV-A range (367.4 nm). The intensity profiles of the two wavelengths with peaks in the UV-C range were determined at three different distances, 1cm, 3cm, and 5cm from the edge of the collimator on a 6cm-by-6cm grid. A rectangle method was used to determine the intensity of the UV LED to include the full width maxima of the wavelength, 10.2 nm, and 13.1 nm, for the 257.7 nm & 280.6 nm respectively. The integration time was set to 'automatic' to ensure the spectrometer was not saturated and 5 scans were used to reduce the signal to noise ratio. A similar approach for characterizing a UV LED was presented in (Gora et al., 2019). The intensity profiles were then used to calculate the UV dose using Equation 13, Equation 14, Equation 15, Equation 16, Equation 17, and Equation 18. Only the intensity profiles of the characterization at a 1 cm distance from the edge of the collimator are displayed in Appendix A: UV Characterization Figures as this was the intensity profile used to calculate the UV dose throughout all of Objective 1.

3.1.2. Replicating the Results of Wang et al. 2020

The standard selected to replicate the results of Wang et al. 2020 was tert-butanol (TBA) as its second order rate constant with hydroxyl radicals ($\cdot\text{OH}$) is reported in literature, $k_{\text{OH}} = 6 * 10^8 \text{ M}^{-1} \text{ s}^{-1}$ (Fang et al., 2014) and it is resistant to UV photolysis and direct oxidation from H_2O_2 . Additionally, TBA has high water solubility, high stability of radical scavenging capacity, and low volatility in the pH range typically seen in drinking water (Wang et al., 2020). The concentrations of the standard solutions were from 25 μM and 333 μM which yielded radical scavenging capacities of $2 \times 10^4 \text{ s}^{-1}$ to $20 \times 10^4 \text{ s}^{-1}$, respectively, which was

the range of ·OH scavenging capacity in real drinking water samples reported in literature (Wang et al., 2020; Kwon et al., 2019).

Methylene blue (MB) was selected as the dye or probe compound because its pK_a value is less than 1, which means that its molecular structure will remain constant through pH that is typically seen in drinking water (Wang et al., 2020). The concentration for MB that was spiked in the standard solutions and in the real water samples was 5 μM. This dose was selected to ensure that MB dominated the absorbance of the water matrix to ensure the UV dose that is achieved in the pure water samples containing TBA (standard solutions) was the same in the real water samples. UV dose is impacted by the absorbance of the sample (see chapter 2.5) and therefore similar absorbance values need to be established to ensure an equivalent UV dose.

The distance from the edge of the collimator to the sample was ~ 1 cm. This distance ensured that the ·OH production rate would not differ by more than 5% from the pure water standard solutions and the real water samples (Wang et al., 2020). Standard solutions and real water samples were spiked with 25 mg L⁻¹ (0.74 mM) of H₂O₂, which was the same used in Wang et al. 2020, and subjected to a UV dose of 200 mJ cm⁻². The UV dose was not reported in Wang et al. 2020. The nominal wavelength of the UV LED device selected was 255 nm as H₂O₂ molar absorption coefficient is higher at shorter wavelengths and Wang et al. 2020 established the external calibration curve using conventional LP mercury lamps which emit UV light at 254 nm.

One mL aliquots were collected before and after UV treatment to analyze initial and final absorbance values. The absorbance was measured using a single scan length at 664 nm, MB's signature wavelength, using a DR6000 UV-Vis spectrophotometer. The color decay rate was calculated using the $\frac{1}{(\ln \frac{[a]_0}{[a]})/t}$ term in Equation 10. Triplicate color decay rates were measured for each standard solution and the color decay rate vs scavenging capacity was plotted in RStudio using ggplot2 and dplyr packages. Triplicate decay rates were measured for the real water samples, which were collected from Lake Ontario, and the scavenging capacity was calculated using the linear regression equation established with the calibration curve and plotted onto the graph.

3.1.3. Adapting the External Calibration Method to UV/Cl

Before a calibration could be established for UV/Cl a key assumption was made. UV/Cl produces multiple radical species including ·OH, ·Cl, ·Cl₂⁻, and ·ClO (Fang et al., 2014). However, only ·OH and ·Cl were

considered when determining the calibration curves. This is because these are the two primary radical species produced in UV/Cl with the highest oxidative potential. Meaning these are the two radical species that will contribute to the degradation of a broad range of contaminants. Additionally, the second order rate constants were not known for the secondary radical species with the selected standard solution. This could be a potential limitation of the study. More research is required on the role of secondary radicals of free chlorine photolysis on contaminant degradation.

TBA was selected as the standard solution as its second order rate constant with $\cdot\text{Cl}$ is reported in literature, $k_{\text{Cl}} = 3.0 \times 10^8 \text{ M}^{-1} \text{ s}^{-1}$ (Fang et al., 2014). Due to UV/Cl producing more radical species its total radical scavenging capacity will always be greater than UV/H₂O₂ (Equation 5). Therefore, the range of concentrations of the standard solutions was selected between 0 μM and 460 μM which yielded radical scavenging capacities of 0 and $40 \times 10^4 \text{ M}^{-1} \text{ s}^{-1}$, respectively, to account for the increase in radical scavenging capacity. The reason a value of $0 \text{ M}^{-1} \text{ s}^{-1}$ was investigated was because the external calibration curves would be applied to standard solutions with a pH of 5 which would intrinsically have a higher radical scavenging capacity than the standard solutions made with pure water. This is because to depress the pH a weak acid was added resulting in higher radical scavenging capacity compared to pure water. Therefore, a comparison between a standard solution in pure water with no TBA added (no added RSC) and a standard solution with a pH of 5 with no added RSC could be made. There were no reported values in literature for the total radical scavenging capacity of UV/Cl or previous studies which conducted a similar analysis. Standard solutions were spiked with 5 mg L^{-1} (0.067 mM) and 7 mg L^{-1} (0.094 mM) of free chlorine.

To depress the pH of standard solutions acetic acid was selected because its second order rate constants with $\cdot\text{OH}$ and $\cdot\text{Cl}$ are reported in literature, $k_{\text{OH}} = 1.57 \times 10^7 \text{ M}^{-1} \text{ s}^{-1}$ and $k_{\text{Cl}} = 2.80 \times 10^8 \text{ M}^{-1} \text{ s}^{-1}$ (NIST Database), because it is a perfect buffer at the desired pH of 5 and is miscible with water and alcohols (Sigma-Aldrich, 2023). The same molar concentrations of TBA were added for both the pure water standard solutions and the standard solutions with a pH of 5. The standard solutions with pH of 5 had a range of radical scavenging capacity between $20 \times 10^4 \text{ s}^{-1}$ and $60 \times 10^4 \text{ s}^{-1}$. The pH was measured using indicator strips and the concentration of acetic acid used in the standard solutions was 666 μM . Due to the variability of molar absorption coefficients at different pH of free chlorine (Yin et al., 2019), nominal wavelengths of 255 nm and 280 nm were investigated to measure the impact utilizing different wavelengths can have on applying the external calibration method.

Methylene blue (MB) was selected as the dye or probe compound in the experiment due to the same reasons outline in Chapter 3.1.2. Unlike with H₂O₂, free chlorine oxidizes MB in water matrices without the formation of radical oxidizing species (Hoang et al., 2022). Therefore, dark experiments (experiments with no UV light) were conducted to measure the contribution of free chlorine to the overall degradation of MB at both pHs, with both free chlorine doses used in the experiment, for the length of time required to achieve a UV dose of 500 mJ cm⁻² and 1000 mJ cm⁻² for each wavelength emitted of the UV LED. To minimize the amount of MB degradation to free chlorine alone, the UV device was turned on at the exact moment free chlorine was spiked into the reactor (Figure 3).

Few studies have been conducted on the effect the water matrices have on contaminant degradation with reactive chlorine species only, so an analysis was also conducted for evaluating the external calibration method utilizing dominantly reactive chlorine species. This was done by spiking the reactor with 10 μM of nitrobenzene, which has high reactivity towards ·OH, $k_{OH} = 4 * 10^9 \text{ M}^{-1} \text{ s}^{-1}$ (NIST Database) and shows negligible reactivity towards reactive chlorine species (Fang et al. 2019). At this concentration of nitrobenzene ·OH radicals are quenched quicker relative to reactive chlorine species (Hoang et al., 2022).

Log reduction values of methylene blue were investigated to measure the impact pH and wavelength have on removing methylene blue. Log reduction values were calculated using Equation 24 below. Where C₀ is the initial concentration of MB and C_t is the concentration of MB after treatment.

$$\text{Log reduction} = \log \left(\frac{C_0}{C_t} \right) [24]$$

One mL aliquots were collected before and after UV treatment to analyze initial and final absorbance values. The absorbance was measured using a single scan length at 664 nm, MB's signature wavelength, using a DR6000 UV-Vis spectrophotometer. The color decay rate was calculated using the $\frac{1}{(\ln \frac{[a]_0}{[a]})/t}$ term in Equation 10. Triplicate color decay rates were measured for each standard solution and the color decay rate vs scavenging capacity was plotted in RStudio using ggplot2 and dplyr packages. Triplicate decay rates were measured for the treated and raw real water samples, which were collected from a treatment plant with a surface water river source in southern Ontario, and the scavenging capacity was calculated using the linear regression equation established with the calibration curve and plotted onto the graph. The pH of the real water samples was depressed using acetic acid. Acetic acid was slowly added to the real water samples while monitoring the pH of the sample using a pH probe. The

concentration required to achieve a pH of 5 in the treated water samples was 1.29 M and in the raw water was 1.65 M.

Statistical significance of wavelength, pH, UV dose, and free chlorine dose on methylene blue log reduction and applying the external calibration method to UV/Cl were determined using two-way analysis of covariance (ANCOVA) tests. ANCOVA is a method of determining if linear regression models are statistically significantly different from each other. Wavelength, pH, UV dose and free chlorine dose were categorical variables in the analysis. For the log reduction analysis, time was the covariate. For the adaptation of the external calibration method, the radical scavenging capacity was the covariate.

To measure if the real water samples had statistically significant calculated radical scavenging capacities, a two-way analysis of variance (ANOVA) test was used. Where pH and wavelength were the tested categorical variables. All statistical tests were done in RStudio. A statistically significant value for this study was a p value of less than or equal to 0.05. A model with an R^2 value greater than or equal to 0.7 was considered to have a strong correlation.

3.1.4. Materials

Table 4: Materials utilized for external calibration method experiments.

Material	Supplier
Nitrobenzene, 99%	Thermofisher
Tert-Butyl Alcohol, 99%	Thermofisher
Methylene Blue	Thermofisher
Sodium Hypochlorite, 10-15%	Thermofisher
Hydrogen Peroxide, 3 wt. %	Thermofisher

3.2. Objective 2: Modelling Required and Optimum UV and Oxidant Doses to Degrade Contaminants of Concern Based on the Radical Scavenging Capacity of the Water Matrix

The contaminant of concern selected for this analysis was Microcystin-LR (MC-LR). Only one cyanotoxin was selected because MC-LR is the most detected cyanotoxin, and to simplify the modelling process. Cyanotoxins are produced from harmful cyanobacterial blooms (also known as harmful algae blooms). Conventional treatment infrastructure is not well equipped to remove cyanobacteria or their toxins, which is why cyanotoxins are classified as contaminants of concern. Additionally, the impacts of climate change on source waters are expected to lead to an increase in the detection of cyanotoxins and could

be a driving input into water utilities considering advanced treatment technologies (Vlad et al., 2014). It is important to note that MC-LR was not used in laboratory experiments conducted, rather, information about its degradation from other studies were used to develop cost estimates presented in Section 4.3. Required doses reported in this study represent all the potential oxidant and UV doses that can be combined to achieve the selected treatment objective(s), while the optimum doses are the best combination of oxidant and UV doses based upon the minimum EED value.

Equation 22, developed by Kwon et al. 2019 was used to predict required dosing parameters for UV/H₂O₂ to treat MC-LR.

To ensure that the methodology used to determine required doses of UV/Cl treatment of MC-LR was correct, the results from Kwon et al. 2019 were replicated for MC-LR degradation with the exact same inputs for UV/H₂O₂ treatment. In Equation 22, H' was isolated and solved for the exact same range of H₂O₂ doses (1-15 mg L⁻¹). K'_d was set to 3.71 J; ε_{H₂O₂} was set to 18.7 M⁻¹ cm⁻¹; φ_{OH} was set to 1; M₀ was set to 100 mol L⁻¹; M_{H'} was set to 10 mol L⁻¹ (1-log reduction); Σk_{s, OH}[S]_I was set to 3*10⁴ s⁻¹; k_{OH, M} was et to 11 *10⁹ M⁻¹ s⁻¹ (Kwon et al., 2019); and k_{OH, H₂O₂} was set to 2.7 *10⁷ M⁻¹ s⁻¹. The inputs are summarized in Table 5 below.

Table 5: Model inputs for replication of Kwon et al., 2019 results. All inputs used were the same as Kwon et al., 2019.

Model Variable	Model Input
[H ₂ O ₂]	1-15 mg L ⁻¹
K' _d	3.71 J
ε _{H₂O₂}	18.7 M ⁻¹ cm ⁻¹
φ _{OH}	1
M ₀	100 mol L ⁻¹
M _{H'}	10 mol L ⁻¹
Σk _{s, OH} [S] _I	3 x 10 ⁴ s ⁻¹
k _{OH, H₂O₂}	2.7 *10 ⁷ M ⁻¹ s ⁻¹
k _{OH, M}	11 *10 ⁹ M ⁻¹ s ⁻¹

To determine the required doses for UV/H₂O₂ in this study almost all inputs from Kwon et al. 2019 were kept the same except that the range of H₂O₂ doses was set to 1-25 mg L⁻¹ as these are values reported in bench, pilot and full-scale studies that researched the use of UV/H₂O₂ for the degradation of contaminants in water (Wang et al 2019; Wang et al. 2020; Tian et al. 2019). Another difference was that there were two radical scavenging capacity values selected to study the impact the RSC has on required and optimum doses. The two values selected were 3 x 10⁴ s⁻¹ and 8 x 10⁴ s⁻¹ as this is the range of ·OH scavenging capacity found in Lake Ontario over the course of a year (Mackey et al. 2022). Lastly, the targeted log reduction of MC-LR was set to 2-log reduction (99%). MC-LR has small maximum allowable concentration according to the Guidelines for Canadian Drinking Water Quality (0.0015 mg L⁻¹) and the World Health Organization (0.001 mg L⁻¹). A study by Hotto et al., 2007 found samples of Lake Ontario had concentrations of MC-LR up to 0.0014 mg/L. Although this value is below Canada’s drinking water guidelines, it does exceed the World Health Organizations recommendations. To account for the potential increase of cyanotoxins resultant of climate change (Vlad et al., 2014), a conservative 2-log reduction of MC-LR was selected. Model inputs are summarized in Table 6 below.

Table 6: Model inputs for required doses for UV/H₂O₂ treatment.

Model Variable	Model Input	Reference
[H ₂ O ₂]	1-25 mg L ⁻¹	Wang et al., 2020
K' _d	3.71 J	Kwon et al., 2019
ε _{H2O2}	18.7 M ⁻¹ cm ⁻¹	Kwon et al., 2019
φ _{OH}	1	Kwon et al., 2019
M ₀	100 mol L ⁻¹	Not applicable
M _{H'}	1 mol L ⁻¹	Not applicable
Σk _{s, OH} [S] _I	3 x 10 ⁴ s ⁻¹ and 8 x 10 ⁴ s ⁻¹	Mackey et al., 2022
k _{OH, H2O2}	2.7 x 10 ⁷ M ⁻¹ s ⁻¹	Kwon et al., 2019
k _{OH, M}	11 x 10 ⁹ M ⁻¹ s ⁻¹	Kwon et al., 2019

To determine optimum doses for 2-log reduction of MC-LR with UV/H₂O₂ treatment, Equation 23 was used.

The values utilized in Equation 23 were similar to the inputs Kwon et al. 2019 used. The a_{254} value was set to 0.02 cm^{-1} as this leads to a UVT of ~96%, a typical value for drinking water; l_{avg} was set to 0.1 m; and η_{UV} was set to 0.3 (30 percent efficiency for LP lamps.) The required energy to produce 1 kg of H_2O_2 was determined by converting the cost per gal of 50% H_2O_2 reported in Mackey et al. 2022 to 2023 CAD by utilizing Equation 1 with the associated CCl cost indexes and dividing that value by the cost of electricity in Ontario (\$/kWh). X was determined to be \$10.62 per kWh. The calculated required UV and H_2O_2 doses to achieve 2-log reduction of MC-LR for both RSC values were utilized as the associated UV and H_2O_2 doses in Equation 23. The minimum value produced from Equation 23 with all associated required doses was selected as the optimum parameters. Model inputs are summarized in Table 7 below.

Table 7: Model inputs for optimum dosing of UV/ H_2O_2 treatment.

Model Variable	Model Input	Reference
a_{254}	0.02 cm^{-1}	Kwon et al., 2019
l_{avg}	0.1 m	Kwon et al., 2019
η_{UV}	0.3	Kwon et al., 2019
X	\$10.62 kWh^{-1}	Mackey et al., 2022

To determine the required doses for 2-log reduction of MC-LR with UV/Cl Equation 22 was modified to include an input that accounts for the degradation of reactive chlorine species. In this analysis $\cdot\text{Cl}$ was considered the only reactive chlorine species contributing to the degradation of MC-LR as it is the primary radical formed in UV/Cl (Guo et al. 2017) and will contribute the most to the degradation of a larger range of contaminants compared to other reactive chlorine species as it has the highest reduction potential (Fang et al. 2014). Equation 23 was modified to Equation 25 below.

$$\ln\left(\frac{[M]_0}{[M]_{H'}}\right) = H' * (k'_d + k'_i + k'_c)$$

$$= H' * \left(\frac{\varepsilon_M * \phi_M * \ln(10)}{U_{254}} + k_{\cdot\text{OH},M} * \frac{\varepsilon_{\text{HOCl}} * [\text{HOCl}] * \phi_{\cdot\text{OH}} * \ln(10)}{U_{254} * (\sum k_{S,\text{OH}}[S]_i + k_{\text{HOCl},\text{OH}}[\text{HOCl}]} + k_{\cdot\text{Cl},M} * \frac{\varepsilon_{\text{HOCl}} * [\text{HOCl}] * \phi_{\cdot\text{Cl}} * \ln(10)}{U_{254} * (\sum k_{S,\text{Cl}}[S]_i + k_{\text{HOCl},\text{Cl}}[\text{HOCl}]} \right) [25]$$

Where [M] is the concentration of micropollutant (mole L^{-1}); H' is the UV fluence (mJ cm^{-2}); k'_d is the fluence based pseudo-first order rate constant for direct UV photolysis ($\text{cm}^2 \text{mJ}^{-1}$); k'_i is the fluence-based pseudo-first-order rate constant for $\cdot\text{OH}$ induced degradation ($\text{cm}^2 \text{mJ}^{-1}$); k'_c is the

fluence-based pseudo-first-order rate constant for $\cdot\text{Cl}$ induced degradation ($\text{cm}^2 \text{mJ}^{-1}$); $k_{\cdot\text{OH},\text{M}}$ is the second order rate constant for the $\cdot\text{OH}$ reaction with the target compound M; $k_{\cdot\text{Cl},\text{M}}$ is the second order rate constant for the $\cdot\text{Cl}$ reaction with the target compound M; ϵ_{M} and ϵ_{HOCl} are the molar absorption coefficients ($\text{M}^{-1} \text{cm}^{-1}$) of micropollutant M and free chlorine, respectively; ϕ_{M} , ϕ_{OH} , and ϕ_{Cl} are the quantum yields of micropollutant M, $\cdot\text{OH}$ production, and $\cdot\text{Cl}$ from free chlorine photolysis, respectively; U_{254} is the molar photon energy at 254 nm; $[\text{HOCl}]$ is the concentration of free chlorine (M); $\Sigma k_{\text{s},\text{OH}}[\text{S}]_i$ is the $\cdot\text{OH}$ scavenging capacity (s^{-1}); $\Sigma k_{\text{s},\text{Cl}}[\text{S}]_i$ is the $\cdot\text{Cl}$ scavenging capacity (s^{-1}); $k_{\text{HOCl},\text{OH}}$ is the second order rate constant with $\cdot\text{OH}$ and free chlorine; and $k_{\text{HOCl},\text{Cl}}$ is the second order rate constant with $\cdot\text{Cl}$ and free chlorine.

The k'_d value was set to 3.71 J (Kwon et al. 2019); $k_{\cdot\text{OH},\text{M}}$ was $11 \times 10^9 \text{ M}^{-1} \text{ s}^{-1}$ (Kwon et al. 2019); $k_{\cdot\text{Cl},\text{M}}$ was $2.25 \times 10^{10} \text{ M}^{-1} \text{ s}^{-1}$ (Zhang et al. 2019); ϵ_{HOCl} was $80 \text{ M}^{-1} \text{ cm}^{-1}$ (Yin et al. 2019); ϕ_{OH} was 1.0 (Mackey et al. 2022); ϕ_{Cl} was 0.28 (Mackey et al. 2022); the log reduction was set to 2-logs; The range of HOCl doses was set from 1-10 mg L^{-1} (Yin et al. 2019; Wang et al. 2019); For effective comparison, the same two $\Sigma k_{\text{s},\text{OH}}[\text{S}]$ values used in the UV/ H_2O_2 analysis, $3 \times 10^4 \text{ s}^{-1}$ and $8 \times 10^4 \text{ s}^{-1}$ were also used; $\Sigma k_{\text{s},\text{Cl}}[\text{S}]$ was $1.14 \times 10^4 \text{ s}^{-1}$ as this was the average of values measured using the external calibration method in Objective 1 of an Ontario surface water drinking water source. This value is complex and currently not well understood (Mackey et al. 2022); $k_{\text{HOCl},\text{OH}}$ was $2 \times 10^9 \text{ M}^{-1} \text{ s}^{-1}$ (Fang et al. 2014); and $k_{\text{HOCl},\text{Cl}}$ was $3 \times 10^9 \text{ M}^{-1} \text{ s}^{-1}$ (Fang et al. 2014). Model inputs are summarized in Table 8 below.

Table 8: Model inputs for required doses for UV/Cl treatment.

Model Variable	Model Input	Reference
[HOCl]	1-10 mg L^{-1}	Yin et al. 2018; Wang et al. 2019
K'_d	3.71 J	Kwon et al., 2019
ϵ_{HOCl}	$80 \text{ M}^{-1} \text{ cm}^{-1}$	Yin et al. 2018
ϕ_{OH}	1	Mackey et al. 2022
M_0	100 mol L^{-1}	Not applicable
$M_{\text{H}'}$	1 mol L^{-1}	Not applicable
$\Sigma k_{\text{s},\text{OH}}[\text{S}]_i$	$3 \times 10^4 \text{ s}^{-1}$ and $8 \times 10^4 \text{ s}^{-1}$	$3 \times 10^4 \text{ s}^{-1}$ and $8 \times 10^4 \text{ s}^{-1}$
$\Sigma k_{\text{s},\text{Cl}}[\text{S}]$	$1.14 \times 10^4 \text{ s}^{-1}$	Experimentally determined.

$k_{OH, M}$	$11 \times 10^9 \text{ M}^{-1} \text{ s}^{-1}$	Kwon et al. 2019
$k_{Cl, M}$	$2.25 \times 10^{10} \text{ M}^{-1} \text{ s}^{-1}$	Zhang et al. 2019
ϕ_{Cl}	0.28	Mackey et al. 2022
$k_{HOCl, OH}$	$2 \times 10^9 \text{ M}^{-1} \text{ s}^{-1}$	Fang et al. 2014
$k_{HOCl, Cl}$	$3 \times 10^9 \text{ M}^{-1} \text{ s}^{-1}$	Fang et al. 2014

To determine optimum doses for Equation 23 was modified to Equation below.

$$\text{Water Factor (WF)} = \frac{1 - 10^{-a_{254} * l_{avg}}}{a_{254} * l_{avg} * \ln 10};$$

$$\text{EED}_{UV/HOCl} = \text{EED}_{UV} + \text{EED}_{HOCl}$$

$$= \left(\frac{2.78 * 10^{-7} * \left(\frac{10 * H'}{WF} \right)}{l_{avg} * \eta_{UV}} \right) + (X * [HOCl]) \quad [26]$$

Where EED_{UV} is the electrical energy dose associated with the UV reactor power requirements (kWh m^{-3}); $\text{EED}_{H_2O_2}$ is the electrical energy dose required for the production of H_2O_2 dosed in the UV/ H_2O_2 process (kWh m^{-3}); WF is the water factor which accounts for the absorbance of the water at 254 nm, a_{254} ; l_{avg} is the average optical pathlength of the reactor; η_{UV} is the UV lamp efficiency; X is the energy requirements to produce 1 kg of sodium hypochlorite in the studied jurisdiction (kWh/kg); and $[\text{HOCl}]_0$ is the free chlorine dose.

The a_{254} value was set to 0.02 cm^{-1} as this leads to a UVT of ~96%, a typical conservative value for drinking water (Mackey et al. 2022); l_{avg} was set to 0.1 m; and η_{UV} was set to 0.3 (30 percent efficiency for LP lamps.) The required energy to produce 1 kg of sodium hypochlorite was determined by the cost per gal of 12.5% sodium hypochlorite reported in Mackey et al. 2022 to 2023 CAD by utilizing Equation 1 with the associated CCl cost indexes and dividing that value by the cost of electricity in Ontario ($\$/\text{kWh}$). X was determined to be \$3.38 per kWh. The calculated required UV and free chlorine doses to achieve 2-log reduction of MC-LR for both RSC values were utilized as the associated UV and free chlorine doses in Equation 25. The minimum value produced from Equation 25 with all associated required doses was selected as the optimum parameters. Model inputs are summarized in Table 9 below.

Table 9: Model inputs for optimum dosing of UV/Cl treatment.

Model Variable	Model Input	Reference
a_{254}	0.02 cm ⁻¹	Mackey et al., 2022
l_{avg}	0.1 m	Kwon et al., 2019
η_{UV}	0.3	Kwon et al., 2019
X	\$3.38 kWh ⁻¹	Mackey et al., 2022

An analysis was conducted to determine required and optimum UV and free chlorine doses when the pH of the water matrix is 5. Since full-scale applications of UV/Cl are often utilized at acidic pH (Mackey et al., 2022) this analysis was conducted to better represent conditions of UV/Cl realized at full-scale. The model inputs for the required doses are pasted in Table 10 below. The same inputs to calculate the optimum doses of UV/Cl treatment at pH of 7 (Table 9) were used at pH of 5, as all prior assumptions were applied to this analysis.

Table 10: Model inputs for required UV and oxidant doses for UV/Cl treatment at a pH of 5.

Model Variable	Model Input	Reference
[HOCl]	1-10 mg L ⁻¹	Yin et al. 2018; Wang et al. 2019
K'_d	3.71 J	Kwon et al., 2019
ϵ_{HOCl}	50 M ⁻¹ cm ⁻¹	Yin et al. 2018
ϕ_{OH}	1.4	Mackey et al. 2022
M_0	100 mol L ⁻¹	Not applicable
M_{H^+}	1 mol L ⁻¹	Not applicable
$\Sigma k_{s, OH}[S]_I$	3 x 10 ⁴ s ⁻¹ and 8 x 10 ⁴ s ⁻¹	Mackey et al., 2022
$\Sigma k_{s, Cl}[S]$	1.14 x 10 ⁴ s ⁻¹	Experimentally determined.
$k_{OH, M}$	11 x 10 ⁹ M ⁻¹ s ⁻¹	Kwon et al. 2019
$k_{Cl, M}$	2.25 x 10 ¹⁰ M ⁻¹ s ⁻¹	Zhang et al. 2019
ϕ_{Cl}	0.8*	Mackey et al. 2022; Yin et al., 2018

Model Variable	Model Input	Reference
$k_{HOCl, OH}$	$2 \times 10^9 \text{ M}^{-1} \text{ s}^{-1}$	Fang et al. 2014
$k_{HOCl, Cl}$	$3 \times 10^9 \text{ M}^{-1} \text{ s}^{-1}$	Fang et al. 2014

* Value is not reported in literature and was estimated using reported values at a pH of 7.

3.3. Objective 3: Conceptualizing the Capital and O&M Costs of UV/H₂O₂ and UV/Cl through the Development of Cost Curves

Direct capital cost curves and O&M cost curves were developed for UV/H₂O₂, and UV/Cl using information available in the peer reviewed literature, Water Research Foundation reports, government documents, and other reputable grey literature sources.

The cost curves for UV/H₂O₂ were created by updating costing information published in USEPA's *Technologies and Costs Document for the Final Long Term 2 Enhanced Surface Water Treatment Rule and Final Stage 2 Disinfectants and Disinfection Byproducts Rule*, which provides detailed costing on utilizing UV disinfection at a UV dose of 40 mJ cm⁻² based upon the capacity of the water treatment plant. This document also provides costing information on H₂O₂ dosing and storage. The UV/H₂O₂ cost curves were developed by combining the cost information of UV disinfection and H₂O₂. UV/H₂O₂ cost curves were compared to Plumlee et al., 2014 and Sharma et al., 2013. More details on these two studies are provided in Section 2.6. Free chlorine was used to calculate quenching costs where the equipment required to monitor, store, and dose the water was already onsite. Mackey et al. 2022 presented costs for 12.5% sodium hypochlorite which was used to calculate the quenching costs. Required dose of HOCl to quench H₂O₂ were determined based off information in Watts, 2012.

The UV/Cl cost curves were developed by combining the same costing information provided for UV disinfection with the cylinder storage chlorine feed system cost estimates published in USEPA's *Estimating Water Treatment Costs: Volume 2 Cost Curves Applicable to 1 to 200 MGD Treatment Plants*. The cylinder storage chlorine system was chosen for this costing exercise as it is applicable to both small and large plant capacities (Crittenden et al., 2012). Additionally, Mackey et al., 2022 provides costing information for 12.5% sodium hypochlorite per gallon, which was used for the O&M costs for the analysis.

All cost curves were developed utilizing the same treatment conditions outlined in Section 3.2. All cost curves were updated to 2023 CAD by using Equation 1, the CCI published in ENR to convert a cost estimate that was developed in a previous year to an equivalent cost in a different year. Error bounds were included in the cost curves and were calculated as +50% and -30% of the calculated cost based on the recommendation for conceptual estimates (McGivney, 2008).

The cost curves presented in this thesis are in general agreement with those published by other researchers (Mackey et al., 2022; Plumlee et al., 2013; Sharma et al., 2013) but they should not be used in lieu of professional cost estimates as they were not rigorously validated against real treatment systems.

4.0. Results and Discussion

4.1. Objective 1: Adapting the External Calibration Method to UV/Cl

4.1.1. Replicating Wang et al. 2020

Figure 6 below illustrates the results of replicating the external calibration method developed for UV/H₂O₂. The black data points are experimental results recorded in the lab while the orange data points indicate the external calibration curve presented in Wang et al. 2020. From inspection of the figure, the experimental results recorded and Wang et al.'s results agree with each other with some slight differences. These differences can be attributed to the different standard solutions used in the recorded experimental results and in Wang et al.'s results. Tert-butanol (TBA) was used in the experimental results while Wang et al. used iso-propanol. TBA was selected because the second order rate constants between ·OH and reactive chlorine species are reported in literature and was used to establish the calibration curves for UV/Cl. Additionally, Wang et al., did not report the UV dose that was used to determine their calibration curve and therefore it is possible that a different UV dose was used in the experiments. However, since the calibration curves are created using the methylene blue colour decay rate, which is a measure of how quickly the methylene blue's colour decays from UV/H₂O₂ treatment, the UV dose should not be important when applying the external calibration method. This is because, assuming a first order rate reaction kinetics between hydroxyl radicals and the standard solution, the rate at which methylene blue is degraded should be the same no matter the UV dose applied as the UV does not significantly contribute to the degradation of MB (Wang et al., 2020).

Another reason for the difference of experimental results and Wang et al.'s results is Wang et al., used LP mercury lamps while a UV LED was used for the experimental results. UV LEDs have a different emission and characterization profile than LP lamps, which can impact the yield of ·OH radicals (Yin et al., 2018), and therefore the rate at which the colour of methylene blue decays. Additionally, Wang et al. had different method of reading the absorbance values of methylene blue which did not require sampling as the absorbance reading was measured within the reactor with a spectrophotometer. In the current study, sampling was required to read the absorbance values from an external UV-Vis measurement device, which may have had an impact on the results.

Overall, the results were successfully replicated and therefore, the external calibration method could confidently be applied to UV/Cl using a similar experimental methodology.

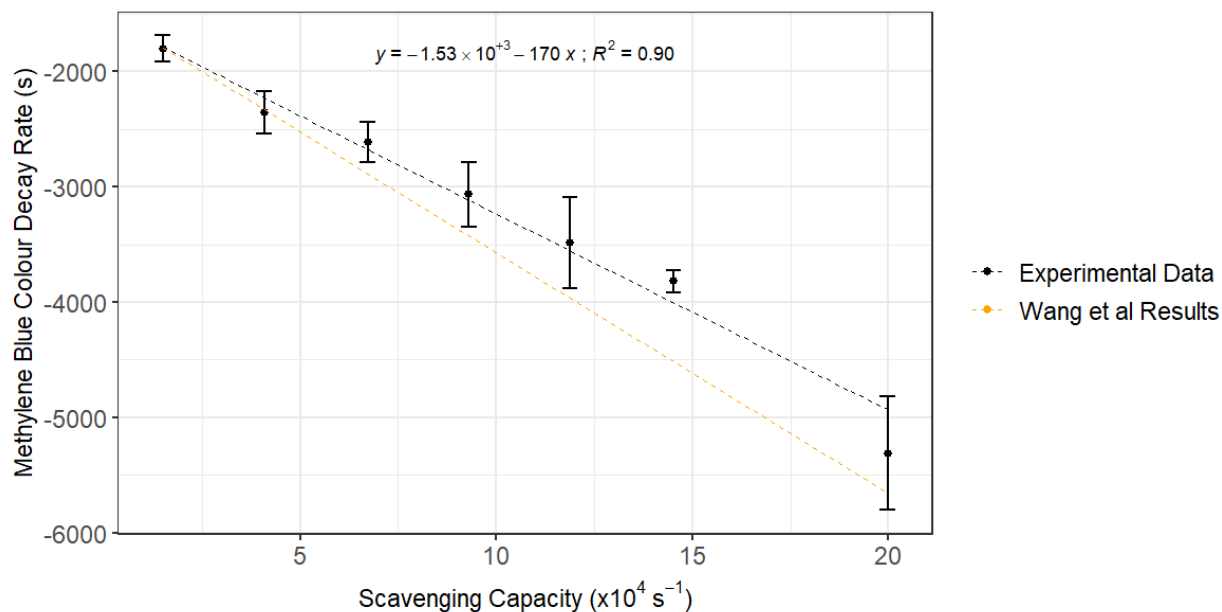


Figure 6: Replicating Wang et al., 2020 results.

4.1.2. Methylene Blue Degradation

Before establishing the external calibration curves for UV/Cl, the impact pH, wavelength, and free chlorine dose have on the removal of the dye used in establishing the external calibration curves, methylene blue, was investigated. UV/Cl is a relatively complex UV AOP and any insight these factors can have on the degradation of contaminants is valuable. Additionally, it is necessary to understand the impact these factors have on the degradation of methylene blue to fully comprehend the impact they can have on applying the external calibration method to UV/Cl.

Theoretically suboptimal conditions are presented to provide empirical evidence of the impact these conditions may have on the degradation of contaminants. The theoretically optimal and suboptimal conditions are based off the results of Yin et al., 2018 where it was determined that the yield of highly oxidative radicals ($\cdot\text{OH}$) in the photolysis of free chlorine is greatest at acidic pH with shorter wavelengths. Conversely, in neutral to basic pH, longer wavelengths were determined to yield more radical species (reactive chlorine species), hence have better and more efficient degradation of contaminants. This is because of the different molar absorption coefficients of OCl^- and HOCl at different wavelengths across the UV emission spectra which are illustrated in Figure 2. The presence of OCl^- vs

HOCl across all pH is illustrated in Figure S. 4. More details of the effect of wavelength and pH have on radical generation is presented in Chapter 2.4. The expected primary radicals at acidic and neutral pH in UV/Cl are illustrated in Figure 7 below. At acidic pH more ·OH are present while at neutral pH more reactive chlorine species are present.

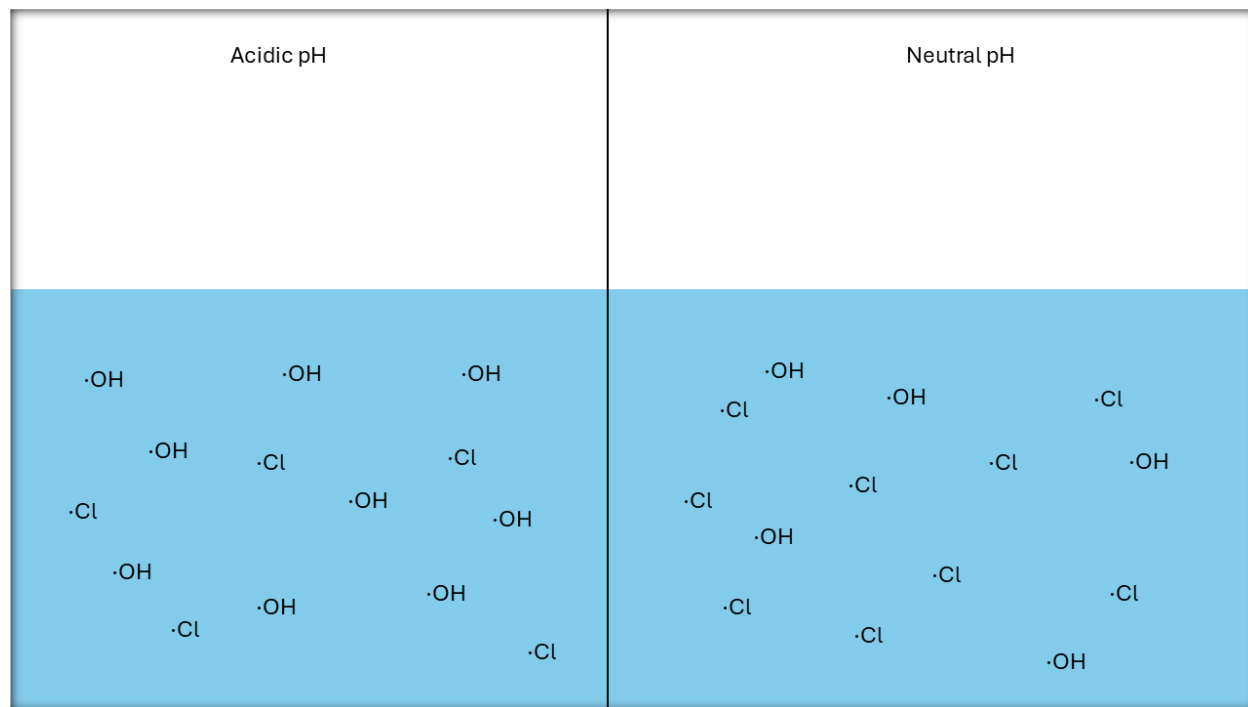


Figure 7: Expected primary radicals in UV/Cl at acidic and neutral pH.

Figure 8 illustrates the degradation of methylene blue vs time at a free chlorine dose of 5 mg L⁻¹. The red data points are the theoretically optimal conditions while the blue data points are the theoretically suboptimal conditions.

It is important to note that the duration of the degradation of methylene blue for the 280 nm was shorter than the duration for the degradation of methylene blue at the 255 nm wavelength. This is because at each wavelength the degradation of methylene blue was subjected to a UV dose of 500 mJ cm⁻² and 1000 mJ cm⁻² and the 280 nm had a greater intensity (shorter time to achieve the same UV dose).

Table 11 reports the statistical significance of pH and wavelength of the data and experimental conditions presented in Figure 9. Based on the two-way analysis of covariance (ANCOVA) results, only wavelength had a statistically significant difference in the removal of methylene blue ($p_{\text{wavelength}} = 0.0001$)

while pH was interestingly not significantly statistically different ($p_{\text{pH}} = 0.51$). This suggests that pH did not impact the efficiency of degradation of methylene blue at these experimental conditions.

Based on the results of Figure 8, the most effective wavelength was 255 nm. As mentioned, the theoretical optimal condition is the condition is the 255 nm wavelength coupled with a pH of 5 due to the photolysis of HOCl producing $\cdot\text{OH}$ (Yin et al., 2018). However, based on these results pH 5 and pH 7 had very similar degradation of methylene blue. At pH 7 you would expect more reactive chlorine present because of the existence of OCl^- . This suggests that reactive chlorine species contribute heavily to the degradation of methylene blue. These results are similar to the results seen in Hoang et al., 2022.

A similar analysis was conducted at a free chlorine dose of 5 mg L^{-1} with a TBA dose of $460 \text{ }\mu\text{M}$ to measure the impact adding scavenging capacity has on the degradation of methylene blue. The results of the analysis are illustrated in Figure 9 below and the ANCOVA statistical significance test is reported in Table 12. Expectantly, there is a reduced efficiency in the degradation of methylene blue at all experimental conditions relative to when no scavenging capacity is added. However, the overall trends seen when there is no added TBA are seen when TBA is added as only wavelength had a statistically significant impact on the degradation of methylene blue. Additionally, the wavelength 255 nm had the best removal of methylene blue for the same UV dose at both pH when no TBA was added (no added RSC). Again, pH had no impact on the efficiency of methylene blue log reduction probably due to the effective contribution of reactive chlorine species to the degradation of methylene blue.

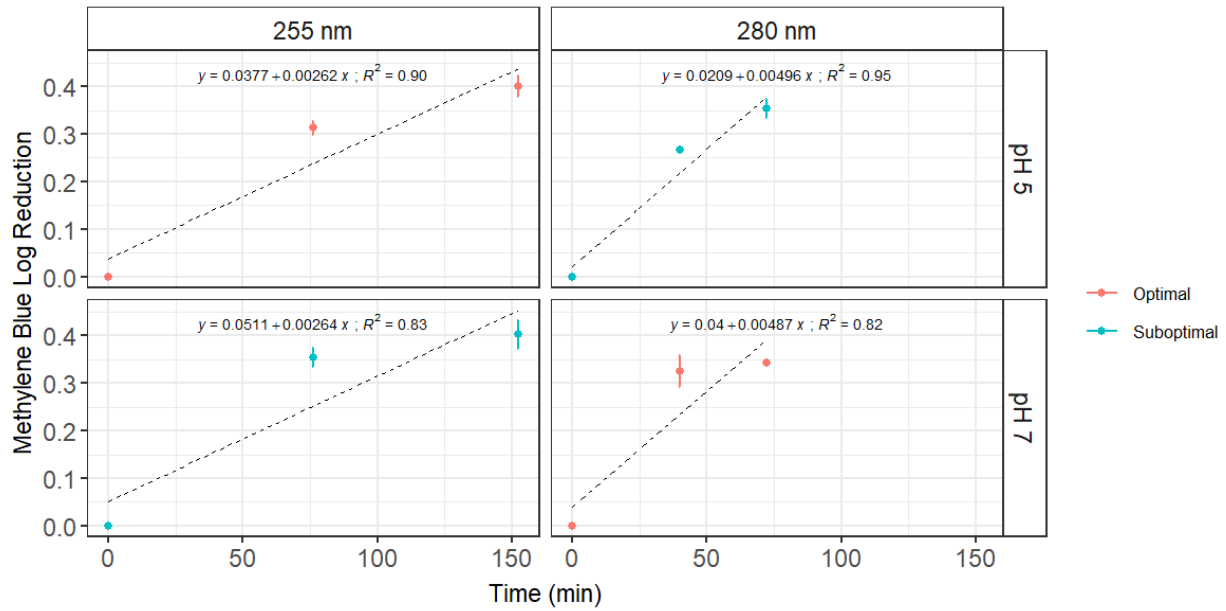


Figure 8: MB log reduction with UV/CI with a free chlorine dose of 5 mg L⁻¹.

Table 11: Statistical significance of wavelength and pH on the degradation of methylene blue at a free chlorine dose of 5 mg L⁻¹.

	F-Value	P-Value	Generalized ETA Squared	Significant?
Wavelength	12.94	0.001	0.32	Yes
pH	0.45	0.51	0.016	No

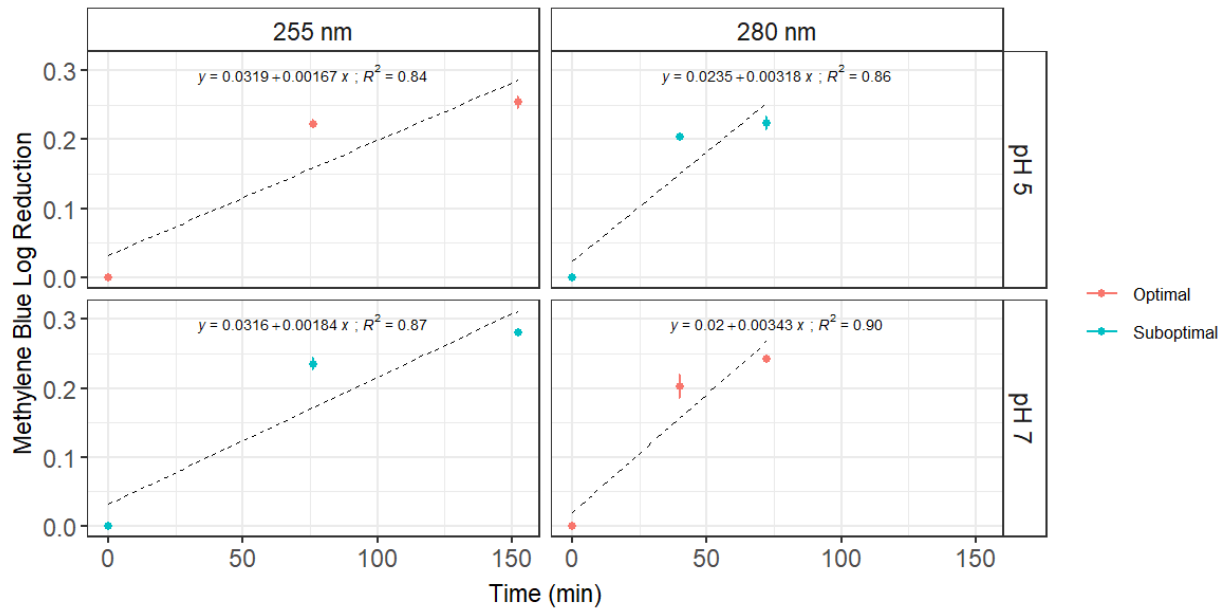


Figure 9: MB log reduction with UV/CI with a free chlorine dose of 5 mg L⁻¹ and a TBA concentration of 460 μM.

Table 12: Statistical significance of wavelength and pH on the degradation of methylene blue at a free chlorine dose of 5 mg L⁻¹ and a TBA dose of 460 μM.

	F-Value	P-Value	Generalized ETA Squared	Significant?
Wavelength	15	<0.001	0.51	Yes
pH	0.62	0.32	0.05	No

The analysis of methylene log reduction was continued for a free chlorine dose of 7 mg L⁻¹ to investigate the impact a change of oxidant dose may have on the results. Figure 10 illustrates the results of the methylene blue degradation and Table 13 reports the results of the ANCOVA statistical significance test. Interestingly, at a free chlorine dose of 7 mg L⁻¹ both the wavelength and pH have a statistically impact on the degradation of methylene blue. This highlights the complexity of UV/Cl as the addition of more oxidant changes the measured impact pH and wavelength have on the efficiency of degradation. A hypothesis for this occurring is that there is more free chlorine available increasing the impact of the radical yield differences of the various chlorine species at the investigated pH values. Another interesting finding is that pH 7 had more efficient degradation of methylene blue than pH 5. It is often assumed that acidic pH is more effective than neutral pH when utilizing UV/Cl to degrade contaminants in water because of the increase yields of ·OH and the relatively lower scavenging capacity of HOCl vs OCl⁻ (Yin et al., 2018; Fang et al., 2014). However, based on the results presented, pH 7 may be more effective for methylene blue specifically, most likely due to its high reactivity towards reactive chlorine species. The most effective combination was pH 7 coupled with a wavelength of 255 nm. Hoang et al., 2022 found similar results where pH 7 had the most effective degradation of methylene blue.

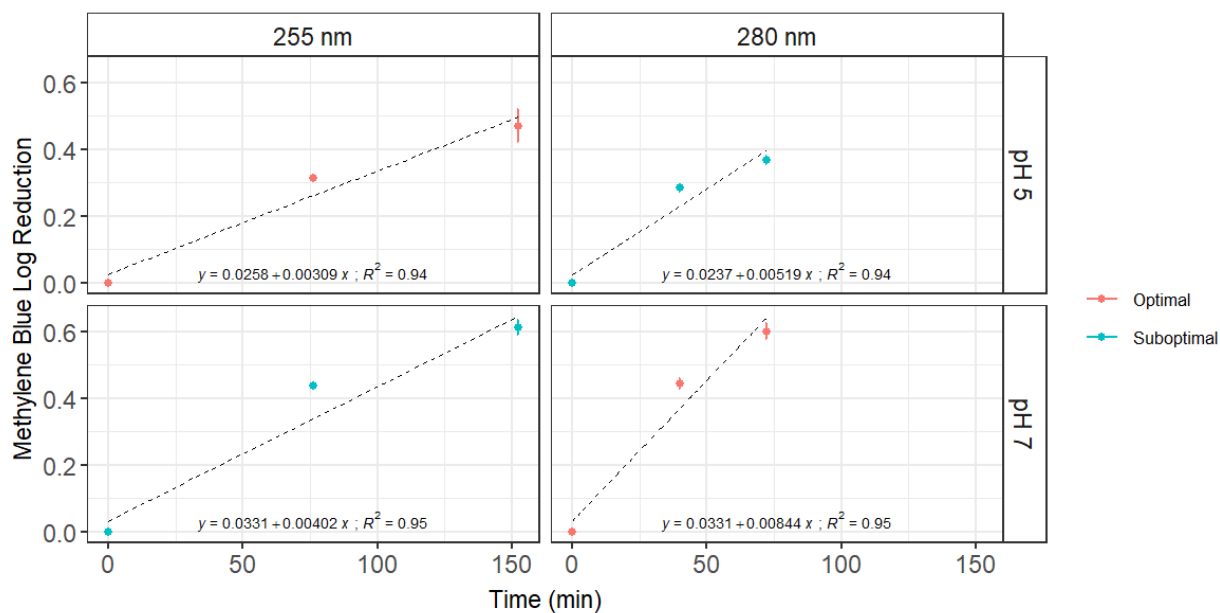


Figure 10: MB log reduction with UV/Cl with a free chlorine dose of 7 mg L⁻¹.

Table 13: Statistical significance of wavelength and pH on the degradation of methylene blue at a free chlorine dose of 7 mg L⁻¹.

	F-Value	P-Value	Generalized ETA Squared	Significant?
Wavelength	47	< 0.001	0.64	Yes
pH	29.68	< 0.001	0.52	Yes

Again, the effect that an increase of scavenging capacity was investigated on the degradation of methylene blue with the results of the degradation presented in Figure 11 and the results of the ANCOVA statistical test reported in Table 14. Like the results of the 5 mg L⁻¹ degradation, similar trends are seen with the addition of TBA. The overall efficiency of the degradation of methylene blue is reduced, as expected, however the same trends of efficiency in relation to the wavelength and pH are consistent with the results when no TBA is added. This suggests that the addition of scavenging capacity from the standard solution has no measurable impact on the optimal conditions of UV/Cl.

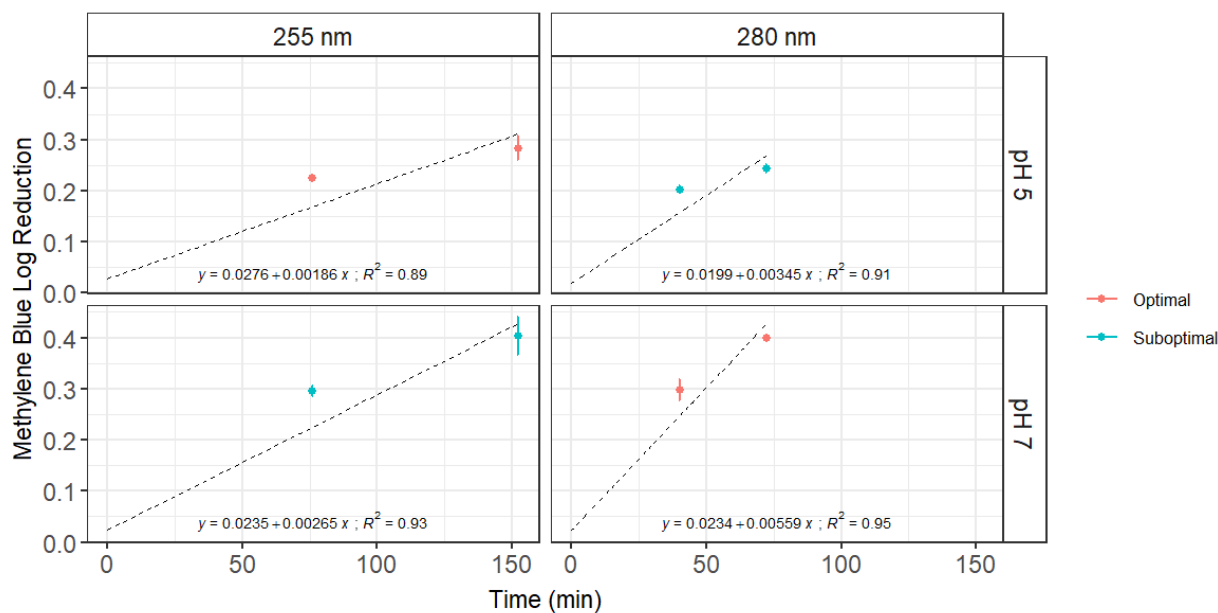


Figure 11: MB log reduction with UV/Cl with a free chlorine dose of 7 mg L⁻¹ and a TBA concentration of 460 μM.

Table 14: Statistical significance of wavelength and pH on the degradation of methylene blue at a free chlorine dose of 7 mg L⁻¹ and a TBA concentration of 460 μM.

	F-Value	P-Value	Generalized ETA Squared	Significant?
Wavelength	47	< 0.001	0.64	Yes
pH	29.68	< 0.001	0.52	Yes

The results of the ANCOVA statistical test on the effect of free chlorine dose on the degradation of methylene blue is reported in Table 15 below. As expected, at both with and without added TBA scenarios, there is a statistically significant impact of free chlorine on the degradation of methylene blue. The greater the free chlorine dose, the more available to photolyze to radical species, increasing the effectiveness of removal.

Table 15: Statistical significance of free chlorine dose on the degradation of methylene blue with and without added scavenging capacity.

	F-Value	P-Value	Generalized ETA Squared	Significant?
Without Scavenger	5.8	0.019	0.08	Yes
With Scavenger	4.6	0.036	0.06	Yes

It is important to note that free chlorine contributes to the degradation of methylene blue in addition to $\cdot\text{OH}$ and reactive chlorine species. The contribution of free chlorine alone to the degradation of methylene blue are illustrated in Figure 12 with the results of the statistical ANCOVA test reported in Table 16. Based on results of the ANCOVA statistical test, neither pH nor free chlorine dose have a statistically significant impact on the degradation of methylene blue with only free chlorine. This suggests that the same contribution of degradation of methylene blue at all pH and free chlorine doses. Therefore, the impact free chlorine has on the results presented in the UV/Cl methylene degradation results are negligible, as at all experimental conditions the same level of degradation from free chlorine occurred. Hoang et al., 2022 demonstrated similar results where pH had little to no impact on the degradation of methylene blue with free chlorine alone.

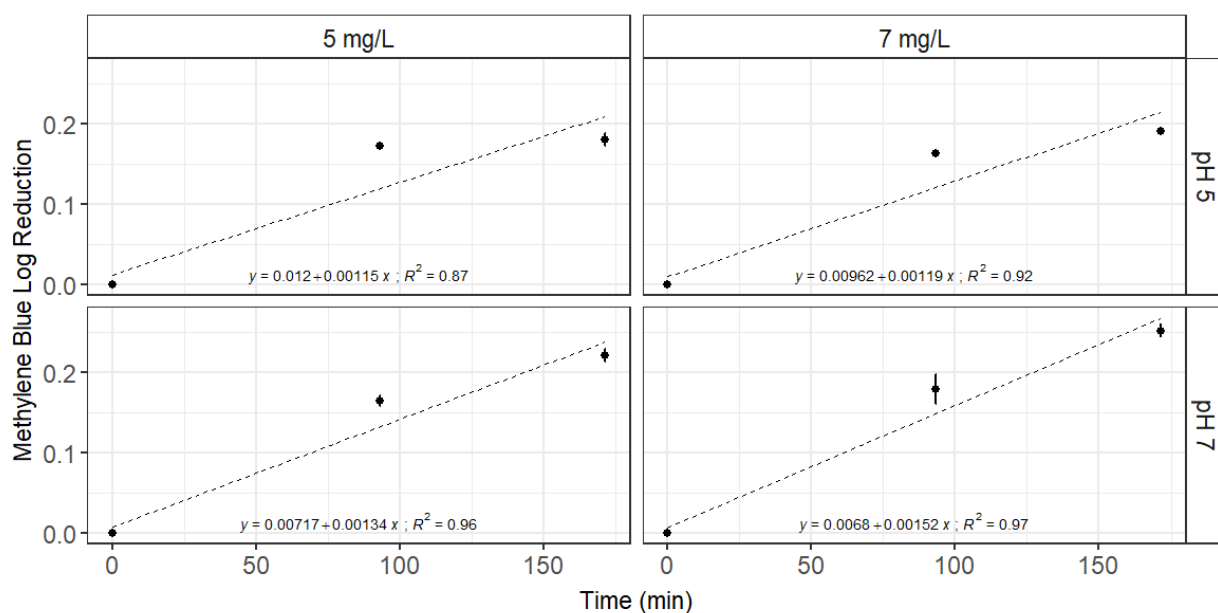


Figure 12: Degradation of methylene blue with only free chlorine (no UV light/dark experiments).

Table 16: Statistical significance of free chlorine dose and pH on the degradation of methylene blue with free chlorine only (no UV light/dark experiments).

	F-Value	P-Value	Generalized ETA Squared	Significant?
HOCl	0.65	0.08	0.01	No
pH	3.2	0.4	0.06	No

The results of the degradation of methylene blue presented above were done spiking deionized water with free chlorine, methylene blue, TBA and acetic acid and are therefore not representative of real

water matrices. To investigate the impact of utilizing real water matrices on methylene blue degradation with UV/Cl, a two-way ANOVA analysis was conducted to analyze statistical significance of wavelength and pH on methylene blue log reduction using treated and raw real water matrices. The real water matrices were collected from a surface water drinking water source in southern Ontario. Previous analyses were conducted on standard solutions which do not necessarily represent the complexity of real water matrices. UV/Cl is a relatively chemically complex AOP and therefore it is valuable to assess the impact wavelength and pH have on contaminant degradation in real water matrices.

Figure 13 below illustrates the mean methylene blue log reduction in treated and raw water samples at pH 5 and 7 utilizing a wavelength of 255 nm and 280 nm and Figure 14 shows the results of the two-way ANOVA tests. The raw water results saw no statistical difference between all experimental conditions investigated. This highlights the importance of retrofitting a UV AOP at the end of the treatment train as the raw water has high scavenging capacity and significantly hindered the efficiency of methylene blue degradation.

In the treated water, both wavelength and pH are statistically significant in the degradation of methylene blue ($p_{\text{wavelength}} = 0.05$, $p_{\text{pH}} < 0.001$). Like the results with the standard solutions with free chlorine dose of 7 mg L^{-1} , pH 7 had the most degradation of methylene blue at both wavelengths in treated water. This again can be attributed to the high reactivity of reactive chlorine species towards methylene blue.

Interestingly, the pH 5 treated water do not produce significantly higher log reduction compared to the raw untreated water. To be consistent throughout the experiments acetic acid was used to depress the pH of the real water samples. However, acetic acid is a weak acid and due to the higher buffer capacity of real water samples compared to standard solutions made with deionized water, a considerably higher concentration of acetic acid was required to depress the pH to 5. The pH of 5 experimental conditions had scavenging capacities were $38\,145 \times 10^4 \text{ s}^{-1}$ larger scavenging capacity than pH 7, due to the added acetic acid. Therefore, it is not entirely a 1:1 comparison. The results do show however, that if the target contaminant is reactive towards reactive chlorine species, then pH adjustment may not necessarily be required.

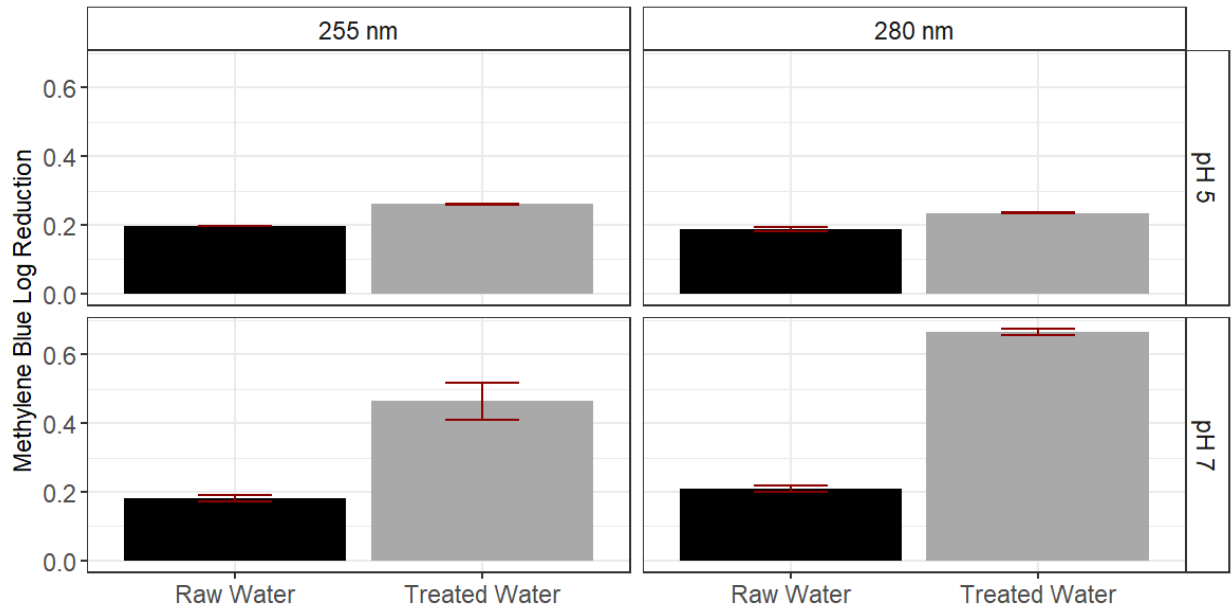
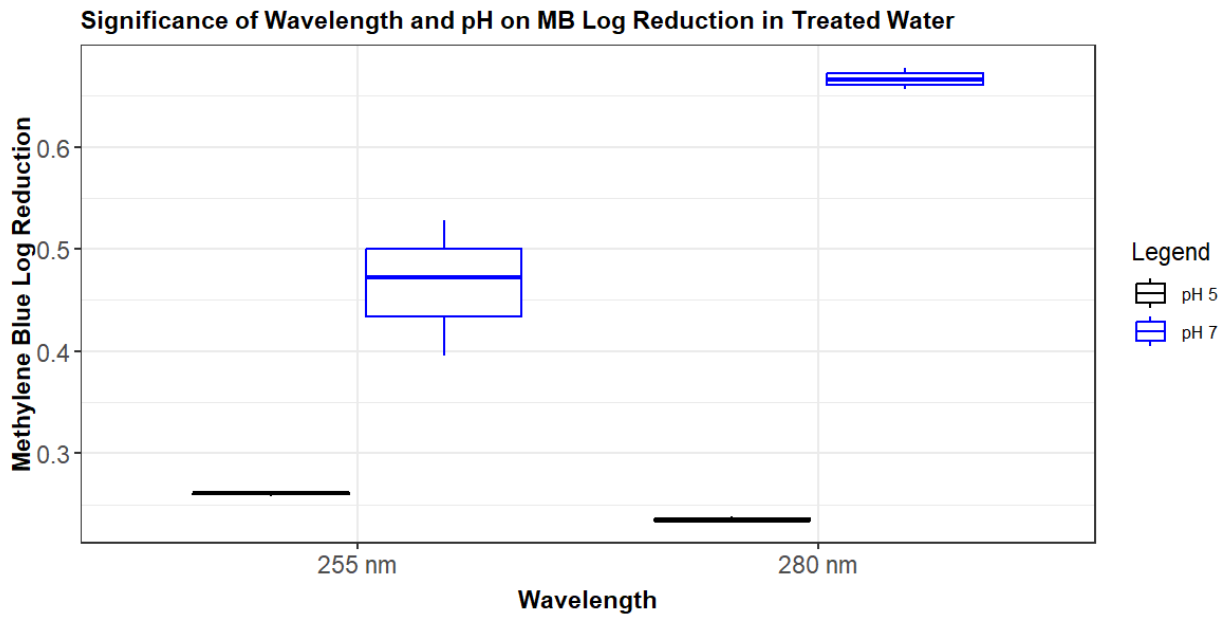
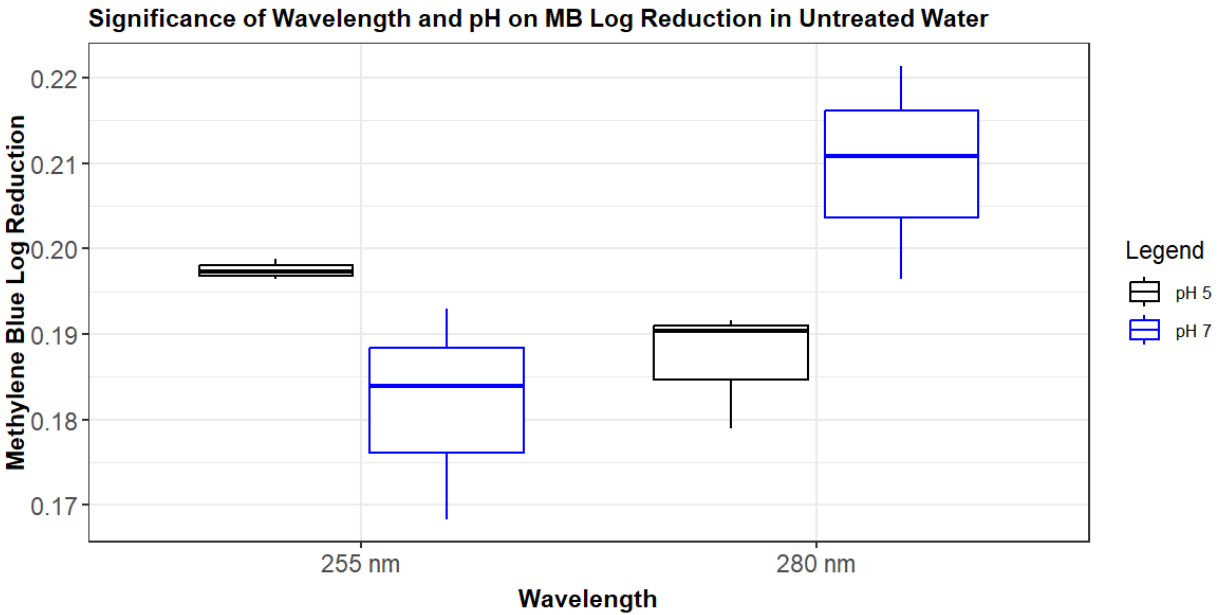


Figure 13: Methylene blue log reduction in real water matrices (free chlorine dose of 7 mg L⁻¹ and UV dose of 500 mJ cm⁻²)



	Sum of Squares	of	Mean of Squares	F-Value	P-Value	Significant?
Wavelength	0.02		0.02	4.44	0.05	Yes
pH	0.3		0.3	57	<0.001	Yes

Figure 14: Statistical significance of wavelength and pH on methylene blue log reduction in treated water (free chlorine dose of 7 mg L⁻¹ and UV dose of 500 mJ cm⁻²)



	Sum of Squares	Mean of Squares	F-Value	P-Value	Significant?
Wavelength	2.24×10^{-4}	2.24×10^{-4}	1.1	0.32	No
pH	3.52×10^{-5}	3.52×10^{-5}	0.17	0.69	No

4.1.3. Summarizing Log Reduction Results

To summarize the results presented in Chapter 4.1.2 both pH and wavelength are statistically significant parameters when degrading methylene blue in the UV/CI. This suggests that when applying the external calibration method to UV/CI wavelength and pH could have a significant impact as they can impact the efficiency of degradation of methylene blue and will therefore likely impact the colour decay rates of methylene blue.

It is commonly assumed that UV/CI should be used at acidic pH to increase yields of radical species and limit radical scavenging of OCl⁻. However, due to methylene blue's high reactivity towards reactive chlorine species if methylene blue was a target contaminant, pH adjustment may not be necessary. This could be true for other contaminants that show high reactivity towards reactive chlorine species and potentially save the utility a significant amount of money when considering retrofitting a UV AOP. For the case of methylene blue (a contaminant that has high reactivity towards reactive chlorine species), based on the log reduction results, a pH of 7 coupled with a wavelength of 255 nm or 280 nm would provide the most efficient removal. However, these are the results of bench scale analysis and may or may not translate to the pilot or full-scale.

Additionally, the results of the degradation experiments show how complex UV/Cl can be in the degradation of methylene. Since UV/Cl can oxidize methylene blue through free chlorine oxidation, reactive chlorine species oxidation, and hydroxyl radical oxidation, this greatly complicates the methylene blue degradation kinematics as seen from the results presented in Chapter 4.1.2. This could impact the practicability of applying the external calibration method specific to UV/Cl with the same accuracy as UV/H₂O₂ because only hydroxyl radicals are solely responsible for the degradation of methylene blue in UV/H₂O₂ oxidation (Wang et al., 2020).

4.1.4. UV/Cl External Calibration Curves

Based on the log reduction results presented in Chapter 4.1.2, it is expected that pH and wavelength will impact how the external calibration method can be applied to UV/Cl. The hypothesis of this analysis is that if there is a statistically significant difference in the regression curves at the different pH and wavelengths tested, separate calibration curves should be established at these conditions to predict the radical scavenging capacity of real water matrices. This is because for the same determined colour decay rate of the sample the curve would predict different radical scavenging capacities for the exact same water matrix. To test this hypothesis, the external calibration curves developed at the different experimental conditions were used to determine the radical scavenging capacity (RSC) of real water matrices from the same source water, comparing the results.

The external calibration method uses the reduction in colour decay rate with the increase in radical scavenging capacity in the standard solutions to create a calibration curve. The color decay rate is a measure of how quickly the dye (methylene blue) is removed in treatment. It does not consider the concentration of the dye as it is calculated using the reduction in absorbance values. If the concentration of the dye were to be considered it can introduce error as the concentration of the dye may not necessarily be directly equal to the absorbance as methylene blue byproducts may be present. That may introduce noise in the absorbance reading which introduces error in the calibration curve between the absorbance and concentration of the dye. Basically, only considering the colour decay and not the concentration decay reduces potential error in the calibration curves (Wang et al., 2020).

UV/Cl is a much more chemically complex UV AOP compared to UV/H₂O₂ (Mackey et al., 2022) because the efficiency in degradation of contaminants is effected by the pH of the water and the wavelength emitted by the UV device (Yin et al., 2018), which is highlighted in the degradation of methylene blue experiments presented in Chapter 4.1.2. Also, the degradation of methylene blue is attributed to free

chlorine, reactive chlorine species, and hydroxyl radicals with UV/Cl (Hoang et al., 2022) whereas in UV/H₂O₂, only hydroxyl radicals contribute. The impact of wavelength and pH was investigated on applying the external calibration method to UV/Cl at a wavelength of 255 nm and 280 nm, and at a pH of 5 and 7.

The results in Figure 15 illustrate the external calibration curves of UV/Cl at a free chlorine dose of 5 mg L⁻¹ and a UV dose of 500 mJ cm⁻². The R² Pearson coefficients had a minimum value of 0.7 across all experimental conditions studied. This means that the external calibration curve can attribute at least 70% of the decrease in colour decay rate to an increase in the radical scavenging capacity. Meaning the external calibration curve created can reasonably be used to predict the radical scavenging capacity.

The 280 nm wavelength had a higher intensity compared to the 255 nm, which is shown in the characterization results presented in Appendix A: UV Characterization Figures. This means that the 280 nm wavelength required less time to achieve a UV dose compared to the 255 nm wavelength. Since the methylene blue log reduction is dependent on time, the 280 nm wavelength results had quicker methylene blue colour decay rates. Additionally, the pH of 5 standards had intrinsically larger radical scavenging capacity values because to depress the pH of the standards acetic acid was added increasing the radical scavenging capacity of the standard solutions, causing the results to be shifted to the right.

Table 17 reports the results of a two-way ANCOVA test that was conducted to measure the impact wavelength and pH have on applying the external calibration method to UV/Cl at the experimental conditions of 5 mg L⁻¹ of free chlorine and a UV dose of 500 mJ cm⁻². Based on the results of the ANCOVA test, both wavelength and pH had a statistically significant impact on the regression curves at all experimental conditions. Meaning each regression curve illustrated is statistically different from each other. If the hypothesis is correct, this suggests that rate at which methylene blue's colour decays from UV/Cl oxidation is dependent on the pH and wavelength of the water matrix at these experimental conditions and separate calibration curves should be created to accurately predict the RSC of the water matrix utilizing the specific pH and wavelength combination. Considering the different radical yields of hydroxyl radicals and reactive chlorine species at the various pH (Yin et al., 2019), this is an expected result however, further validation of the bench scale results at pilot and full-scale is required. Additionally, validation could be done at the bench scale using modified versions of type 1 or type 2 methods (requires LC-MS) for determining RSC presented in Chapter 2.3 and comparing the results of the external calibration curve.

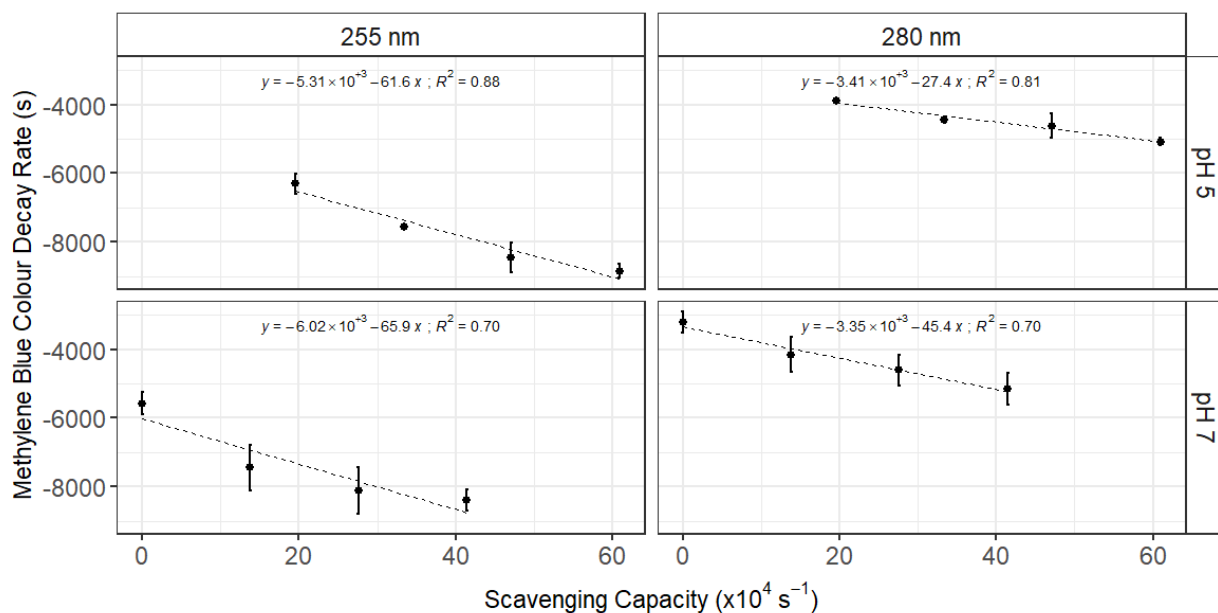


Figure 15: UV/Cl external calibration curves at free chlorine dose of 5 mg L⁻¹ and UV dose of 500 mJ cm⁻².

Table 17: Statistical significance of pH and wavelength on the colour decay rate with experimental conditions 5 mg L⁻¹ free chlorine and 500 mJ cm⁻² UV dose.

	F-Value	P-Value	Generalized ETA Squared	Significant?
Wavelength	497.8	< 0.001	0.93	Yes
pH	15.4	< 0.001	0.28	Yes

Figure 16 presents the results of the calibration curves applied for the experimental conditions of 5 mg L⁻¹ and a UV dose of 1000 mJ cm⁻². From the R² Pearson correlation coefficients the external calibration curves could attribute at least 71% of the decrease in the methylene blue colour decay rates to an increase in radical scavenging capacity of the standard solutions. Meaning the external calibration curves could be reasonably be used to predict the radical scavenging capacity of the standard solutions.

Table 18 shows that, similarly to the results for 5 mg L⁻¹ and 500 mJ cm⁻², both the wavelength and pH is statistically significant when applying the calibration curves at the experimental conditions of 5 mg L⁻¹ and 1000 mJ cm⁻². Again, if the hypothesis is correct, this suggests that the rate at which methylene blue's colour decays from UV/Cl oxidation is dependent on the pH of the water matrix and wavelength of the UV device. Although these are expected results, they still need to be validated. More information on how these results can be validated is presented in Chapter 4.1.7.

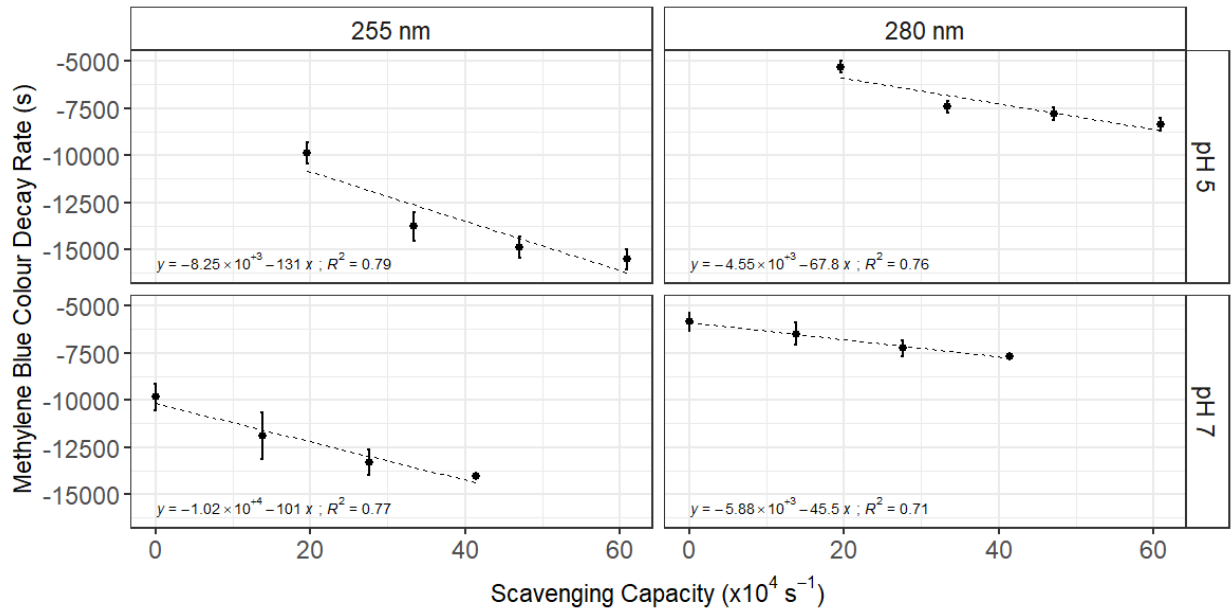


Figure 16: UV/Cl external calibration curves at free chlorine dose of 5 mg L⁻¹ and UV dose of 1000 mJ cm⁻².

Table 18: Statistical significance of pH and wavelength on the colour decay rate with experimental conditions 5 mg L⁻¹ free chlorine and 1000 mJ cm⁻² UV dose.

	F-Value	P-Value	Generalized ETA Squared	Significant?
Wavelength	604.4	< 0.001	0.94	Yes
pH	9.0	0.005	0.52	Yes

The results in Figure 17 illustrate the external calibration curves of UV/Cl at a free chlorine dose of 7 mg L⁻¹ and a UV dose of 500 mJ cm⁻². The R² Pearson coefficients had a minimum value of 0.74 across all experimental conditions studies. This means that the external calibration curve can attribute at least 74% of the decrease in colour decay rate to an increase in the radical scavenging capacity. Again, the external calibration curve created can reasonably be used to predict the radical scavenging capacity at these experimental conditions.

Table 19 reports the results of a two-way ANCOVA statistical test. Like all the results presented, both wavelength and pH had a statistically significant impact on the linear regression curves of the external calibration method at all experimental conditions.

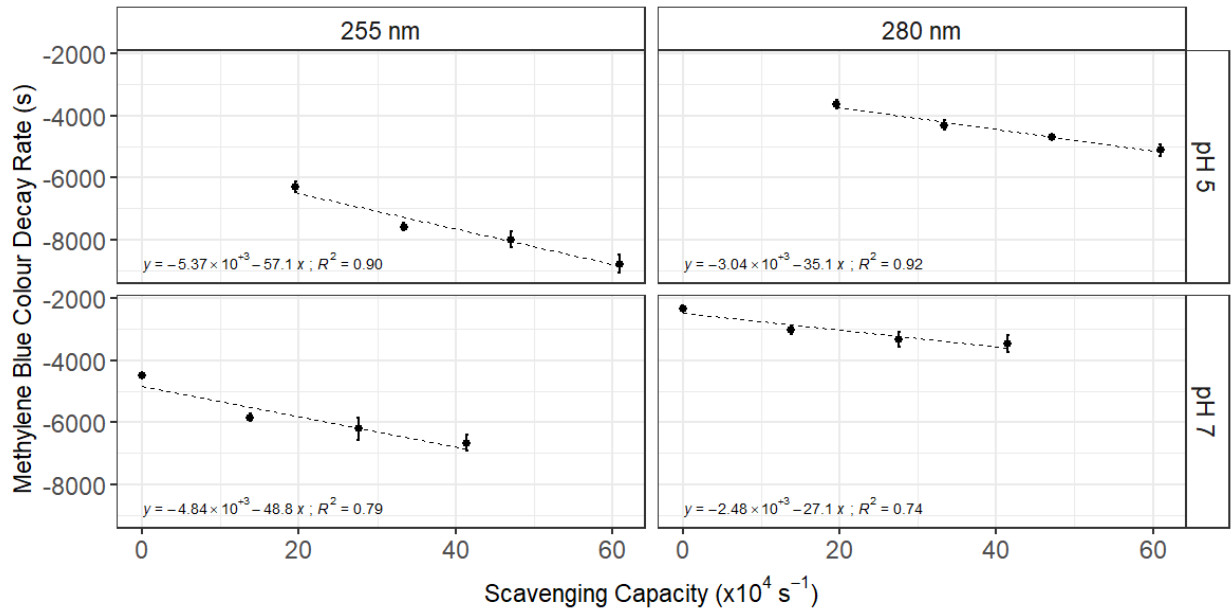


Figure 17: UV/Cl external calibration curves at free chlorine dose of 7 mg L^{-1} and UV dose of 500 mJ cm^{-2} .

Table 19: Statistical significance of pH and wavelength on the colour decay rate with experimental conditions 7 mg L^{-1} free chlorine and 500 mJ cm^{-2} UV dose.

	F-Value	P-Value	Generalized ETA Squared	Significant?
Wavelength	1200.3	< 0.001	0.97	Yes
pH	57.2	<0.001	0.60	Yes

Figure 18 presents the results of the calibration curves applied for the experimental conditions of 7 mg L^{-1} and a UV dose of 1000 mJ cm^{-2} . From the R^2 Pearson correlation coefficients the external calibration curves could attribute at least 73% of the decrease in the methylene blue colour decay rates to an increase in radical scavenging capacity of the standard solutions. Again, the external calibration curve could be reasonably be used to predict the radical scavenging capacity of the standard solutions.

Table 20 shows that, similarly to all results presented at all experimental conditions, pH and wavelength have a statistically significant impact on the linear regression curves of the external calibration method of UV/Cl.

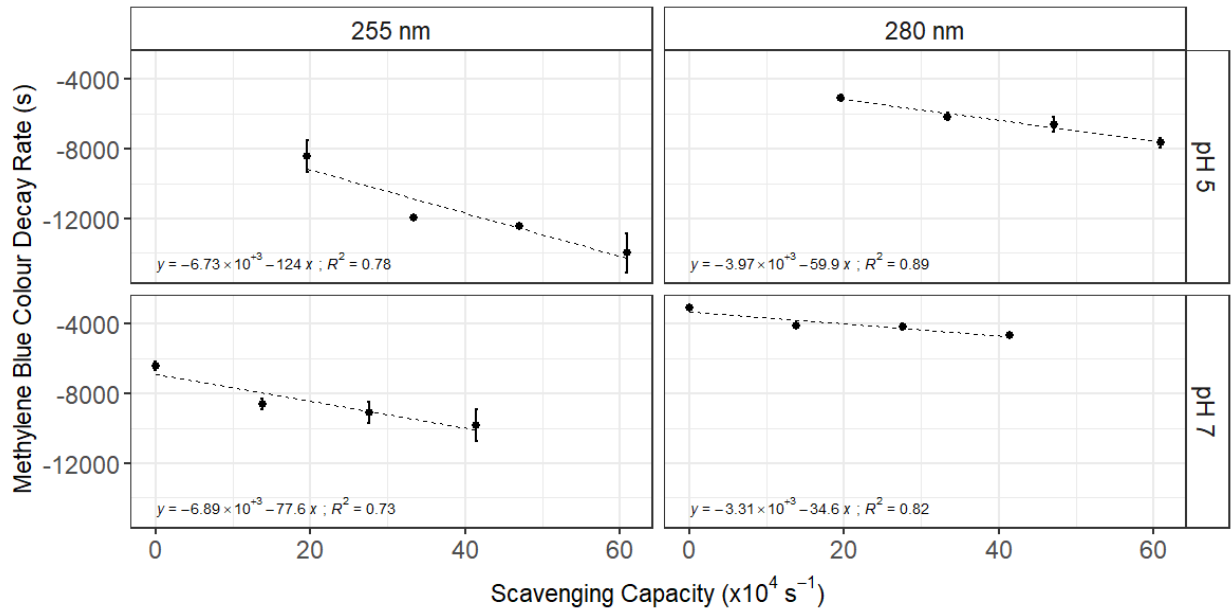


Figure 18: UV/Cl external calibration curves at free chlorine dose of 7 mg L^{-1} and UV dose of 1000 mJ cm^{-2} .

Table 20: Statistical significance of pH and wavelength on the colour decay rate with experimental conditions 7 mg L^{-1} free chlorine and 1000 mJ cm^{-2} UV dose.

	F-Value	P-Value	Generalized ETA Squared	Significant?
Wavelength	561.9	< 0.001	0.93	Yes
pH	30.1	<0.001	0.43	Yes

4.1.5. Comparing Similar Real Water Matrices Radical Scavenging Capacity Values Determined with the External Calibration Method.

This section compares the radical scavenging capacity values (RSC) calculated using the external calibration method of real water matrices. The external calibration method was used to calculate the RSC of raw untreated water and treated water from the same sources at the same time and therefore should have similar a similar water matrix makeup. As mentioned in Chapter 4.1.4, comparing the results of the calculated RSC values of a similar water matrix makeup is the most effective way of measuring the impact that pH and wavelength have on applying the external calibration method to UV/Cl.

The raw water samples were collected from a surface water river source in southern Ontario and the treated water samples were collected from a water treatment plant that utilizes a conventional

treatment train (coagulation, flocculation, sedimentation, filtration, and chlorine disinfection) to treat the raw water from the same river source.

The experimental conditions that were used to investigate the impact wavelength and pH have on the external calibration method were a free chlorine dose of 7 mg L^{-1} and a UV dose of 500 mJ cm^{-2} . To reiterate, the hypothesis is as follows: if there is a statistically significant difference in the colour decay rates, then the predicted RSC values of a similar water matrix will be significantly different.

Figure 19 shows the results of the predicted RSC values of the raw and treated water at each experimental condition. It is important to note that the same molar concentration was added to both the raw and treated water (0.094 mM). However as presented in Appendix D: Residual Free Chlorine Concentration of Treated Water Samples, in the treated water samples there was anywhere between 0.4 mg L^{-1} - 1.1 mg L^{-1} of residual free chlorine and therefore the concentration of free chlorine was greater when determining the colour decay rate of the treated water samples than when calibrating the external calibration curve with the standard solutions and determining the colour decay rate of the raw water samples. This means that the predicted RSC values of the treated water samples are less than what they should be for a dose of 7 mg L^{-1} of free chlorine.

Table 21 shows the summarized values of the average RSC values at the studied experimental conditions of both the raw water and treated water samples. As mentioned above, the treated water samples are smaller than what they should be for a dose of 7 mg L^{-1} due to residual chlorine present in the samples. There is an expected and apparent difference in the average RSC values of the raw water samples compared to the treated water samples. This highlights the importance of retrofitting a UV/AOP at the end of the treatment train due to the much smaller RSC of the water matrix.

Table 21 also summarizes the statistical significance of wavelength and pH on the determined RSC value of the water matrix. Based on the two-way ANOVA test, wavelength had a statistically significant impact on the RSC values of both the raw and treated water samples, while pH only had a statistically significant impact on the treated water samples. Since UV AOP treatment would be implemented at the end of the treatment train therefore would more likely be subjecting treatment to water matrices like the treated water samples, it is more effective to consider the results of the treated water samples. In the treated water samples, the results of the ANOVA tests confirm the hypothesis that the statistical significance difference of the colour decay rates will cause statistically significant determined RSC values for a similar water matrix makeup. Therefore, the targeted pH of the water matrix and selected wavelength of the UV

device will impact how the external calibration method can be applied to UV/Cl and therefore independent and reactor specific external calibration curves should be developed to accurately determine the RSC value.

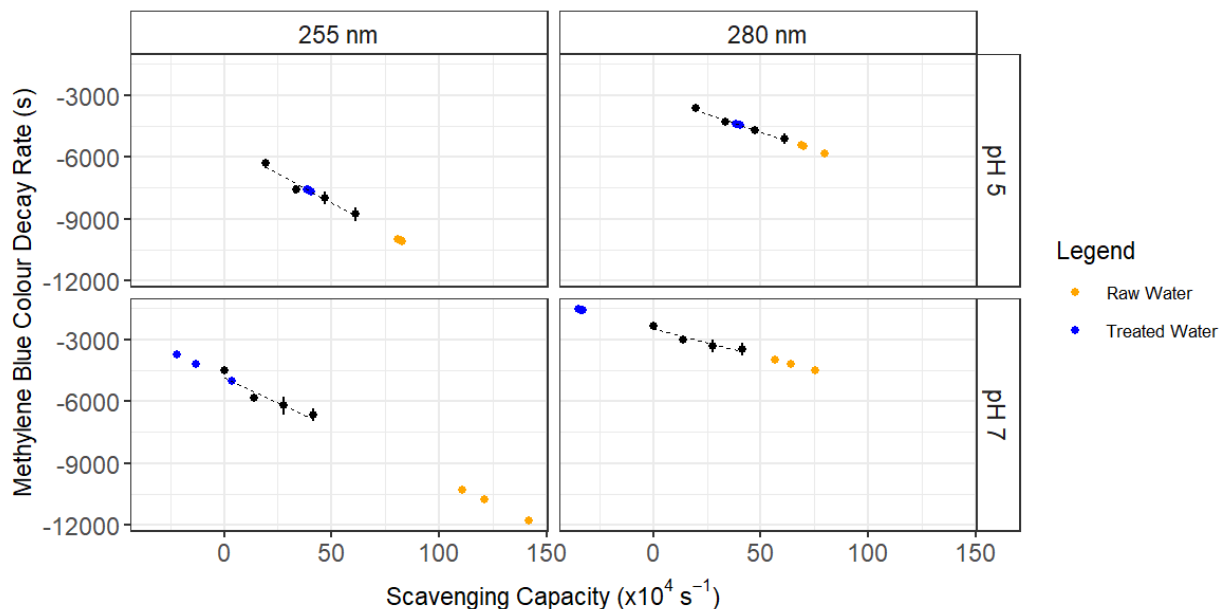


Figure 19: UV/Cl external calibration curves at free chlorine dose of 7 mg L^{-1} and UV dose of 500 mJ cm^{-2} with results of radical scavenging capacities of real water samples from a source water source in Southern Ontario. The black points are the external calibration curve for the mentioned chlorine and UV dose presented in Figure 17.

Table 21: Summarizing the average determined radical scavenging capacity (RSC) values of a similar water matrix to compare external calibration curves at the studied experimental conditions. Highlighted values indicate a negative RSC value which is a result of residual chlorine being present in the treated water. The concentration of free chlorine was greater than 7 mg L^{-1} in the treated water samples which was the free chlorine dose used to develop the external calibration curves. Statistical significance of pH and Wavelength on the determined RSC value is also presented in the table. A p-value of 0.05 or less is considered statistically significant.

pH	Wavelength (nm)	Avg Treated Water RSC ($\times 10^4 \text{ s}^{-1}$)	Avg Raw Water RSC ($\times 10^4 \text{ s}^{-1}$)
5	255	39	82
7	255	-10	124
5	280	40	73
7	280	-3.4	65
<i>Statistical Significance (ANOVA) of pH and Wavelength on Determined RSC Values</i>			
Condition		P-Value	
pH (Raw Water)		0.1	
pH (Treated Water)		0.05*	
Wavelength (Raw Water)		0.007*	
Wavelength (Treated Water)		<0.001*	

* Indicates statistical significance.

4.1.6. Summarizing Results of Applying the External Calibration Method to UV/Cl

Overall, based on the Pearson R^2 coefficients of all the experimental conditions tested, the external calibration method could be reasonably be applied to UV/Cl as the smallest R^2 value was 0.7 (threshold for statistical significance was set to 0.7). Therefore, at least 70% of the decrease in colour decay rate could be attributed to an increase of the radical scavenging capacity of the standard solutions. Since UV/Cl is much more chemically complex than UV/H₂O₂, the external calibration curve is not as effectively applied. This is because free chlorine, reactive chlorine species, and hydroxyl radicals all contribute to the degradation of methylene blue in the UV/Cl AOP (Hoang et al., 2022), while only hydroxyl radicals contribute to the degradation of methylene blue in the UV/H₂O₂ (Wang et al., 2020). Therefore, UV/Cl is not as predictable in the degradation of methylene blue resulting in less reliable external calibration curves.

Additionally, based on the results of the bench scale experiments, wavelength and pH both impact the determined RSC value for a similar water matrix makeup, and reactor specific external calibration curves should be developed to accurately determine the total radical scavenging capacity in a UV/Cl reactor. This complicates the process of validating the results of the external calibration curves developed for UV/Cl as there are more variables that can impact the results of the RSC value compared to UV/H₂O₂.

Furthermore, Table 22, Table 23, Table 24, and Table 25 present the statistical significance of the free chlorine dose (presented as HOCl dose) and UV dose on the colour decay rates of methylene blue. Interestingly both free chlorine dose and UV dose have a statically significant impact on the linear regression curves of the external calibration method. Therefore, based on the results of these bench scale studies, if the external calibration method were to be applied at the full scale to UV/Cl, and used to calculate the RSC to adjust the UV/Cl operating conditions (free chlorine dose, UV dose), the external calibration method would need to be corrected for these operational changes. Basically, once the operating conditions change to optimize for the RSC of the water matrix, the external calibration method would no longer be accurately predicting the RSC. Again, further highlighting the complexity of adapting this method to UV/Cl. Therefore, it may not necessarily be feasible to adapt the external calibration in the same approach that it is for UV/H₂O₂. Future research steps are presented in Chapter 4.1.7 .

Table 22: Statistical significance of free chlorine dose and UV dose on the application of the external calibration method to UV/Cl at pH 7 and a wavelength of 255 nm.

	F-Value	P-Value	Generalized	Significant?
--	---------	---------	-------------	--------------

			ETA Squared	
Free Chlorine	111.2	< 0.001	0.76	Yes
UV Dose	718.4	<0.001	0.98	Yes

Table 23: Statistical significance of free chlorine dose and UV dose on the application of the external calibration method to UV/Cl at pH 5 and a wavelength of 255 nm.

	F-Value	P-Value	Generalized ETA Squared	Significant?
Free Chlorine	4.1	0.05	0.1	Yes
UV Dose	397.5	<0.001	0.95	Yes

Table 24: Statistical significance of free chlorine dose and UV dose on the application of the external calibration method to UV/Cl at pH 7 and a wavelength of 280 nm.

	F-Value	P-Value	Generalized ETA Squared	Significant?
Free Chlorine	268.6	< 0.001	0.88	Yes
UV Dose	656.7	<0.001	0.97	Yes

Table 25: Statistical significance of free chlorine dose and UV dose on the application of the external calibration method to UV/Cl at pH 5 and a wavelength of 280 nm.

	F-Value	P-Value	Generalized ETA Squared	Significant?
Free Chlorine	6.08	0.02	0.14	Yes
UV Dose	721.6	<0.001	0.97	Yes

4.1.7. Future Research Steps

Due to the complexity of methylene blue degradation from UV/Cl, the external calibration method is not as effectively applied to UV/Cl compared to UV/H₂O₂. Although, it would be valuable to apply the method specifically to UV/Cl, accounting for both reactive chlorine species and ·OH scavenging, it may be more feasible to utilize the original method developed for UV/H₂O₂ to determine optimum conditions for UV/Cl. Figure 20 demonstrates a simple representation on how this could be done at a pilot or full-scale treatment plant. The treatment train routes a separate line before the UV/Cl reactor to use the external calibration method to determine the ·OH radical scavenging capacity only. Therefore, bench scale experiments should be conducted to measure the impact the variation of ·OH radical scavenging capacity has on the degradation of target contaminants in UV/Cl. This can be conducted by obtaining real water matrices from various sources at different times of the year (ensuring different water matrix makeups

and $\cdot\text{OH}$ radical scavenging capacities) then using the external calibration curve to measure the $\cdot\text{OH}$ radical scavenging capacity of these water matrices. Then, the same water matrices should be spiked with a target contaminant and free chlorine, and then subjected to UV treatment. The degradation of the target contaminant (MC-LR for example) should be tracked and the degradation vs the $\cdot\text{OH}$ radical scavenging capacity should be plotted and analyzed. Different experimental conditions such as pH and wavelength could be adjusted and monitored as well. This same analysis could be conducted with UV/H₂O₂ and compare the results of UV/Cl.

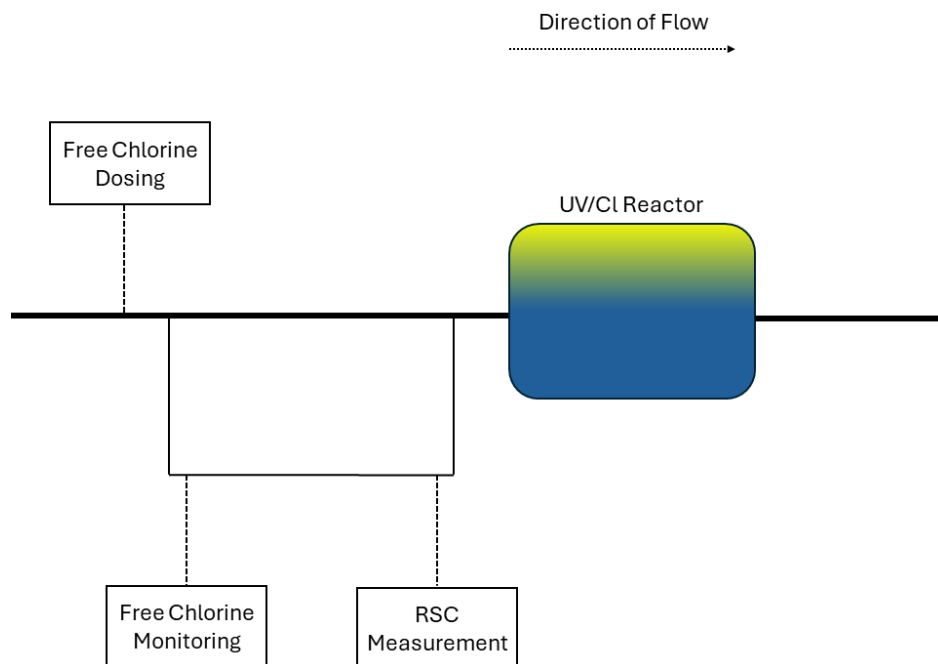


Figure 20: Schematic of how the external calibration method could be utilized to determine real time measurements of the radical scavenging capacity (RSC) to optimize the reactor's operating conditions.

Additionally, bench scale tests of type 1 and type 2 methods of determining the radical scavenging capacity presented in Chapter 2.3 could be modified for UV/Cl and be compared to the calculated radical scavenging capacity values using the external calibration curves of UV/Cl. This can be used to verify and improve the results of this study.

Lastly, nitrogen species, specifically ammonia, can extremely impact the feasibility of UV/Cl implementation at full-scale treatment plants (Mackey et al., 2022). Ammonia quickly reacts with free chlorine to form chloramines (Weil and Morris 1949). The presence of ammonia results in two major issues for UV/Cl. The first issue is that there will be less free chlorine available for photolysis and therefore could reduce the yield of $\cdot\text{OH}$ and reactive chlorine species. The second issue is that

chloramines are heavy radical scavengers, therefore the presence of ammonia reduces the concentration of free chlorine available while simultaneously increasing the radical scavenging capacity of the water matrix. Therefore, it would be valuable to measure the impact that ammonia has on establishing the external calibration curve for UV/Cl. An ammonia solution can be spiked into the standard solutions at various concentrations to specify the impact ammonia can have on the radical scavenging capacity of UV/Cl.

4.2. Objective 2: Modelling Optimum Dosing Requirements to Degrade Contaminants of Concern Based on the Radical Scavenging Capacity of the Water Matrix

The second objective of this research was to model optimum dosing requirements to degrade microcystin-LR (MC-LR) based on the radical scavenging capacity (RSC) of the water matrix so that these doses can be used to develop cost curves in objective three. It is important to note that no laboratory experiments were conducted with MC-LR and was selected for strictly for modelling purposes. UV/AOPs have shown great performance in the degradation of cyanotoxins, and with the potential increase in prevalence of harmful algal blooms resultant of climate change (Vlad et al., 2014), may need to be retrofitted to impacted water utilities to ensure the safety of their effluent water quality.

Since the modelling approach in this research was like the approach taken by Kwon et al., 2019, the results in Kwon et al., 2019 were replicated to ensure the correct methodology was taken to obtain results. This analysis is conducted in Appendix E: Replicating Kwon et al., 2019. The results show the required doses for 1-log reduction of MC-LR with UV/H₂O₂ treatment and are the exact results presented in Kwon et al., 2019. Therefore, it can be concluded that the correct methodology was achieved, and the analysis could be reasonably transferred to other water quality and treatment assumptions.

The required and optimum doses for 2-log reduction of MC-LR with UV/H₂O₂ are presented in Figure 21 below. Two curves were developed to illustrate the impact the RSC has on required and optimum doses for treatment with UV/H₂O₂. The difference in RSC studied is representative of the changes of ·OH demand in Lake Ontario over the course of a year (Mackey et al. 2022) and could be the variation seen in the reactor of full-scale UV AOPs where Lake Ontario is the source water. To clarify, the ·OH demand is the scavenging capacity of the water matrix specific to ·OH. The two curves represent the required doses to achieve 2-log reduction of MC-LR. Basically, at any point of the curve (oxidant dose, UV dose), that combination of oxidant and UV dose will meet the treatment objectives.

Due to the large energy requirements to produce H_2O_2 (Rosenfeldt et al. 2006), optimum doses for treatment with UV/ H_2O_2 tend to have smaller doses of H_2O_2 and larger UV doses as the optimum doses are calculated based on minimum electrical energy dose. This limits capital costs but leads to higher O&M costs which is shown from the results in Chapter 4.3. Based on the results of the analysis, the optimum dose for 2-log reduction of MC-LR using UV/ H_2O_2 with an RSC of $3 \times 10^4 \text{ s}^{-1}$ is a H_2O_2 dose of 2.4 mg L^{-1} and a UV dose of 776 mJ cm^{-2} . While with an RSC of $8 \times 10^4 \text{ s}^{-1}$ the optimum H_2O_2 dose is 1 mg L^{-1} with a UV dose of 1130 mJ cm^{-2} . To reiterate, optimum doses were calculated by minimizing the electrical energy dose (EE/O) and are based on the minimum energy requirements to treat MC-LR to the subjected treatment standards.

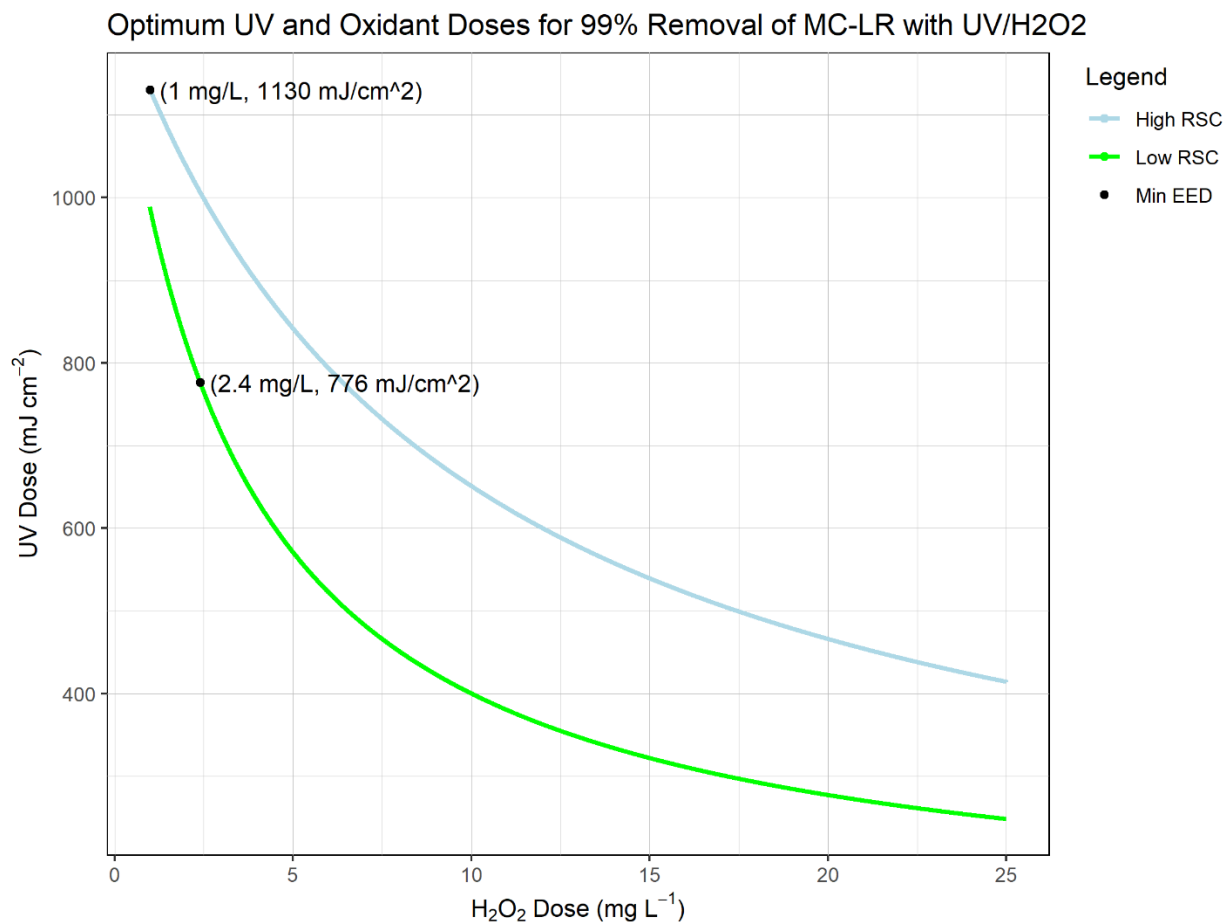


Figure 21: Required and optimum doses for 2-log reduction of MC-LR with UV/ H_2O_2 . Optimum doses are based on minimum energy requirement to treat MC-LR. The high RSC corresponds to a value of 8×10^4 and the low RSC corresponds to a value of $3 \times 10^4 \text{ s}^{-1}$.

The required and optimum doses for 2-log reduction of MC-LR with UV/Cl treatment at neutral pH are presented in Figure 22 below. The same analysis was conducted with UV/Cl as with UV/H₂O₂. The relatively higher RSC's optimum free chlorine dose is 2.4 mg L⁻¹ coupled with a UV dose of 820 mJ cm⁻². While the relatively lower RSC's optimum dose is 1.86 mg L⁻¹ coupled with a UV dose of 772 mJ cm⁻². Interestingly, UV/Cl is not as impacted by the increase of RSC as UV/H₂O₂ as UV/H₂O₂'s optimum oxidant dose changes 140% and its UV dose changes 30% due to the different RSC values, while UV/Cl's optimum oxidant dose only changes 22% and UV dose only 6%. This can be attributed to the reactive chlorine species that are generated in UV/Cl that also contribute to the degradation of MC-LR. In situations where the target contaminant is not susceptible to reactive chlorine species degradation, UV/Cl may see a much larger impact in the variation of RSC. The susceptibility of the target contaminant to reactive chlorine species should be considered when looking to retrofit UV/Cl.

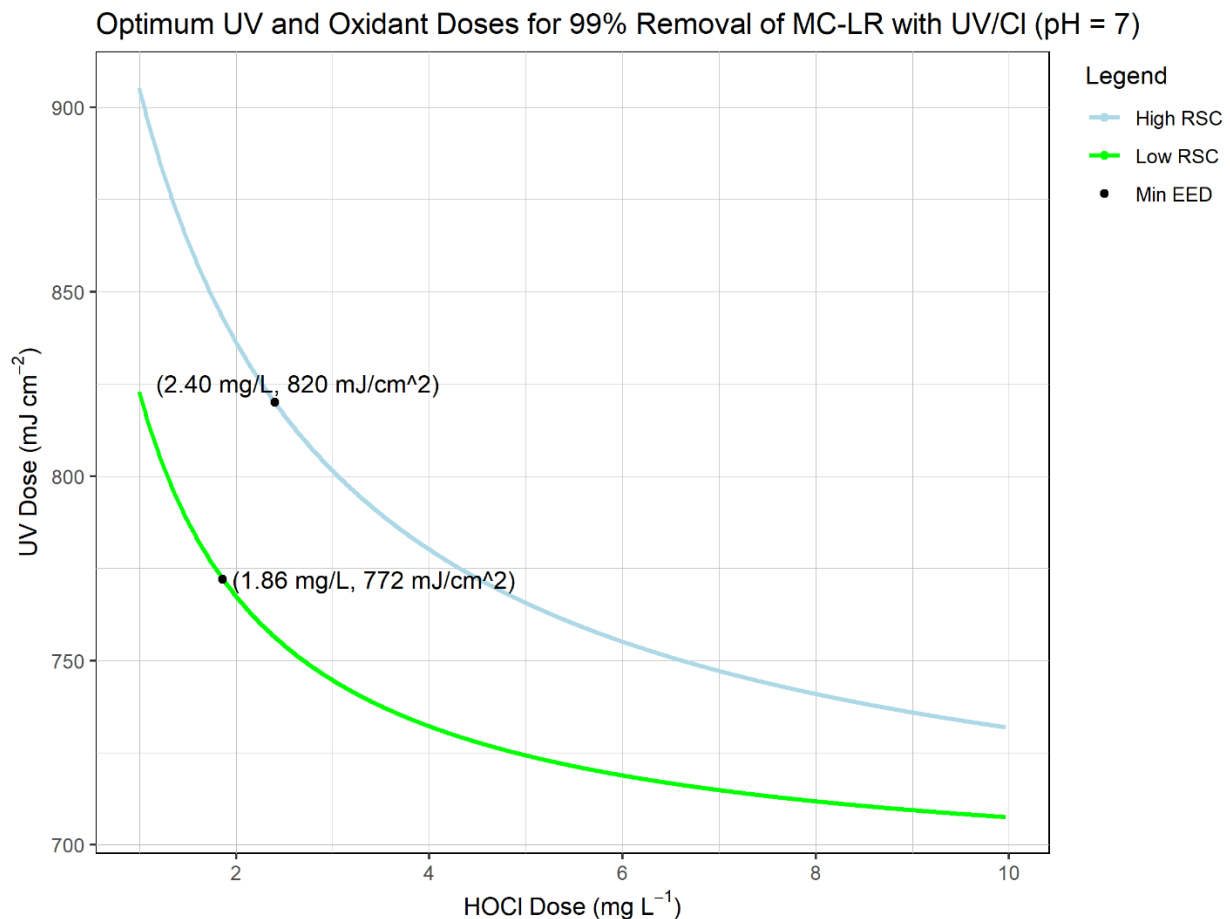


Figure 22: Required and optimum doses for 2-log reduction of MC-LR with UV/Cl at neutral pH. Optimum doses are based on minimum energy requirement to treat MC-LR. The high RSC corresponds to a value of 9.14×10^4 and the low RSC corresponds to a value of $4.14 \times 10^4 \text{ s}^{-1}$.

Figure 23 below presents the required and optimum doses for 2-log reduction of MC-LR with UV/Cl treatment at acidic pH. It is commonly assumed that UV/Cl is more efficient at acidic pH due to higher quantum yield of radicals, and the smaller RSC of HOCl compared to OCl⁻ (Yin et al., 2018; Mackey et al., 2022; Fang et al., 2014). The optimum UV and free chlorine doses for the relatively lower RSC value is 730 mJ cm⁻² and 1.72 mg L⁻¹, respectively. The optimum UV and free chlorine doses for the relatively higher RSC value is 770 mJ cm⁻² and 2.08 mg L⁻¹, respectively. Comparing to the optimum doses determined for UV/Cl at neutral pH, the optimum UV doses and free chlorine doses calculated for acidic pH were about 6% and 10% lower, respectively. These were expected results because of the increase of quantum yield of ·OH and ·Cl in the model inputs.

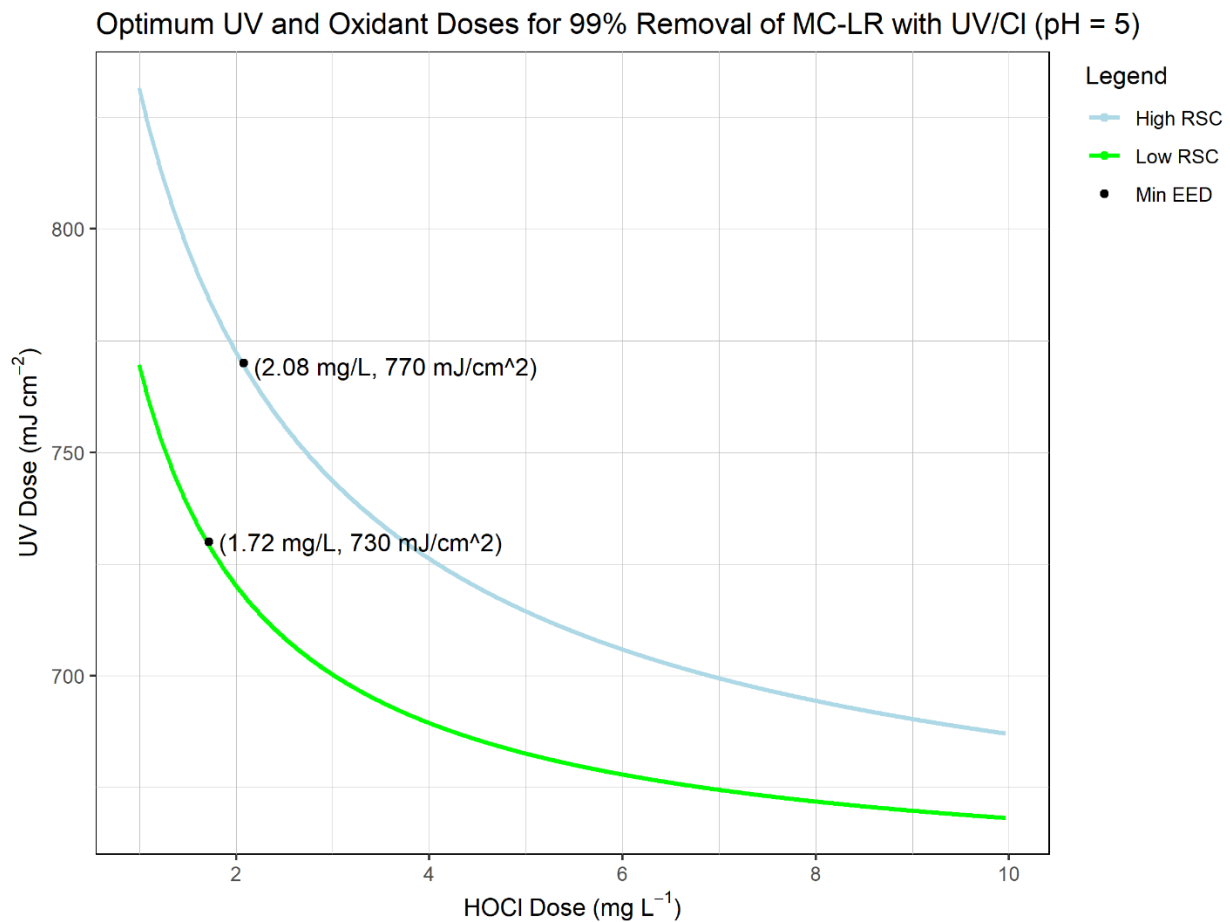


Figure 23: Required and optimum doses for 2-log reduction of MC-LR with UV/Cl at acidic pH. Optimum doses are based on minimum energy requirement to treat MC-LR. The high RSC corresponds to a value of 9.14×10^4 and the low RSC corresponds to a value of $4.14 \times 10^4 \text{ s}^{-1}$.

The optimum doses presented above are used in Chapter 4.3 to develop capital and O&M cost curves. An important caveat to the predicted optimum doses of UV/Cl is that they do not consider the

ammonium concentration in the water matrix which could greatly impact the available free chlorine in the UV/Cl reactor. When developing actual models to predict optimum operating conditions for UV/Cl, the ammonium concentration needs to be analysed as its impact on predicted free chlorine concentration vs the actual free chlorine concentration in the reactor is significant (Mackey et al. 2022). However, ammonium is typically a concern in wastewater treatment and not as much in drinking water treatment which is why it was not considered in the modelling approach.

It is important to note that alternative methods, such as dissolved air flotation and granular activated carbon, have also shown to be effective in the removal of algal blooms and cyanotoxins (Vlad et al., 2014). Adding redundancy into water treatment trains is invaluable to ensure that water utilities can always produce safe and potable water. UV/AOPs can be retrofitted into water treatment plants to increase the resilience of water utilities to climate change and population growth.

4.2.1. Future Research Steps

The next step for this aspect of the research would be to validate the modelling results of the predicted required doses to achieve targeted treatment objectives through bench and pilot scale experiments. The RSC of the treated water would be measured and recorded while MC-LR is spiked and treated with UV/H₂O₂ or UV/Cl. The degradation of MC-LR for a given UV and oxidant dose would be recorded and compared to the results presented by the model. In addition to validation, the bench and pilot scale experiments could be used to improve the model. A preliminary suggestion on how to improve the model based on a literature review would be to incorporate the UVT of the water matrix as it is commonly incorporated as a model input to determine dosing requirements for full-scale implementation of UV/AOPs (Mackey et al., 2022). The recommended variables to record for bench and pilot scale experiments to validate the predicted required doses from the model are listed below:

- Recorded RSC
- Recorded UVT
- UV Dose
- Oxidant Dose
- Initial Concentration of MC-LR
- Final Concentration of MC-LR
- Actual Log-Reduction
- Predicted Log-Reduction

4.3. Objective 3: Conceptualize the Capital and O&M Costs of UV/H₂O₂ and UV/Cl Through the Development of Cost Curves

4.3.1. Capital Costs of UV/H₂O₂

From the analysis conducted in Chapter 4.2, the optimum H₂O₂ and UV doses for the relatively low radical scavenging capacity (RSC) are 2.4 mg L⁻¹ and 776 mJ cm⁻², respectively. For the relatively higher RSC, the optimum H₂O₂ and UV dose are 1 mg L⁻¹ and 1130 mJ cm⁻², respectively. The optimum doses were calculated based upon the treatment objectives and water quality assumptions outlined in the second objective. The water quality and treatment objectives applied to build the cost curves of UV/H₂O₂ are summarized in Table 26 below.

Table 26: Water quality and treatment objectives that were used to build cost curves for UV/H₂O₂.

Assumption	Value
Target Contaminant	MC-LR
Log reduction	2
pH	7
Absorbance of the water matrix	0.02 cm ⁻¹
Radical scavenging capacity of the water matrix	Low RSC: 3 x 10 ⁴ s ⁻¹ ; High RSC: 8 x 10 ⁴ s ⁻¹

Figure 24 below shows the calculated capital costs to meet the treatment objectives using UV/H₂O₂ for a relatively high RSC compared to a relatively low RSC. The dotted red and green lines indicate error bounds of +50% and -30%, respectively, and were included based upon recommendations for conceptual estimates (McGivney, 2008). The cost curves presented in Figure 24 are the cost associated to build a UV/H₂O₂ reactor without any prior infrastructure in place. Therefore, they are not necessarily indicative of a retrofit.

To reiterate, the impact the variation of RSC has on capital costs were investigated to measure the importance of accurately determining the RSC to maximize cost savings. The impact the variation of RSC has on UV/H₂O₂ capital costs are quite substantial. There is as much as a ~30% increase in capital costs to treat MC-LR at a high RSC versus a low RSC. Considering the capital costs for these systems, based on the cost curves presented can cost upwards of \$1 billion CAD for very large treatment plants. The difference in cost can be upwards of \$300 million CAD. This certainly highlights the importance of accurately determining the RSC to minimize costs, especially at very large treatment plants. To give context, a drinking water treatment plant with a design capacity of 1500 MLD is about 1.6x greater than Toronto's largest drinking water treatment plant, R.C Harris (City of Toronto, 2022).

Figure 25 below illustrates the percent contribution of UV equipment versus H₂O₂ storage and dosing at both high and low RSC situations. At both situations, UV equipment heavily dominates the required capital costs to build the UV/H₂O₂ reactor at all design treatment capacities. Therefore, based on these results, it can be concluded that larger required UV doses will induce larger capital costs for UV/H₂O₂.

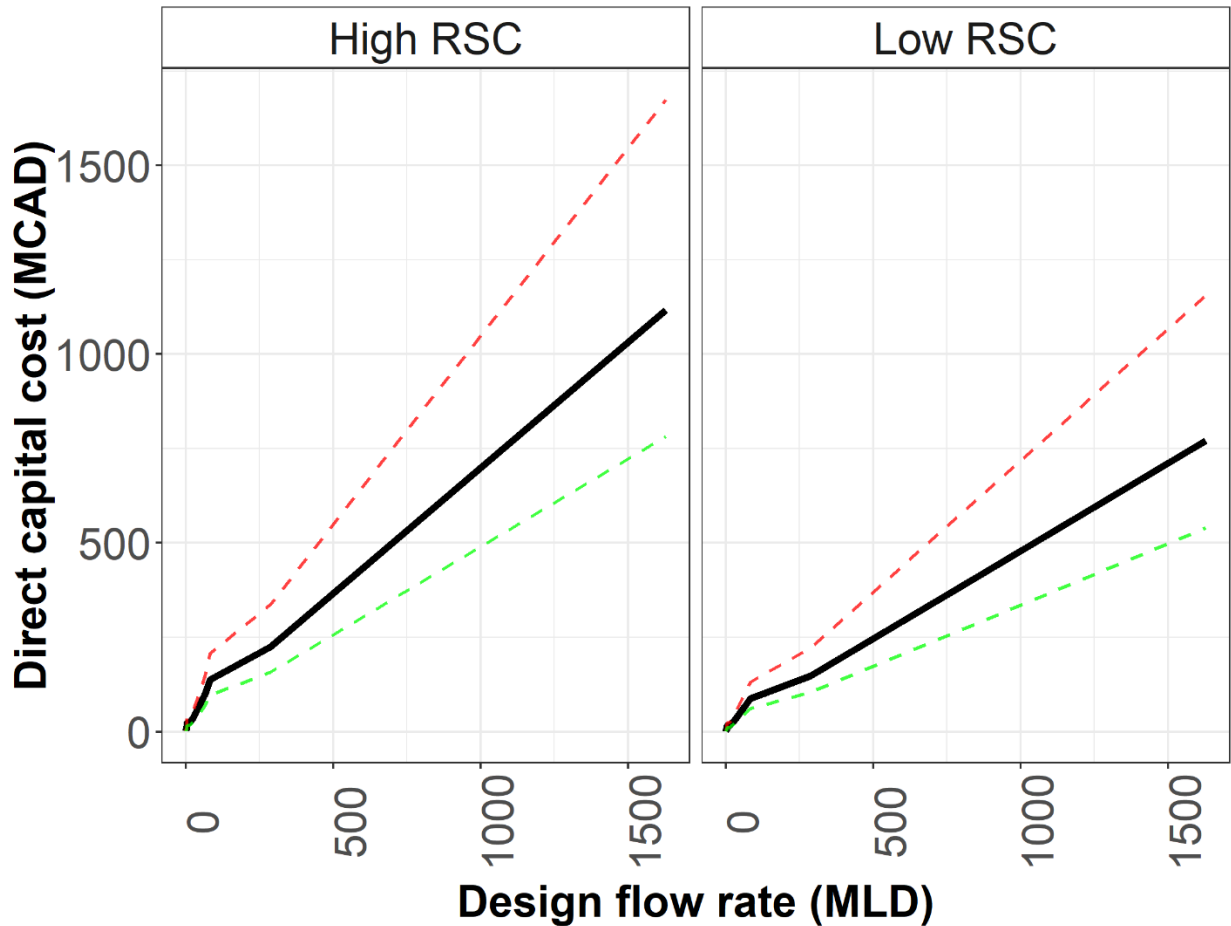


Figure 24: Capital cost curves for UV/H₂O₂ to achieve 2-log reduction of MC-LR. The dotted red and green lines indicate error bounds of +50% and -30%, respectively.

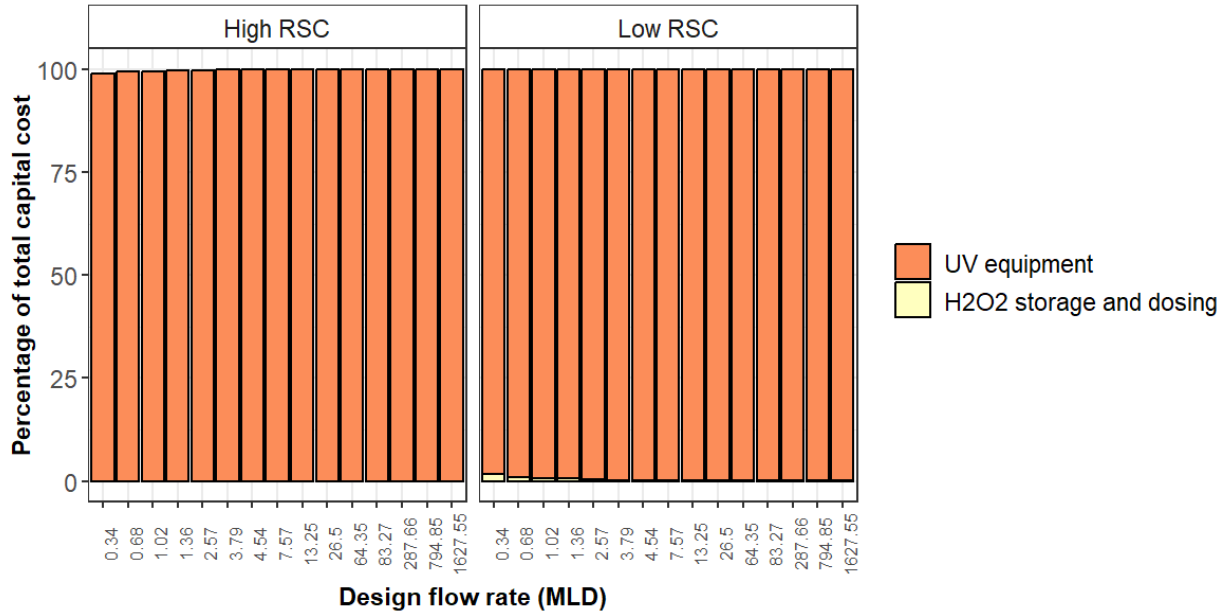


Figure 25: Percent contribution of UV equipment and H₂O₂ storage and dosing to overall capital costs.

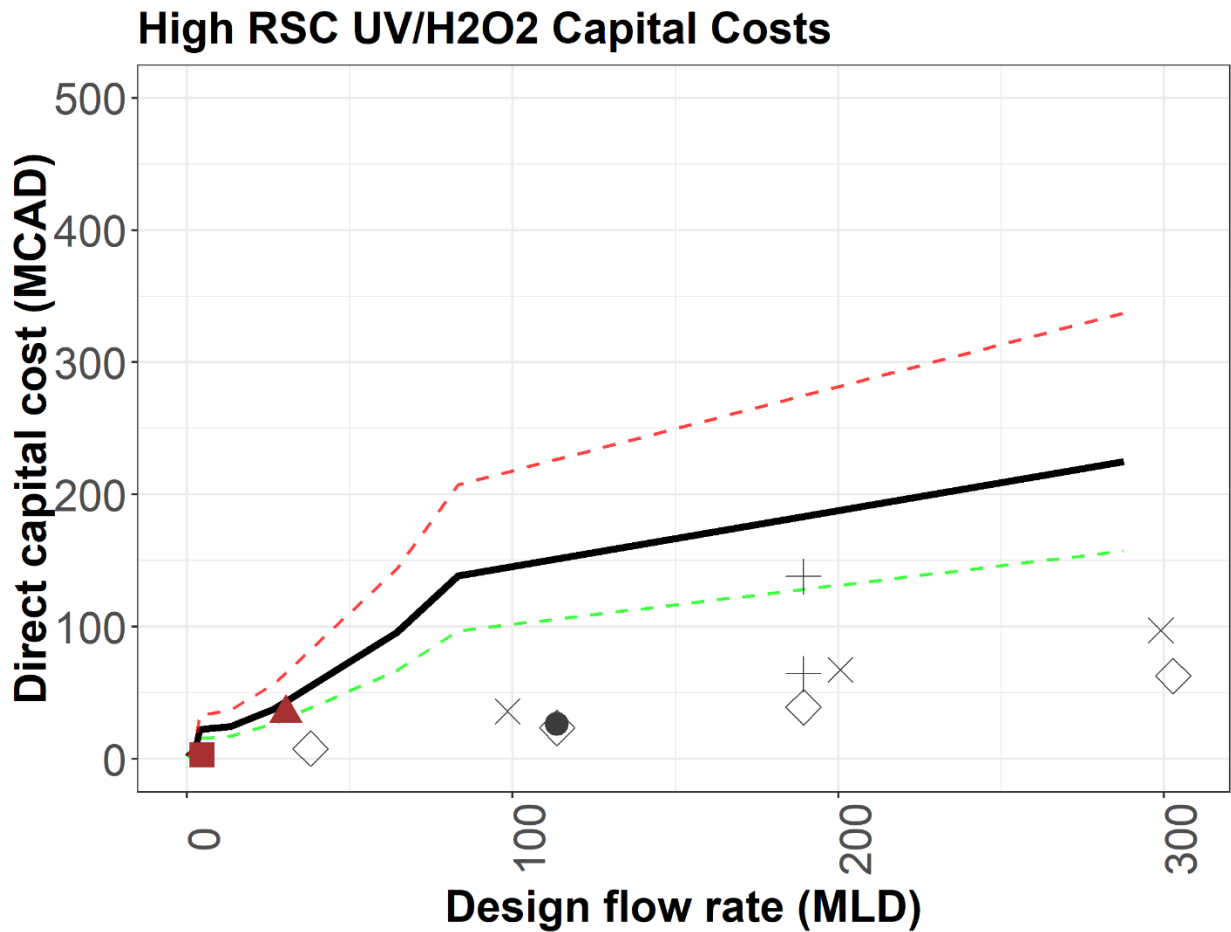


Figure 26: Comparison of capital costs calculated for high RSC to reported full-scale installations of UV/H₂O₂ listed in industry magazines, conference proceedings, and other online sources (red points), and conceptual estimates conducted by researchers through the consultation of equipment vendors (black points). The dotted red and green lines indicate +50% and -30% of the calculated cost, respectively.

Figure 26 above and Figure 27 below compare the capital costs calculated in the analysis to full-scale costs listed in industry magazines, conference proceedings and other online sources (Water and Wastes Digest, 2018; Civil Engineering Magazine, 2011; Biggs, 2020; Regional Development Corporation, 2022; City of Monton, 2021) and are the points in red on the figures. The costs were also compared to conceptual estimates conducted by researchers through the consultation of equipment vendors (Plumlee et al., 2014; Cotton et al., 2006; Dore et al., 2014) and are the black points on the figures. All cost estimates compared were updated to 2023 CAD using the ENR cost indexes.

Based on the comparison, it can be concluded that the conceptual estimates can accurately predict costs for treatment plants with relatively small design capacities. However, as the treatment plant's design capacity increases, the capital cost analysis conducted seems to overestimate the costs these systems may have. An important caveat is that the reported costs do not have the same water quality assumptions or treatment objectives. However, it still can be likely concluded that the cost estimates for treatment plants with a design capacity greater than 100 MLD are overestimated. However, due to the little cost information of full-scale systems at large scale sizes, it is difficult to make improvements to the cost curves to describe the costs of larger treatment plants more accurately. The overestimation is likely due to the fact that the reported costs for UV were for a UV dose of 40 mJ cm⁻². To calculate costs for a UV dose of 776 mJ cm⁻² for example, the reported costs were multiplied by a factor of 776/40. This is probably where the overestimation is occurring as there is more than likely an economy of scale.

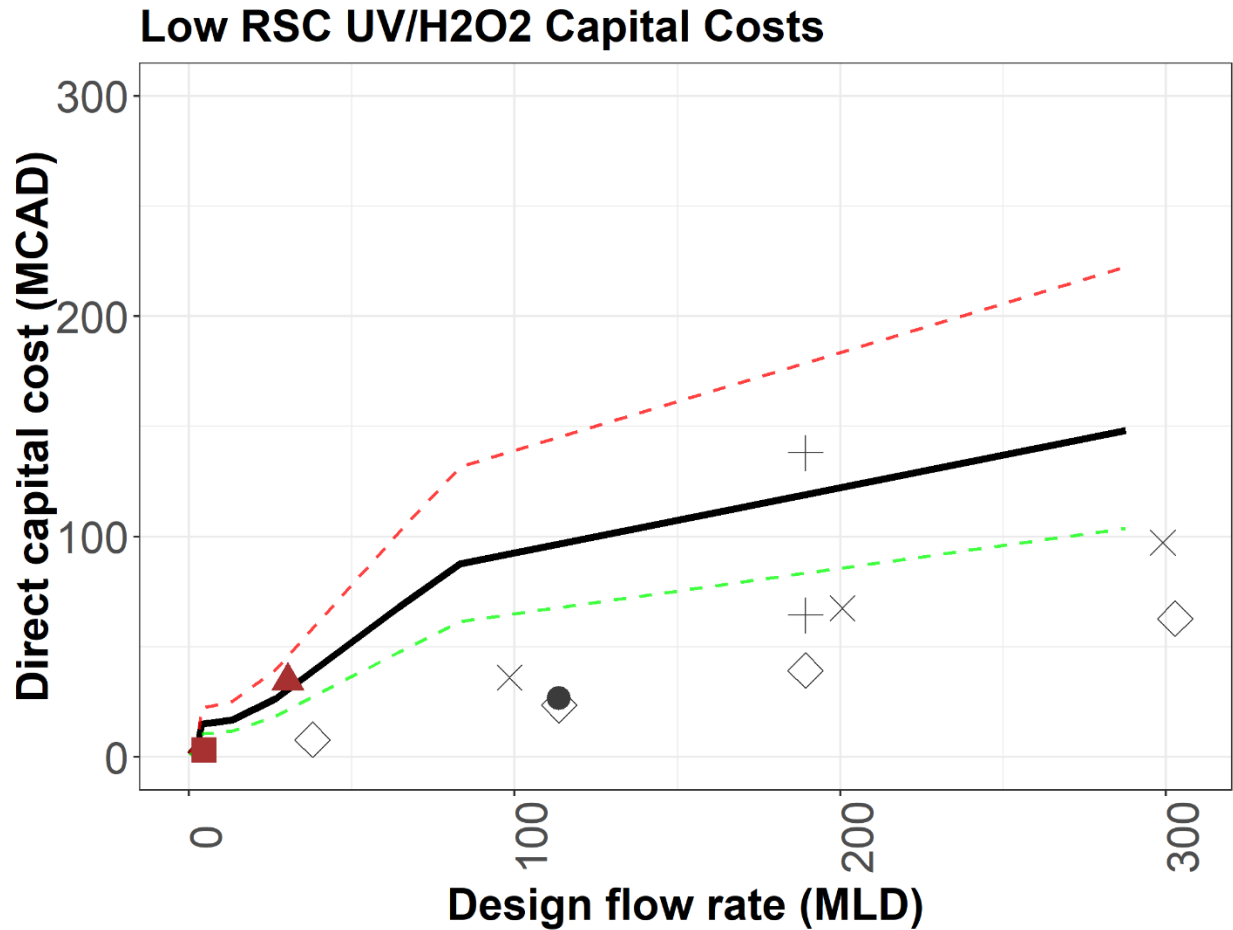


Figure 27: Comparison of capital costs calculated for low RSC to reported full-scale installations of UV/H₂O₂ listed in industry magazines and conference proceedings (red points) and conceptual estimates conducted by researchers through the consultation of equipment vendors (black points). The dotted red and green lines indicate +50% and -30% of the calculated cost, respectively.

4.3.2. Capital Costs for UV/Cl

From the analysis conducted in Chapter 4.2 the optimum free chlorine and UV doses for the relatively low RSC are 1.86 mg L⁻¹ and 772 mJ cm⁻², respectively. For the relatively higher RSC, the optimum free chlorine and UV dose are 2.4 mg L⁻¹ and 820 mJ cm⁻², respectively. The optimum doses were calculated based upon the treatment objectives and water quality assumptions outlined in the second objective. The water quality and treatment objectives applied to build the cost curves of UV/Cl are summarized in Table 27 below. The pH adjustment doses were not used to calculate capital costs, only O&M costs which are discussed in Chapter 4.3.5. It is important to note that the RSC of UV/Cl is larger than the RSC of UV/H₂O₂ strictly because of more reactive species present in UV/Cl versus UV/H₂O₂. The RSC of UV/Cl will have intrinsically larger value for UV/Cl compared to UV/H₂O₂ due to the increased yield of radical species.

Table 27: Water quality and treatment objectives that were used to build cost curves for UV/H2O2.

Assumption	Value
Target Contaminant	MC-LR
Log reduction	2
pH	7
Absorbance of the water matrix	0.02 cm ⁻¹
Radical scavenging capacity of the water matrix	Low RSC: 4.14 x 10 ⁴ s ⁻¹ ; High RSC: 9.14 x 10 ⁴ s ⁻¹

The capital costs calculated for the relatively high and low RSC's are presented in Figure 28 below. The costs presented assume no prior infrastructure in place and are not necessarily indicative of a retrofit. The dotted red lines and green lines indicate a +50% and -30% error bounds and were included based on recommendations for conceptual cost estimates (McGivney, 2008). Interestingly, there is only a maximum difference of about 5% in the calculated costs for the relatively high RSC compared to the relatively low RSC. However, because the capital costs of large treatment plants can be upwards of \$1 billion CAD, a 5% difference could be upwards of \$50 million CAD in estimated capital costs to treat MC-LR. Based on these results, understanding the RSC of the water matrix could lead to major cost savings especially for large treatment plants.

Figure 29 below compares the percent contribution of UV equipment and sodium hypochlorite dosing and storage to overall capital costs. At both RSC values and at all design treatment plants, UV equipment dominates the contribution to overall capital costs. The smaller treatment plant capacities (0.34-2.57 MLD) show a larger contribution from NaOCl but are still less than 10% of the overall capital costs. Therefore, based on the results of this analysis, larger UV doses will induce larger capital costs when constructing UV/Cl reactors.

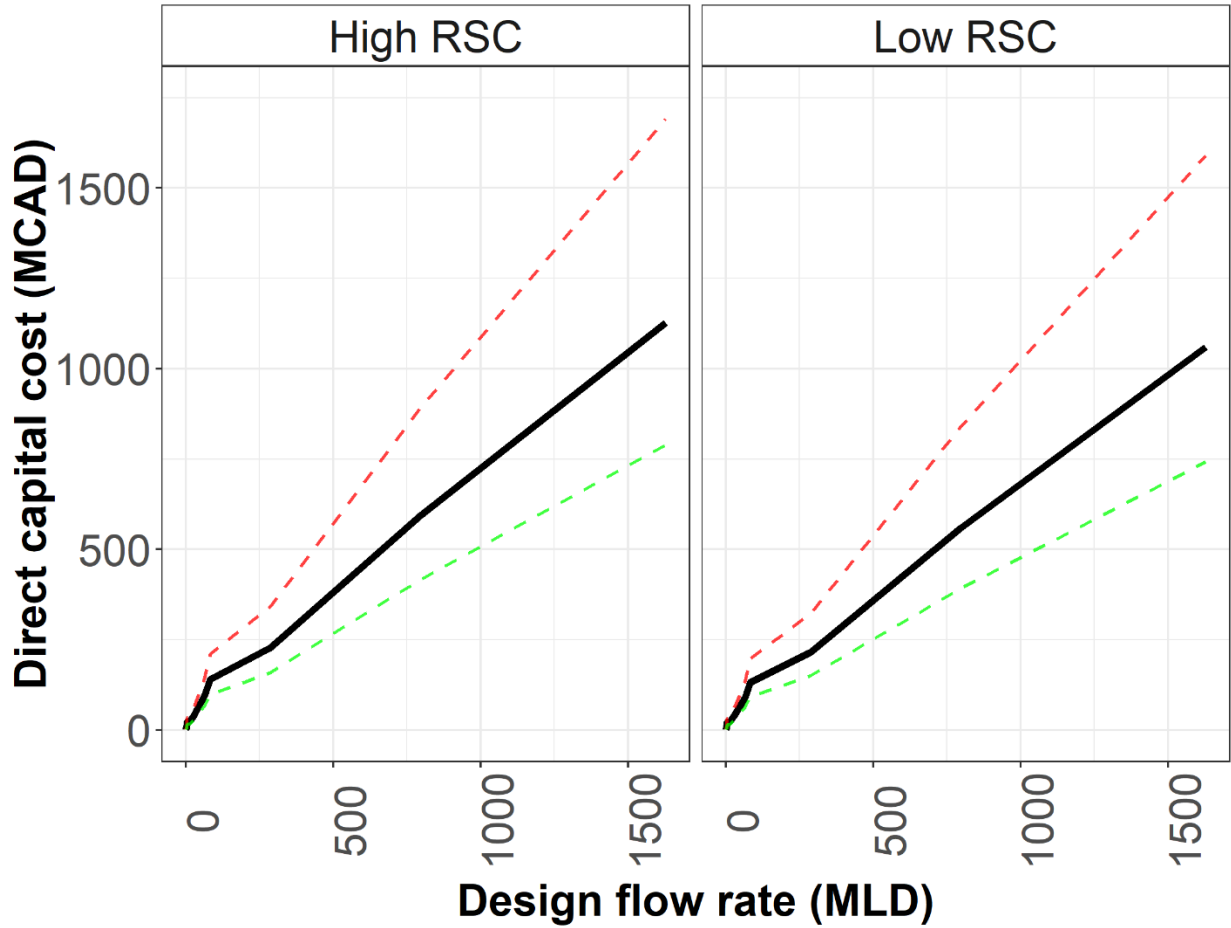


Figure 28: Capital cost curves for UV/Cl to achieve 2-log reduction of MC-LR. The dotted red and green lines indicate error bounds of +50% and -30%, respectively.

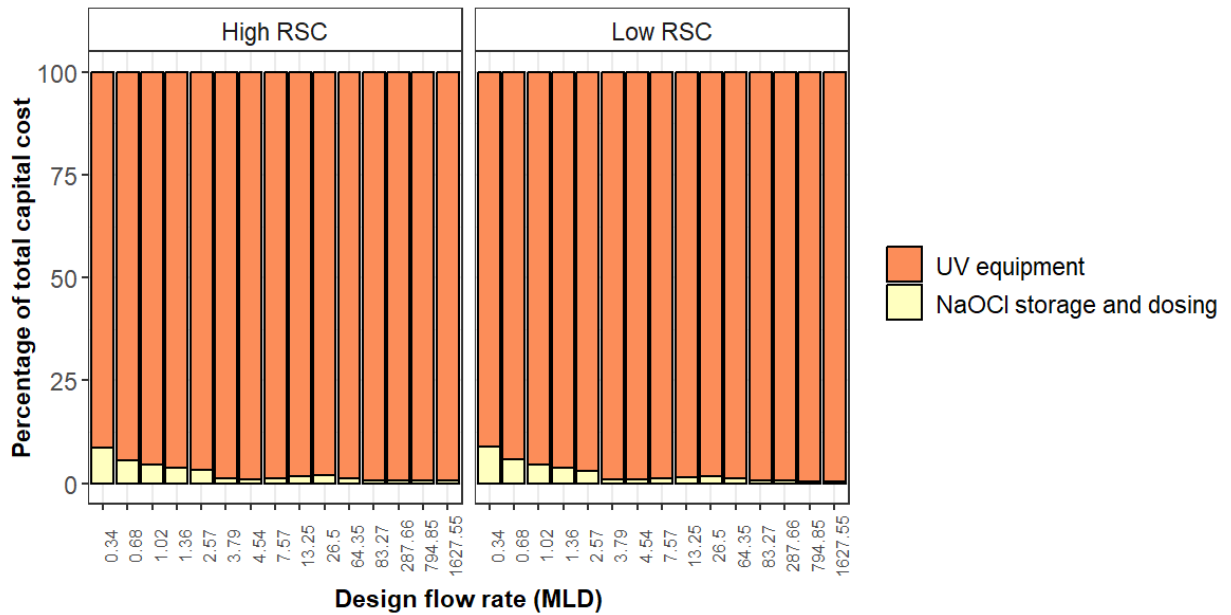


Figure 29: Percent contribution of UV equipment and NaOCl storage and dosing to overall capital costs.

4.3.3. Comparison of Capital Costs

Comparing the capital costs of UV/H₂O₂ to UV/Cl, UV/H₂O₂ is significantly more affected by the variation of RSC compared to UV/Cl. This can be attributed to MC-LR's high reactivity towards reactive chlorine species, which minimizes the impact the variation of RSC has on calculated optimum dosing requirements, therefore reducing the variation of costs associated with constructing the UV/AOP reactor. Comparing the estimated costs to construct both UV/H₂O₂ and UV/Cl, at the relatively high RSC there is no more than about a 4% difference between the estimated capital costs, with UV/H₂O being the slightly cheaper option. Comparing the two relatively low RSC cost estimates, UV/H₂O₂ has about 30% lower estimated capital costs. Based on these results, it can be concluded that UV/H₂O₂ does have the advantage regarding capital costs compared to UV/Cl for the same treatment objectives.

It is also important to note that the capital costs are more than likely overestimated for treatment plants with design capacities greater than 100 MLD. This can be concluded from the analysis in Chapter 4.3.1 which compared the capital cost estimates of UV/H₂O₂ to reported full-scale costs and other conceptual estimates conducted by researchers. This analysis could only be conducted with UV/H₂O₂ because, to the authors knowledge, no full-scale costs of UV/Cl have been reported. The assumption is that similarly to UV/H₂O₂, the capital costs for treatment plants larger than 100 MLD are likely overestimated for UV/Cl as well. Once full-scale costs are reported for larger treatment plants, adjustments can be made to the capital cost curves to better represent and predict costs associated with constructing UV/H₂O₂ and UV/Cl reactors.

4.3.4. O&M Costs for UV/H₂O₂

The yearly O&M costs for two log reduction of MC-LR using UV/H₂O₂ are presented in Figure 31 below. Again, the costs to treat MC-LR in water with a relatively high radical scavenging capacity and a relatively low radical scavenging capacity were compared to measure how important accurately determining the radical scavenging capacity is for minimizing costs. Interestingly, the O&M costs for the lower radical scavenging capacity are greater than the O&M costs for the larger radical scavenging capacity. This is because the calculated optimum H₂O₂ dose for the lower radical scavenging capacity was larger (2.4 mg L⁻¹ versus 1 mg L⁻¹). From Figure 32, costs associated with H₂O₂ heavily dictate the O&M costs of UV/H₂O₂ as quenching H₂O₂ with free chlorine becomes a quite substantial cost at treatment plants with larger

capacities. Resulting in an increase of O&M costs with respect to larger H₂O₂ doses. Based on this, the optimum doses calculated for UV/H₂O₂ minimize capital costs but result in increased O&M costs when the water matrix is assumed to have a larger radical scavenging capacity. This highlights a potential issue in the modelling approach taken to obtain optimum doses for treatment of MC-LR. Due to the large energy requirement to produce H₂O₂ (Rosenfeldt et al. 2006), optimum doses for water quality with higher radical scavenging capacity, and therefore less optimal conditions, favour smaller H₂O₂ doses coupled with larger UV doses. However, this is only true for treatment plants with design capacities greater than or equal to 26.5 MLD. Treatment plants with design capacities equal to or less than 7.57 MLD have O&M costs that are heavily resultant from maintenance. Thus, the O&M costs are greater for larger UV doses. Therefore, the potential issue with the modelling approach is linked to treatment plants with larger design capacities. More research is required to better understand the costs associated with UV/AOPs at larger design capacities. The estimated yearly O&M costs go up to about \$25 million CAD for the higher RSC and about 35 million CAD for the lower RSC.

To clarify, quenching refers to reducing the concentration of H₂O₂ in the water before it reaches the distribution system. H₂O₂ can't enter the distribution system and therefore, some mechanism of removal is required. A process flow diagram of UV/H₂O₂ is presented in Figure 30. The HOCl dose in this diagram is used to both quench H₂O₂ and provide secondary disinfection.

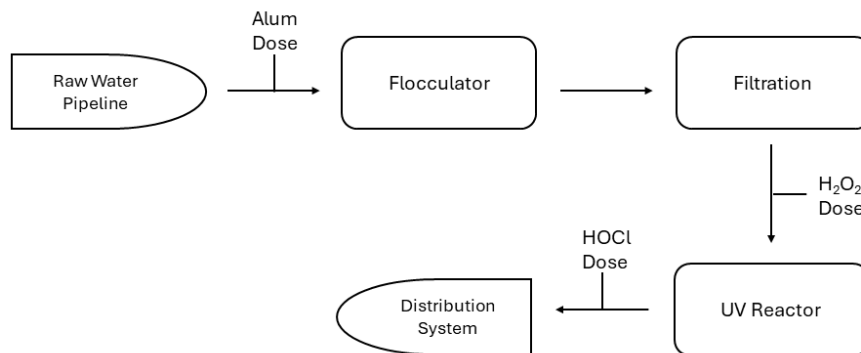


Figure 30: Process flow diagram of conventional drinking water treatment retrofitted with a UV/H₂O₂ reactor.

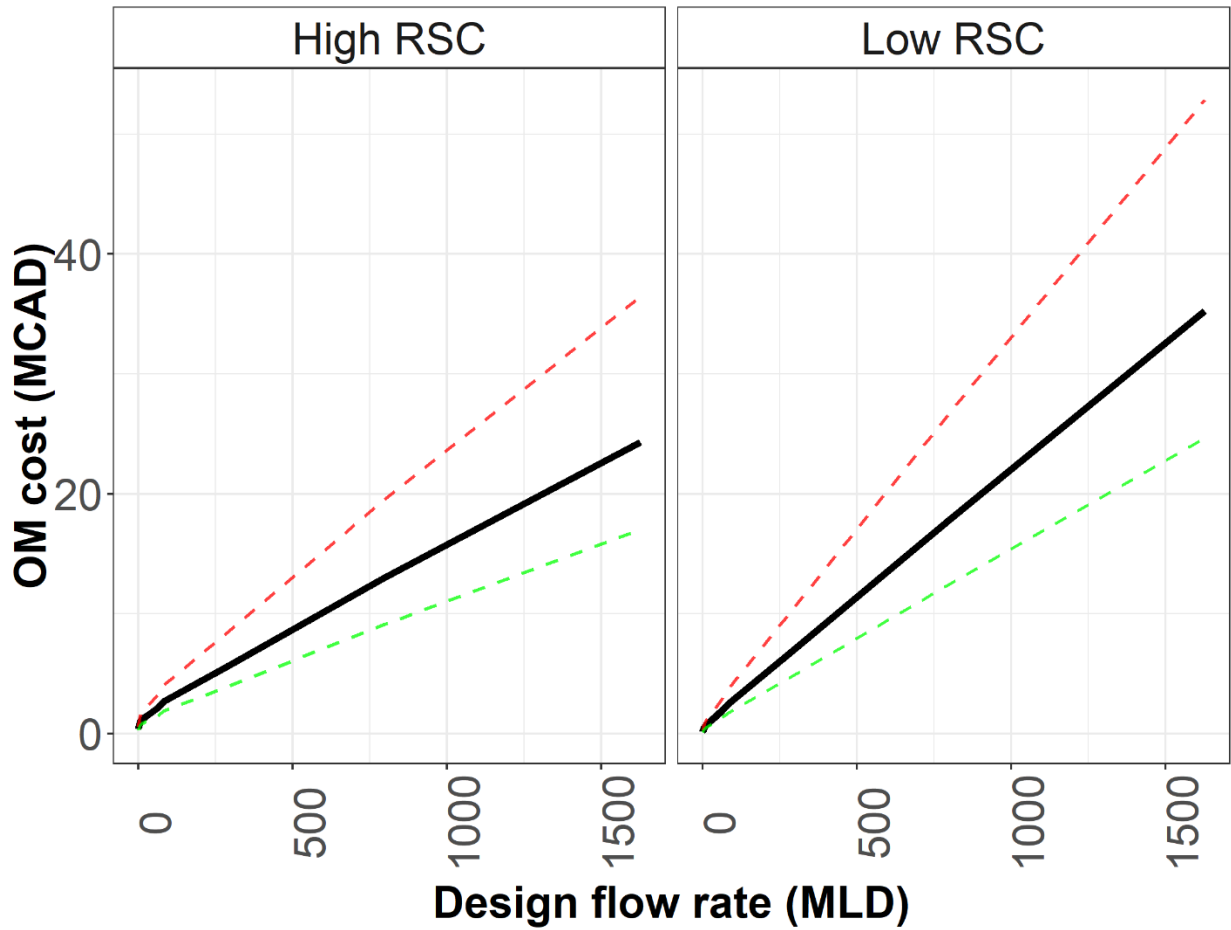


Figure 31: O&M cost curves for UV/H₂O₂ to achieve 2-log reduction of MC-LR. The dotted red and green lines indicate error bounds of +50% and -30%, respectively.

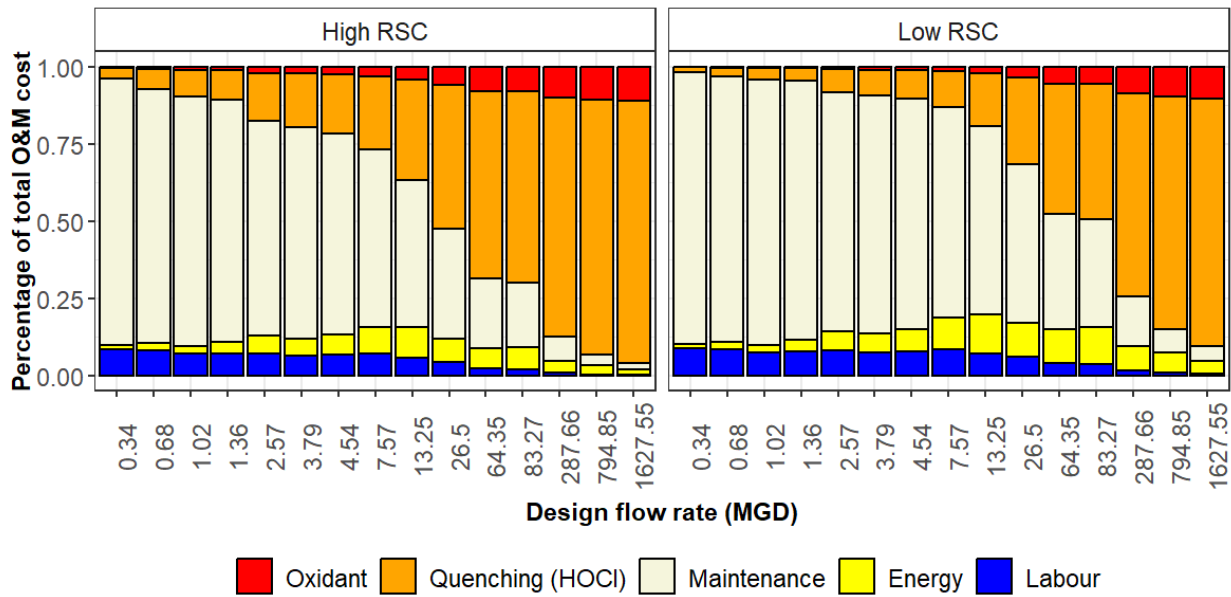


Figure 32: Percent contribution of H₂O₂ costs, quenching costs, maintenance, energy, and labour costs to overall O&M costs.

4.3.5. O&M Costs for UV/Cl

Two scenarios of yearly O&M costs are compared for UV/Cl, one situation where pH adjustment is required, and one where pH adjustment is not required. This was done because it is often assumed that full-scale adaptations of UV/Cl should operate at acidic pH to ensure the most efficient and effective degradation of contaminants (Mackey et al., 2022; Fang et al., 2014). Although, there is evidence in literature that UV/Cl can be effective at degradation of contaminants at neutral pH (Tian et al., 2020; Wang et al., 2018). Additionally, UV/Cl coupled with MP UV lamps or UV LEDs that emit UV light at UVB wavelengths (280-320 nm) at pH > 7 can generate a high yield of radical species potentially making basic pH a viable option for UV/Cl as well. (Yin et al., 2018).

Figure 33 below illustrates the yearly O&M costs to achieve two log-reduction of MC-LR with UV/Cl treatment without pH adjustment. Expectantly, the low RSC has lower required yearly O&M costs compared to the higher RSC, with a maximum difference of \$1 million CAD. From Figure 34, the free chlorine dose heavily influences O&M costs for treatment plants with design capacities equal to or greater than 298 MLD while maintenance heavily influence O&M costs for treatment plants with design capacities less than or equal to 83 MLD. The estimated yearly O&M costs for the high RSC and low RSC situations are as much as approximately \$10 million and \$9 million CAD, respectively.

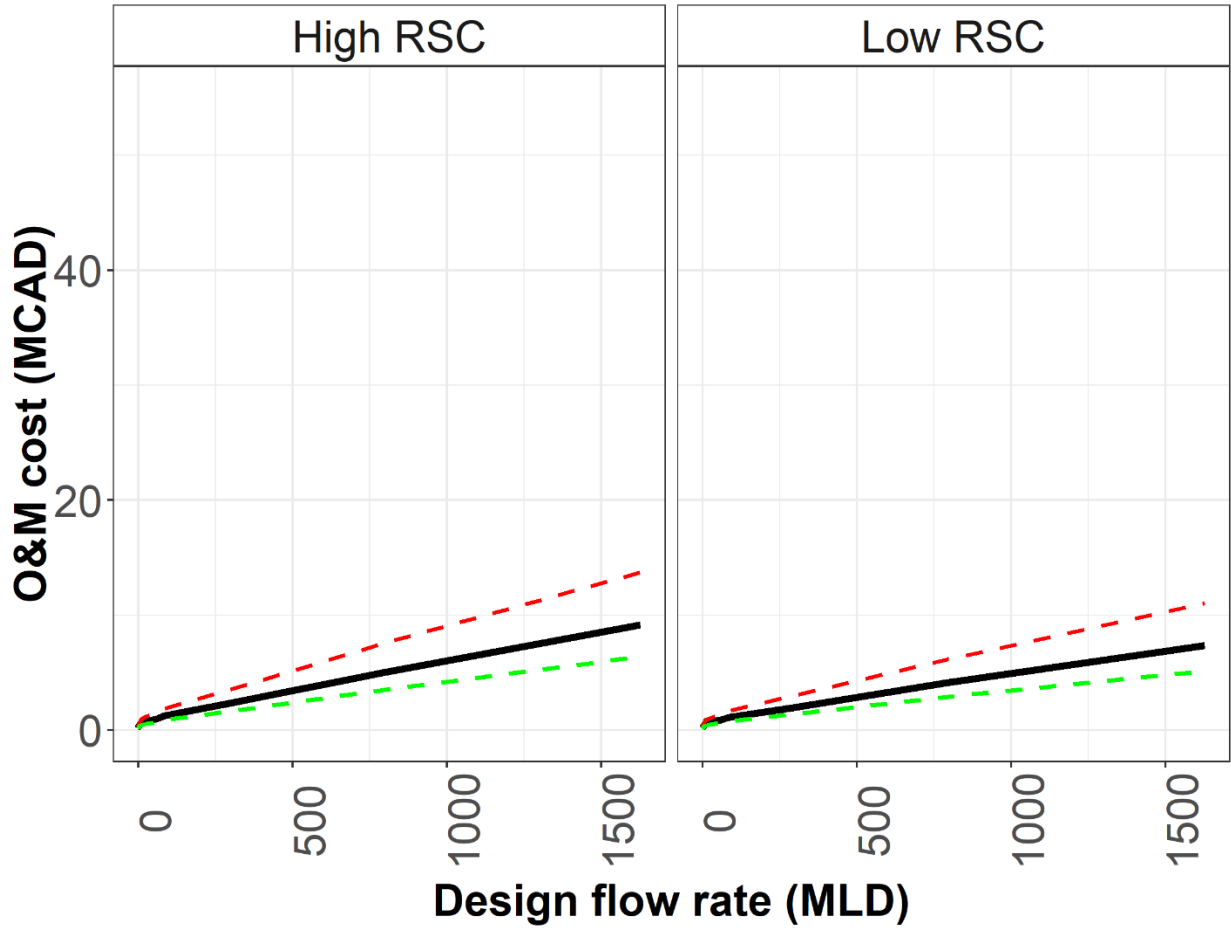


Figure 33: O&M cost curves for UV/Cl to achieve 2-log reduction of MC-LR with no pH adjustment. The dotted red and green lines indicate error bounds of +50% and -30%, respectively.

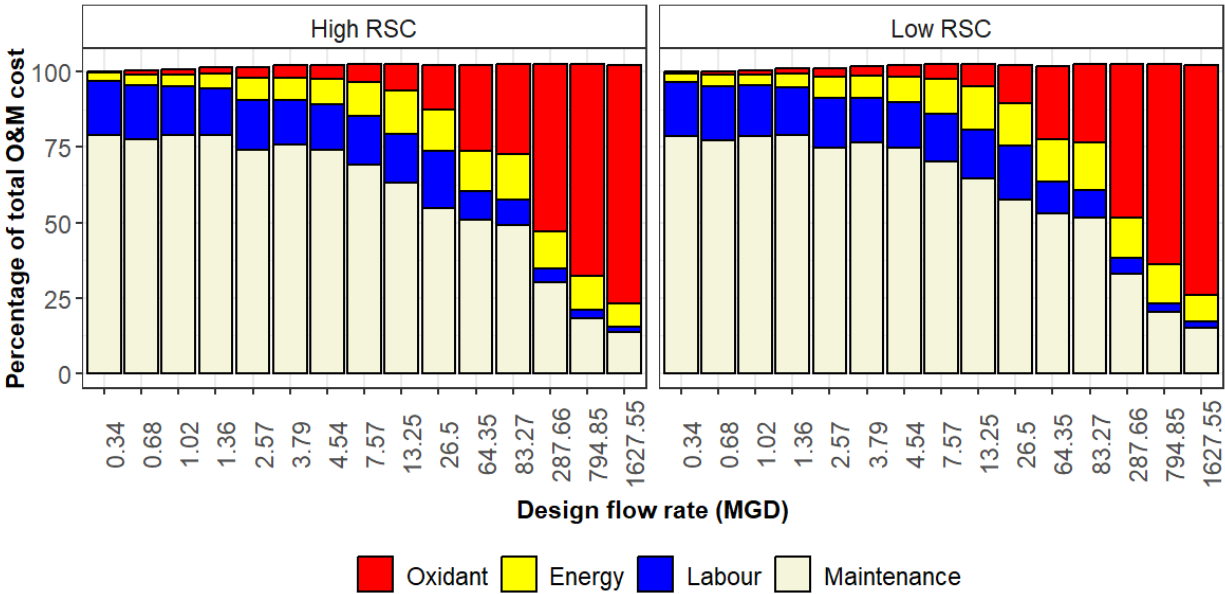
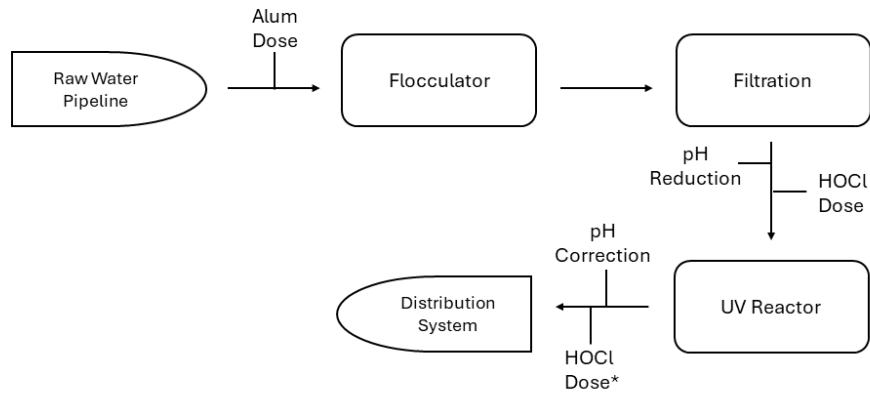


Figure 34: Percent contribution of NaOCl costs, quenching costs, maintenance, energy, and labour costs to overall O&M costs.

Figure 36 below illustrates the yearly O&M costs to achieve two log-reduction of MC-LR with UV/Cl treatment with pH adjustment. Again, the low RSC has lower required yearly O&M costs compared to the higher RSC, with a maximum difference of approximately \$1 million CAD. Figure 37 shows that the free chlorine dose combined with the pH adjustment chemicals heavily dominates the O&M costs for treatment plants with design capacities equal to or greater than 26 MLD while maintenance dominates yearly O&M costs for treatment plants with design capacities less than or equal to 13 MLD. The estimated yearly O&M costs for the high RSC and low RSC situations are as much as approximately \$22 million and \$23 million CAD, respectively.

Comparing the yearly O&M costs of when pH adjustments are required vs when pH adjustments are not required, there is a clear cost benefit to water treatment plants that do not require pH adjustments. With pH adjustments the yearly O&M costs are double the amount if no pH adjustment is required. Additionally, the pH adjustment costs were conducted assuming little to no buffer capacity of the water matrix (post-coagulation), therefore, if the in-situ water quality has high buffer capacity, the costs for pH adjustment would be even greater. Therefore, if pH adjustment is not required either because the in-situ water quality is naturally acidic, or because UV/Cl shows effective and efficient degradation of the target contaminant at neutral pH, or because the in-situ water quality is naturally basic, and free chlorine is coupled with UV light emitted at UVB wavelengths, UV/Cl can be cost effective.

A process flow diagram of a conventional water treatment plant retrofitted with a UV/Cl reactor is presented in Figure 35 below which shows where pH reduction and pH correction would occur in the plant.



* May not be required. Dependent on the HOCl dose leaving the reactor.

Figure 35: Process flow diagram of conventional drinking water treatment retrofitted with a UV/Cl reactor.

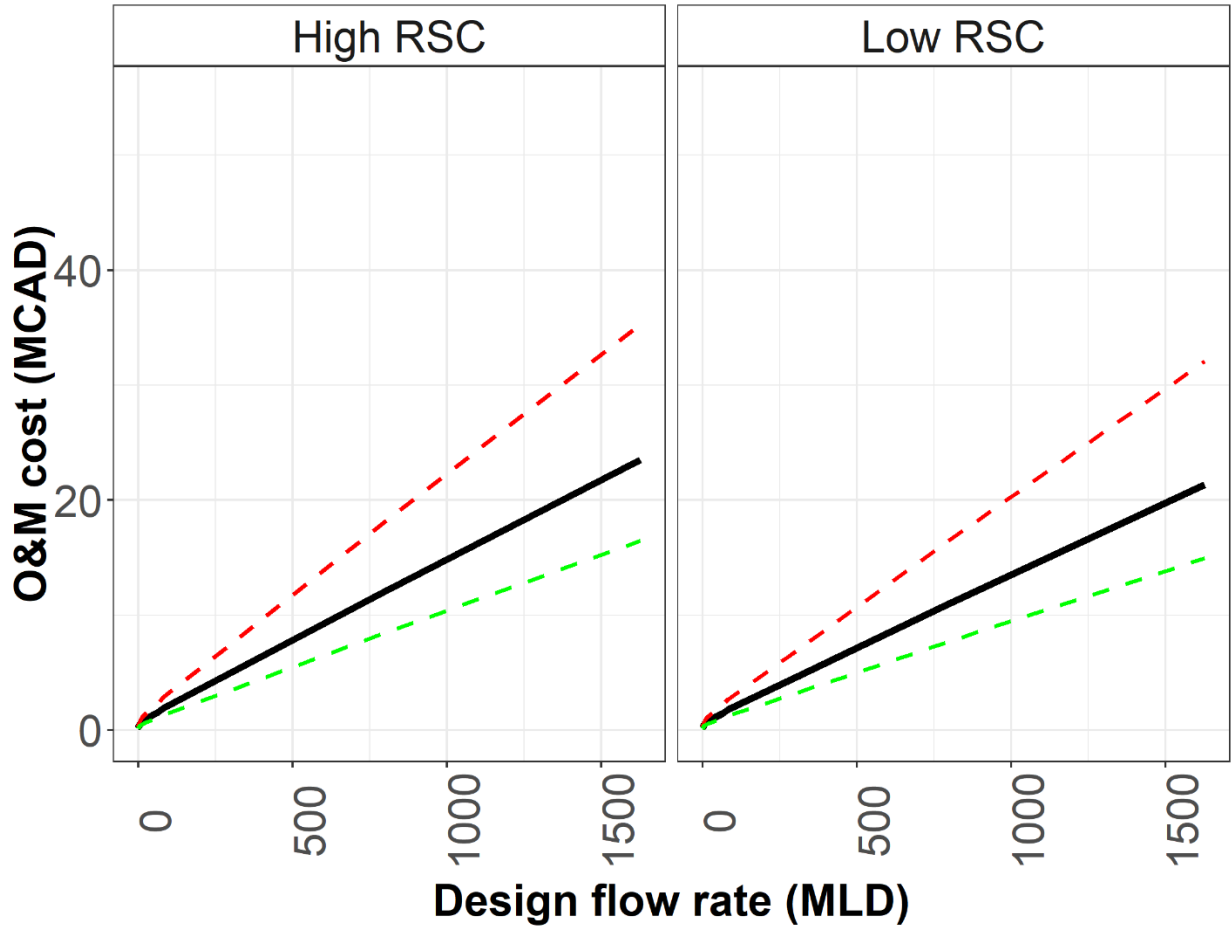


Figure 36: O&M cost curves for UV/Cl to achieve 2-log reduction of MC-LR with pH adjustment. The dotted red and green lines indicate error bounds of +50% and -30%, respectively.

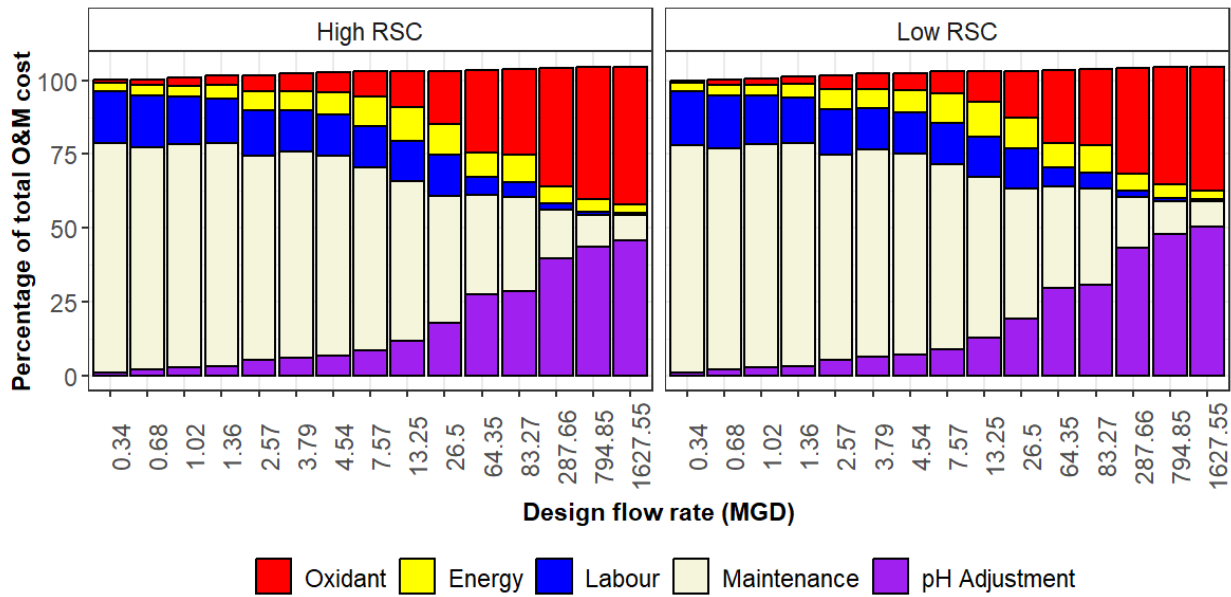


Figure 37: Percent contribution of NaOCl costs, quenching costs, maintenance, energy, pH adjustment and labour costs to overall O&M costs.

4.3.6. Comparison of O&M Costs

Comparing the O&M costs of UV/Cl to UV/H₂O₂, UV/Cl has the clear advantage for yearly O&M costs, especially if pH adjustment is not required. Based on the cost estimates, UV/Cl, without pH adjustment, could be as much as three times less costly annually to treat MC-LR to the same treatment objectives. Recall from Chapter 4.3.3, UV/H₂O₂ had the advantage for capital costs compared to UV/Cl. The cheaper annual O&M costs of UV/Cl could offset the larger capital costs in as much as twelve years and as little as three years. Therefore, long-term, without pH adjustment UV/Cl may be the best option. However, if pH adjustment is required, it may be more prudent to select UV/H₂O₂, as the O&M costs become much more comparable. Additionally, the pH adjustment costs were calculated assuming little to no buffer capacity of the water matrix and therefore costs for water with high alkalinity may require larger doses of sulfuric acid resulting in even greater yearly O&M costs. Therefore, based on the analysis presented in the research, when pH adjustment is not required UV/Cl is the recommended choice, and where pH adjustment is required, UV/H₂O₂ is the recommended choice.

4.3.7. Seasonality Analysis

The O&M costs calculated and presented in sections 4.3.4 and 4.3.5 assume that the UV/AOP is operating all year long. Therefore, these calculated costs are calculated as a worst-case scenario. Algal blooms most often occur in the summer and fall months so cyanotoxins may only be present in the source water in these seasons, meaning the UV AOP reactor would only need to operate during the summer and fall months. Although algal blooms can also be present during winter and spring months, hence the worst-case scenario presented in the previous sections (Province of British Columbia, 2022).

The cost curves presented in this section estimate the yearly cost to operate UV/Cl and UV/H₂O₂ only during the summer and fall months when cyanotoxins would typically be present in the source water. It is important to note that only having the UV/AOP operate in the summer and fall months would not impact capital costs as the reactor would still need to be constructed.

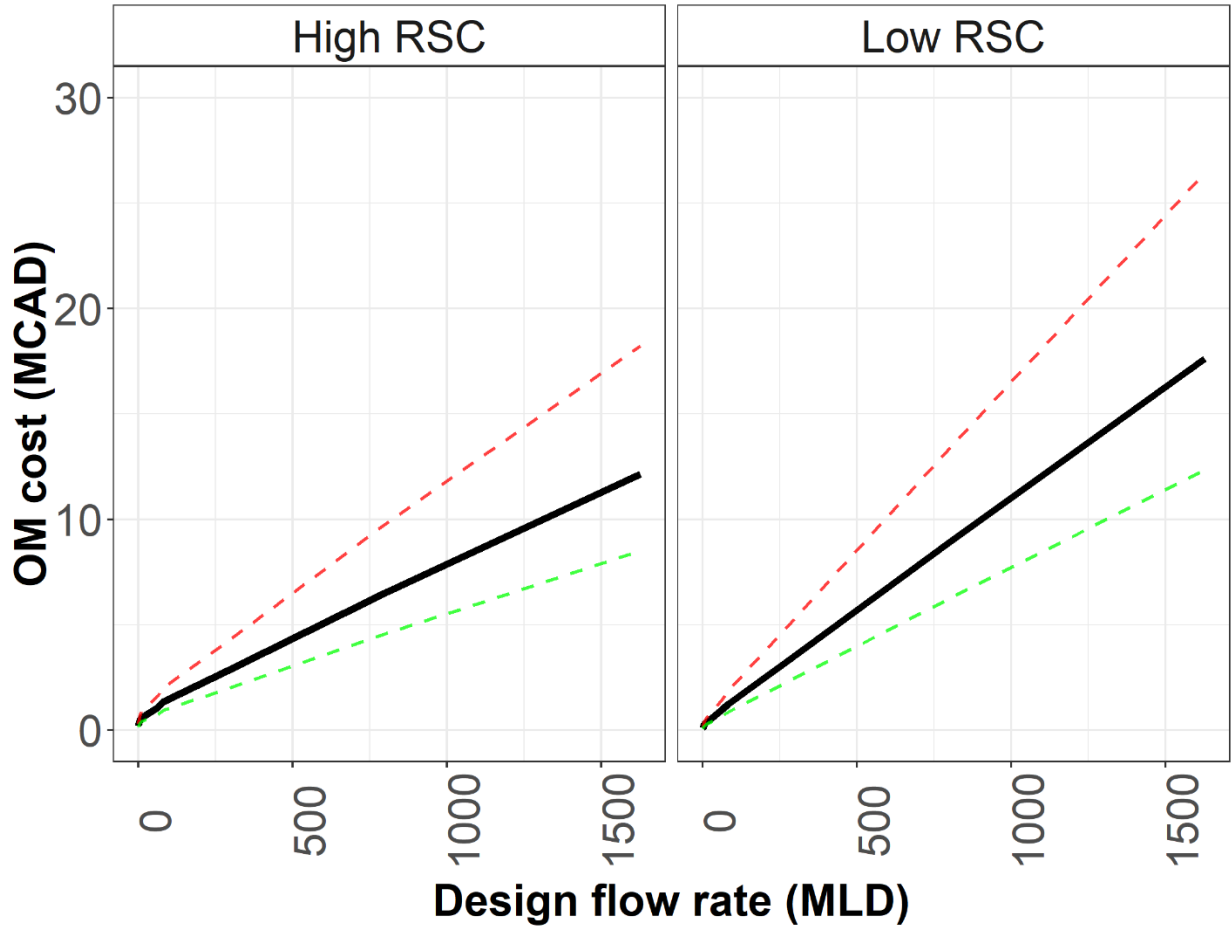


Figure 38: Seasonal O&M cost curves for UV/H₂O₂ to achieve 2-log reduction of MC-LR. The dotted red and green lines indicate error bounds of +50% and -30%, respectively.

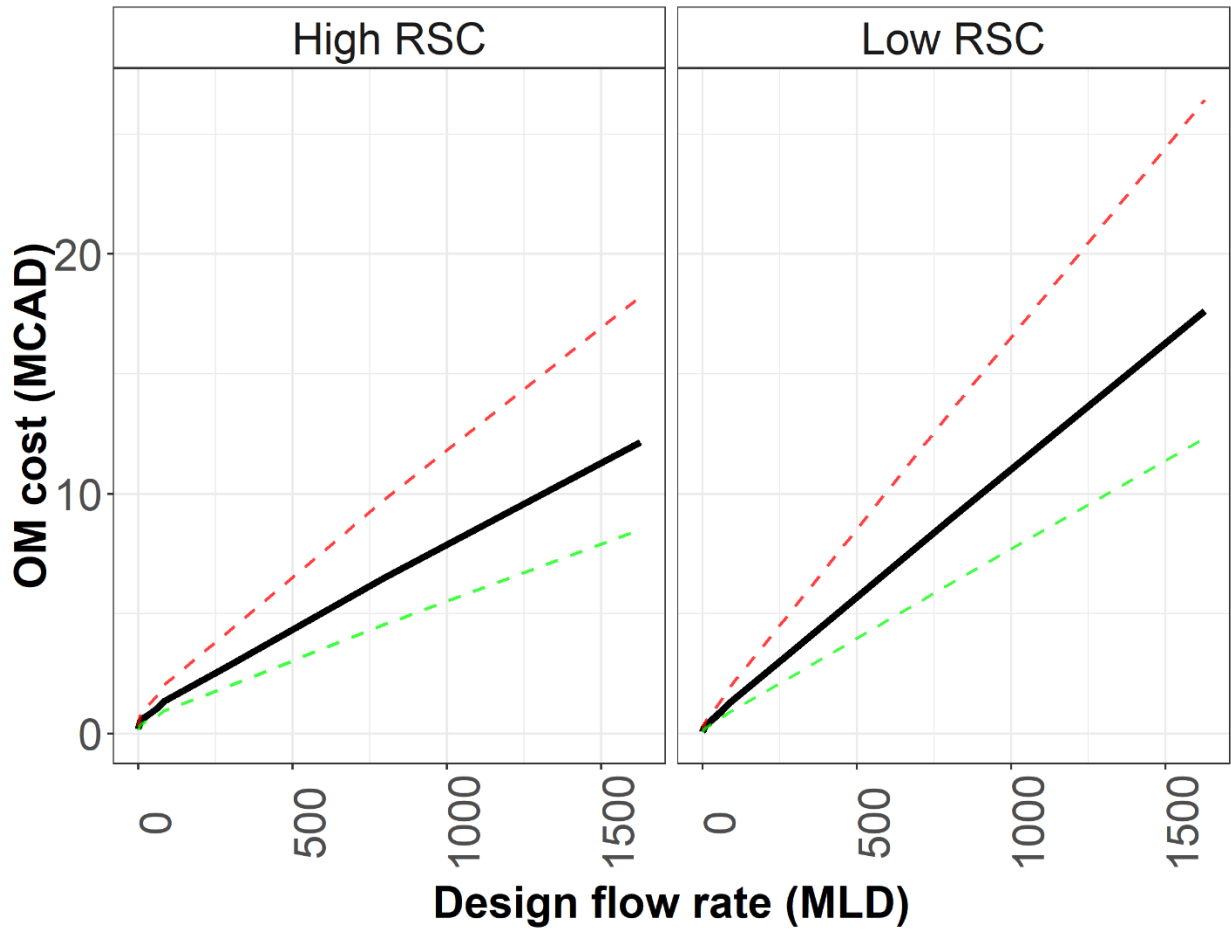


Figure 39: Seasonal O&M cost curves for UV/Cl to achieve 2-log reduction of MC-LR with no pH adjustment. The dotted red and green lines indicate error bounds of +50% and -30%, respectively.

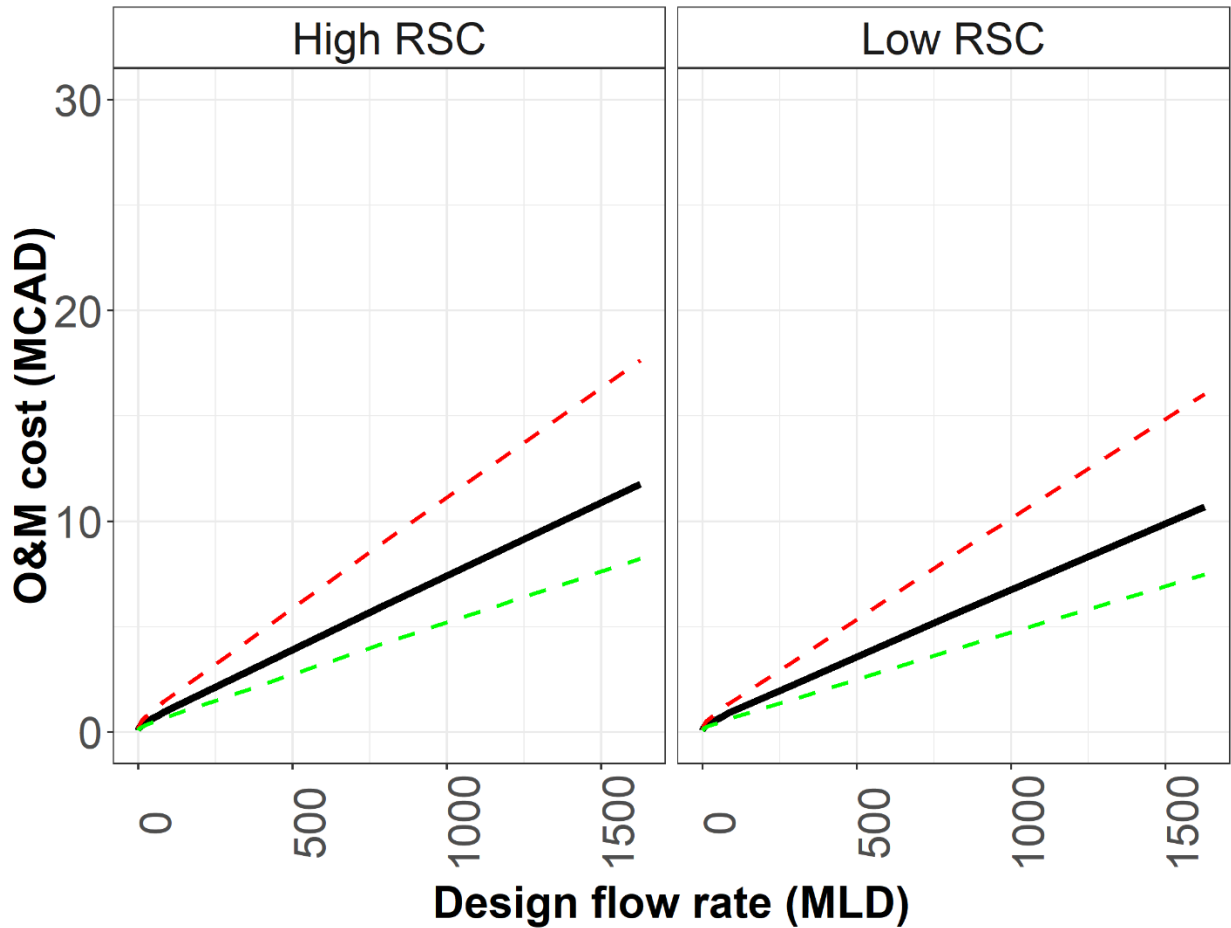


Figure 40: Seasonal O&M cost curves for UV/Cl to achieve 2-log reduction of MC-LR with pH adjustment. The dotted red and green lines indicate error bounds of +50% and -30%, respectively.

4.3.8. Comparison of Previous Cost Curves

Figure 41 and Figure 42 below show a comparison of previous capital costs and O&M cost estimates created for UV/H₂O₂. The previous cost curves were developed using a range of UV and H₂O₂ doses that were utilized in literature to treat contaminants using UV/H₂O₂. The previous cost curves were not constructed using UV and oxidant doses to achieve a certain treatment goal. They were constructed to demonstrate the potential variance of capital and O&M costs using UV/H₂O₂ with the wide range of reported UV and oxidant doses in literature. This comparison highlights the significance of measuring the radical scavenging capacity to be used to determine optimum UV and H₂O₂ doses as it can lead to more precise cost curves.

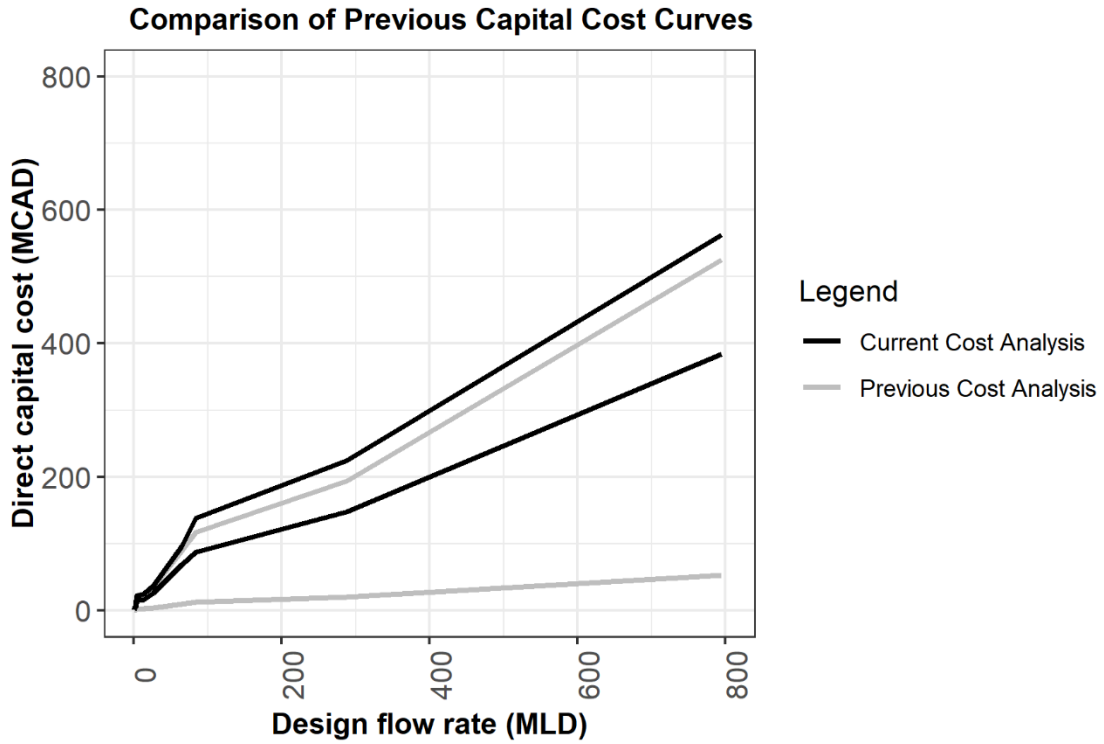


Figure 41: Comparison of previous capital cost curves versus current cost curves developed for UV/H₂O₂.

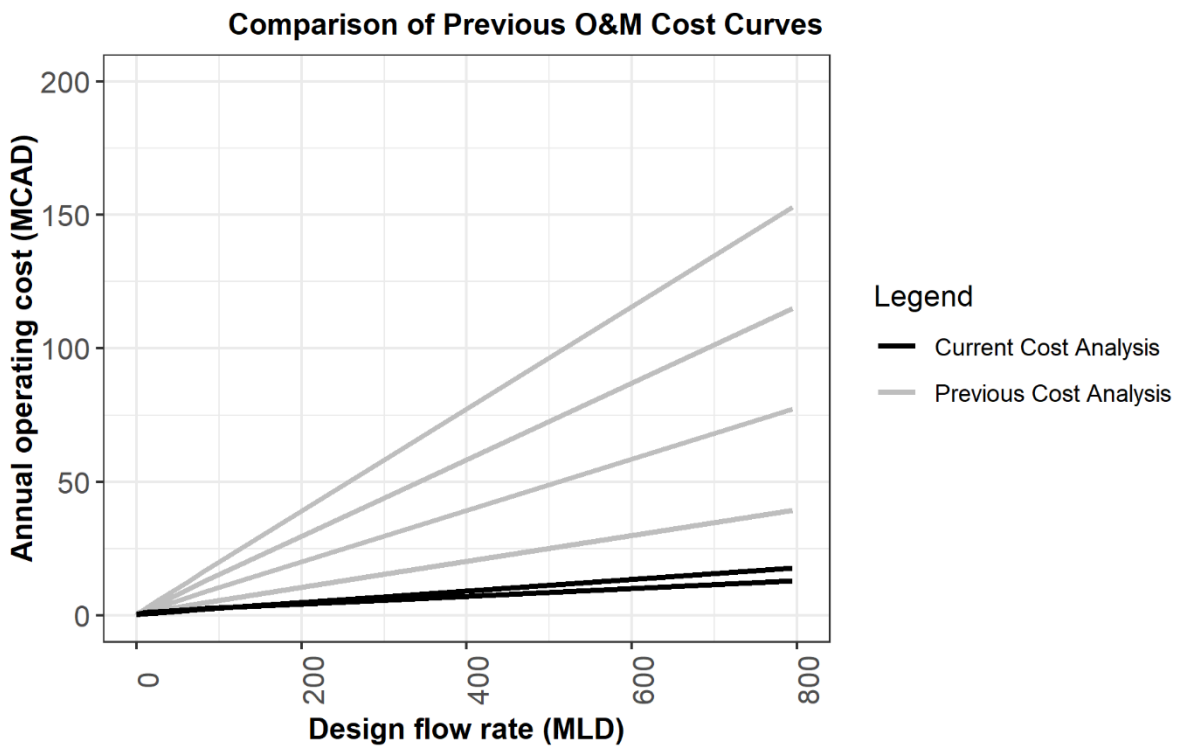


Figure 42: Comparison of previous capital cost curves versus current cost curves developed for UV/H₂O₂.

4.3.9. Future Research Steps

The most significant step for this aspect of the research is to better characterise the costs for treatment plants with larger design capacities. From the analysis conducted in Chapter 4.3.1, the capital costs of treatment plants with larger design capacities of both UV/H₂O₂ and UV/Cl are likely overestimated. Additionally, the model that calculated the optimum doses for UV/H₂O₂ reduces capital costs but increases O&M costs of treatment plants with larger design capacities. Therefore, more research is required to better characterize costs for UV/AOPs with treatment plants with design capacities larger than 100 MLD by retooling the model used to calculate optimum doses, especially for UV/H₂O₂ and using reported costs of these systems at larger scales to assist in the methodology of estimating costs. This could be done by potentially iterating between the modelling task and the cost curves to optimize for minimum costs rather than just the electrical energy dose.

5.0. Conclusions and Future Research Implications

5.1. Future Research Implications

Future research recommendations for each objective are outlined at the end of their respective results section in Chapter 4.0. This section discusses the potential implications of this research in the future and its applicability to the drinking water industry.

In the absence of real time data, UV/AOPs are designed for the worst-case scenario (lowest UVT and highest RSC). This means that UV/AOPs are often over-designed inflating already large capital and O&M costs. The external calibration method can be used to provide real time data of the radical scavenging capacity of water matrices which can then in turn be used to calculate optimum doses to achieve targeted treatment objectives utilizing a UV/AOP. This will optimize the system, reducing costs. A device has already been developed that uses the external calibration method to quickly quantify the $\cdot\text{OH}$ scavenging capacity of water matrices. If the $\cdot\text{OH}$ scavenging capacity can be used to accurately predict the optimum dosing requirements of UV/Cl or if the complexities of external calibration method specific to UV/Cl can be simplified, the operating conditions of a UV/Cl AOP reactor can be optimized in real time reducing costs.

If the required modelled doses can be validated, and the optimum dosing algorithm minimizes for costs rather than just electrical energy dose, this model can use the radical scavenging capacity reading provided through the external calibration method to predict optimum dosing requirements for a UV/H₂O₂ or UV/Cl reactor which can be used to update the operating conditions of the reactor in real time reducing costs.

The cost curves could be used as a preliminary tool to assess whether UV/Cl or UV/H₂O₂ would be the most cost-effective option for given in-situ water quality. General cost curves should never be used in-lieu of site-specific calculations which is why these cost curves should be used as a preliminary feasibility assessment.

5.2. Conclusions

To conclude this study, it is important to reiterate the objectives of this research. The objectives are listed below with conclusions identified.

1. *Evaluate the application of the external calibration method to UV/Cl.*

Due to the highly complex nature of UV/Cl, the external calibration method is not as effective at measuring the radical scavenging capacity of water matrices specific to UV/Cl. The contribution to the degradation of methylene blue from reactive chlorine species, $\cdot\text{OH}$, and free chlorine seem to result in less effective prediction of the radical scavenging capacity. Additionally, both free chlorine dose and UV dose have a statistically significant impact on the linear regression curves of the external calibration method. Therefore, if the external calibration method were to be applied at the full scale to UV/Cl and used to calculate the radical scavenging capacity to adjust the UV/Cl operating conditions (free chlorine dose, UV dose), the external calibration method would need to be corrected for these operational changes. Again, highlighting the fact that it is not as effective at predicting the radical scavenging capacity compared to the original method developed for UV/H₂O₂.

Based on the results of the log reduction experiments, methylene blue is best removed at pH 7. This means that pH adjustments may not necessarily be required to remove contaminants like methylene blue which have large reactivity towards reactive chlorine species. It is often assumed that acidic pH is necessary for optimal efficiency of contaminants due to high radical yield of $\cdot\text{OH}$ and the reduced radical scavenging capacity of HOCl relative to OCl⁻ (Yin et al., 2018; Fang et al., 2014). However, the results from this study suggest that this may not necessarily be the case for specific contaminants which would reduce required O&M costs to operate a UV/Cl reactor.

2. *Model optimum dosing requirements for UV/Cl to degrade MC-LR based on radical scavenging capacity of the water matrix.*

The model favours small H₂O₂ doses for larger radical scavenging capacity values because it optimizes based upon the minimum electrical energy dose and H₂O₂ has large energy requirements to produce. This then leads to larger calculated O&M costs for a small radical scavenging capacity value which intuitively should not happen. This aspect of the modelling approach needs to be corrected by iterating between the modelling task and the cost curves to minimize for costs rather than just the electrical energy dose. Additionally, the modelling results for required doses should be validated using bench and pilot scale experiments.

3. *Conceptualize the capital and O&M costs of UV/H₂O₂ and UV/Cl through the development of cost curves.*

The results of the cost curves indicated that UV/H₂O₂ had a slight capital cost advantage compared to UV/Cl. Although the capital costs were built with the assumption that there is no prior infrastructure installed and are therefore not indicative of a retrofit. In addition, the calculated capital costs are likely overestimated, probably due to the scaling factor used to calculate costs for the optimum UV doses when the reported costs were for a UV dose of 40 mJ cm⁻². There is an economy of scale missing from the capital cost curves.

UV/Cl had significant O&M cost savings compared to UV/H₂O₂ when no pH adjustment was required. If pH adjustment was required, UV/H₂O₂ became much more competitive in respect to O&M costs and will likely be the most overall cost-effective option. A pH adjustment may not be required if the in-situ water quality has acidic pH, or if the variation of the pH is deemed not significant in the degradation of the target contaminant using UV/Cl. The cost curves developed were in general agreement with the analysis conducted by the Water Research Foundation.

References

- Al Afifi, F., Jasim, S., & Mohseni, M. (2023). Microcystin-LR Removal by Ozone (O₃) and Vacuum-UV (VUV): The Effect of Chloride Ions. *Ozone: Science & Engineering*, 1–13.
<https://doi.org/10.1080/01919512.2023.2264339>
- Amano, H., Collazo, R., Santi, C. D., Einfeldt, S., Funato, M., Glaab, J., Hagedorn, S., Hirano, A., Hirayama, H., Ishii, R., Kashima, Y., Kawakami, Y., Kirste, R., Kneissl, M., Martin, R., Mehnke, F., Meneghini, M., Ougazzaden, A., Parbrook, P. J., ... Zhang, Y. (2020). The 2020 UV emitter roadmap. *Journal of Physics D: Applied Physics*, 53(50), 503001. <https://doi.org/10.1088/1361-6463/aba64c>
- Andrades, J. A., Lojo-López, M., Egea-Corbacho, A., & Quiroga, J. M. (2022). Comparative Effect of UV, UV/H₂O₂ and UV/H₂O₂/Fe on Terbutylazine Degradation in Natural and Ultrapure Water. *Molecules*, 27(14), Article 14. <https://doi.org/10.3390/molecules27144507>
- Asaithambi, P., Alemayehu, E., Sajjadi, B., & Aziz, A. R. A. (2017). Electrical energy per order determination for the removal pollutant from industrial wastewater using UV/Fe²⁺/H₂O₂ process: Optimization by response surface methodology. *Water Resources and Industry*, 18(Complete), 17–32.
<https://doi.org/10.1016/j.wri.2017.06.002>
- Biggs, J. (2020). *Tucson Water's AOP Treatment Facility: Transformation Of Tucson Water's CERCLA-To Drinking Water Program After 25 Years*.
- Boehlert, B., Strzepek, K. M., Chapra, S. C., Fant, C., Gebretsadik, Y., Lickley, M., Swanson, R., McCluskey, A., Neumann, J. E., & Martinich, J. (2015). Climate change impacts and greenhouse gas mitigation effects on U.S. water quality. *Journal of Advances in Modeling Earth Systems*, 7(3), 1326–1338.
<https://doi.org/10.1002/2014MS000400>

- Bolton, J. R., & Stefan, M. I. (2002). Fundamental photochemical approach to the concepts of fluence (UV dose) and electrical energy efficiency in photochemical degradation reactions. *Research on Chemical Intermediates*, 28(7–9), 857–870. <https://doi.org/10.1163/15685670260469474>
- Canada, H. (2014, October 22). *Guidelines for Canadian Drinking Water Quality—Summary Tables* [Guidance]. <https://www.canada.ca/en/health-canada/services/environmental-workplace-health/reports-publications/water-quality/guidelines-canadian-drinking-water-quality-summary-table.html>
- Chaves, F. P., Gomes, G., Della-Flora, A., Dallegrave, A., Sirtori, C., Saggiaro, E. M., & Bila, D. M. (2020). Comparative endocrine disrupting compound removal from real wastewater by UV/Cl and UV/H₂O₂: Effect of pH, estrogenic activity, transformation products and toxicity. *Science of The Total Environment*, 746, 141041. <https://doi.org/10.1016/j.scitotenv.2020.141041>
- City of Moncton. (2021). *2020 Water Quality Annual Report: Moncton/Riverview/Dieppe*. City of Moncton.
- City of Toronto. (2022). *DRINKING WATER SYSTEM Annual Report*. City of Toronto.
- Cotton, C. A & Collins, J. R. (2006). *Dual Purpose UV Light; Using UV Light for Disinfection and for Taste and Odour Oxidation*.
- Crittenden, J., Trussell, Rhodes, Hand, David, Howe, Kerry, & Tchobanoglous, George. (2012). *MWH's Water Treatment: Principles and Design, Third Edition* (1st ed.). John Wiley & Sons, Ltd. <https://doi.org/10.1002/9781118131473>
- Diebel, J & Catalano, L. (2011). Providing for Aurora. *Civil Engineering Magazine*.
- Dore, M. (2014). *Global Drinking Water Management and Conservation: Optimal Decision Making*. Springer.

- Erik J. Rosenfeldt, Karl G. Linden, Silvio Canonica, & Urs von Gunten. (2006). Comparison of the efficiency of d
OH radical formation during ozonation and the advanced oxidation processes O₃/H₂O₂ and UV/H₂O₂.
Water Research, 40, 3695–3704.
- Erin D. Mackey, Ron Hofmann, Adam Festger, & Catherine Vanyo. (2022). *UV-Chlorine AOP in Potable Reuse: A
Guidance Manual to Assessment and Implementation*. California Water Boards State Water Resources
Control Board.
- Fang, J., Fu, Y., & Shang, C. (2014). The Roles of Reactive Species in Micropollutant Degradation in the UV/Free
Chlorine System. *Environmental Science & Technology*, 48(3), 1859–1868.
<https://doi.org/10.1021/es4036094>
- Gora, S. L., Rauch, K. D., Ontiveros, C. C., Stoddart, A. K., & Gagnon, G. A. (2019). Inactivation of biofilm-bound
Pseudomonas aeruginosa bacteria using UVC light emitting diodes (UVC LEDs). *Water Research*, 151,
193–202. <https://doi.org/10.1016/j.watres.2018.12.021>
- Guo, K., Wu, Z., Shang, C., Yao, B., Hou, S., Yang, X., Song, W., & Fang, J. (2017). Radical Chemistry and
Structural Relationships of PPCP Degradation by UV/Chlorine Treatment in Simulated Drinking Water.
Environmental Science & Technology, 51(18), 10431–10439. <https://doi.org/10.1021/acs.est.7b02059>
- Hoang, N. T., Manh, T. D., Nguyen, V. T., Thy Nga, N. T., Mwazighe, F. M., Nhi, B. D., Hoang, H. Y., Chang, S. W.,
Chung, W. J., & Nguyen, D. D. (2022). Kinetic study on methylene blue removal from aqueous solution
using UV/chlorine process and its combination with other advanced oxidation processes. *Chemosphere*,
308, 136457. <https://doi.org/10.1016/j.chemosphere.2022.136457>
- Hotto, A. M., Satchwell, M. F., & Boyer, G. L. (2007). Molecular Characterization of Potential Microcystin-
Producing Cyanobacteria in Lake Ontario Embayments and Nearshore Waters. *Applied and
Environmental Microbiology*, 73(14), 4570–4578. <https://doi.org/10.1128/AEM.00318-07>

- Huang, Y., Li, Y., Kong, M., D. Dionysiou, D., & Lei, L. (2021). Degradation of atrazine in the electrochemical LED-UV/Cl² system: The role of [•]OH and Cl[•]. *Environmental Science: Water Research & Technology*, 7(9), 1630–1642. <https://doi.org/10.1039/D1EW00039J>
- Huaying Liu, Zhi Chao Hou, & Yingjie Li. (n.d.). *Modeling degradation kinetics of gemfibrozil and naproxen in the UV/chlorine system: Roles of reactive species and effects of water matrix | Elsevier Enhanced Reader*. <https://doi.org/10.1016/j.watres.2021.117445>
- James R. Bolton & Karl G. Linden. (2003). *Standardization of Methods for Fluence (UV Dose) Determination in Bench-Scale UV Experiments*. <https://ascelibrary.org/doi/epdf/10.1061/%28ASCE%290733-9372%282003%29129%3A3%28209%29>
- Kheyrandish, A., Mohseni, M., & Taghipour, F. (2017). Development of a method for the characterization and operation of UV-LED for water treatment. *Water Research*, 122, 570–579. <https://doi.org/10.1016/j.watres.2017.06.015>
- Krupińska, I. (2020). Impact of the Oxidant Type on the Efficiency of the Oxidation and Removal of Iron Compounds from Groundwater Containing Humic Substances. *Molecules*, 25(15), 3380. <https://doi.org/10.3390/molecules25153380>
- Kudesia, V. P. (n.d.). *Kinetics of Reaction of Isopropyl Alcohol with Aqueous Chlorine*. 4.
- Kwon, M., Kim, S., Jung, Y., Hwang, T.-M., Stefan, M. I., & Kang, J.-W. (2019). The Impact of Natural Variation of OH Radical Demand of Drinking Water Sources on the Optimum Operation of the UV/H₂O₂ Process. *Environmental Science & Technology*, 53(6), 3177–3186. <https://doi.org/10.1021/acs.est.8b05686>
- Lado Ribeiro, A. R., Moreira, N. F. F., Li Puma, G., & Silva, A. M. T. (2019). Impact of water matrix on the removal of micropollutants by advanced oxidation technologies. *Chemical Engineering Journal*, 363(Complete), 155–173. <https://doi.org/10.1016/j.cej.2019.01.080>

- Li, M., Li, W., Wen, D., Bolton, J. R., Blatchley, E. R., & Qiang, Z. (2019). Micropollutant Degradation by the UV/H₂O₂ Process: Kinetic Comparison among Various Radiation Sources. *Environmental Science & Technology*, 53(9), 5241–5248. <https://doi.org/10.1021/acs.est.8b06557>
- Luo, C., Ma, J., Jiang, J., Liu, Y., Song, Y., Yang, Y., Guan, Y., & Wu, D. (2015). Simulation and comparative study on the oxidation kinetics of atrazine by UV/H₂O₂, UV / HSO₅ – and UV/S₂O₈²⁻. *Water Research*, 80, 99–108. <https://doi.org/10.1016/j.watres.2015.05.019>
- Martijn, A. J. (2015). *Impact of the Water Matrix on the Effect and the Side Effect of MP UV/H₂O₂ Treatment for the Removal of Organic Micropollutants in Drinking Water Production* [Ph.D.]. Wageningen University and Research.
- Matamoros, V., & Salvadó, V. (2013). Evaluation of a coagulation/flocculation-lamellar clarifier and filtration-UV-chlorination reactor for removing emerging contaminants at full-scale wastewater treatment plants in Spain. *Journal of Environmental Management*, 117, 96–102. <https://doi.org/10.1016/j.jenvman.2012.12.021>
- McGivney, W., & Kawamura, S. (2008). *Cost Estimating Manual for Water Treatment Facilities*. John Wiley & Sons, Inc.
- Miklos, D. B., Remy, C., Jekel, M., Linden, K. G., Drewes, J. E., & Hübner, U. (2018). Evaluation of advanced oxidation processes for water and wastewater treatment – A critical review. *Water Research*, 139, 118–131. <https://doi.org/10.1016/j.watres.2018.03.042>
- Morgan, M. S., Van Trieste, P. F., Garlick, S. M., Mahon, M. J., & Smith, A. L. (1988). Ultraviolet molar absorptivities of aqueous hydrogen peroxide and hydroperoxyl ion. *Analytica Chimica Acta*, 215, 325–329. [https://doi.org/10.1016/S0003-2670\(00\)85294-0](https://doi.org/10.1016/S0003-2670(00)85294-0)

- Morris, J. C. (1966). The Acid Ionization Constant of HOCl from 5 to 35°. *The Journal of Physical Chemistry*, 70(12), 3798–3805. <https://doi.org/10.1021/j100884a007>
- Mundy, B., Kuhnel, B., Hunter, G., Jarnis, R., Funk, D., Walker, S., Burns, N., Drago, J., Nezgod, W., Huang, J., Rakness, K., Jasim, S., Joost, R., Kim, R., Muri, J., Nattress, J., Oneby, M., Sosebee, A., Thompson, C., ... Schulz, C. (2018). A Review of Ozone Systems Costs for Municipal Applications. Report by the Municipal Committee – IOA Pan American Group. *Ozone: Science & Engineering*, 40(4), 266–274. <https://doi.org/10.1080/01919512.2018.1467187>
- National Institute of Standards Technology. (2024). *NDRL/NIST Solution Kinetics Database on the Web* [Dataset].
- Plumlee, M. H., Stanford, B. D., Debroux, J.-F., Hopkins, D. C., & Snyder, S. A. (2014). Costs of Advanced Treatment in Water Reclamation. *Ozone: Science & Engineering*, 36(5), 485–495. <https://doi.org/10.1080/01919512.2014.921565>
- Pousty, D., Mamane, H., Cohen-Yaniv, V., & Bolton, J. R. (2022). Ultraviolet actinometry – Determination of the incident photon flux and quantum yields for photochemical systems using low-pressure and ultraviolet light-emitting diode light sources. *Journal of Environmental Chemical Engineering*, 10(3), 107947. <https://doi.org/10.1016/j.jece.2022.107947>
- Province of British Columbia. (n.d.). *What causes an algae bloom?* Province of British Columbia. Retrieved 28 July 2024, from <https://www2.gov.bc.ca/gov/content/environment/air-land-water/water/water-quality/algae-watch/what-are-algae/causes-of-an-algae-bloom>
- R Gumerman, R Culp, & R Clark. (1979). The cost of granular activated carbon adsorption treatment in the U.S. *Journal of the American Water Resources Association*, 71(11), 690–696.

- Rabani, J., Mamane, H., Pousty, D., & Bolton, J. R. (2021). Practical Chemical Actinometry—A Review. *Photochemistry and Photobiology*, 97(5), 873–902. <https://doi.org/10.1111/php.13429>
- Reece Lima-Thompson & Stephanie Gora. (2023). Techno-Economic Assessment of the Application of Advanced Oxidation Processes for the Removal of Seasonal and Year-Round Contaminants from Drinking Water. In *Advanced Oxidation Processes for Micropollutant Remediation* (1st ed., p. 28). CRC Press.
- Regional Development Corporation. (2022). *P. of N. B. Investment in Moncton's Drinking Water System*. Regional Development Corporation.
- Ruderman, G., Caffarena, E., Mogilner, I., & Tolosa, E. J. (1998). Hydrogen Bonding of Carboxylic Acids in Aqueous Solutions—UV Spectroscopy, Viscosity, and Molecular Simulation of Acetic Acid. *Journal of Solution Chemistry*, 27, 935–948. <https://doi.org/10.1023/A:1022615329598>
- Sgroi, M., Snyder, S. A., & Roccaro, P. (2021). Comparison of AOPs at pilot scale: Energy costs for micropollutants oxidation, disinfection by-products formation and pathogens inactivation. *Chemosphere*, 273, 128527. <https://doi.org/10.1016/j.chemosphere.2020.128527>
- Shahi, N. K., Maeng, M., Choi, I., & Dockko, S. (2021). Degradation effect of ultraviolet-induced advanced oxidation of chlorine, chlorine dioxide, and hydrogen peroxide and its impact on coagulation of extracellular organic matter produced by *Microcystis aeruginosa*. *Chemosphere*, 281, 130765. <https://doi.org/10.1016/j.chemosphere.2021.130765>
- Shu, Z., Singh, A., Klamerth, N., McPhedran, K., Bolton, J. R., Belosevic, M., & Gamal El-Din, M. (2016). Pilot-scale UV/H₂O₂ advanced oxidation process for municipal reuse water: Assessing micropollutant degradation and estrogenic impacts on goldfish (*Carassius auratus* L.). *Water Research*, 101, 157–166. <https://doi.org/10.1016/j.watres.2016.05.079>
- Sigma-Aldrich. (2023). *Acetic Acid Safety Data Sheet*. Sigma-Aldrich.

- Smith, E. J., Davison, W., & Hamilton-Taylor, J. (2002). Methods for preparing synthetic freshwaters. *Water Research*, 36(5), 1286–1296. [https://doi.org/10.1016/S0043-1354\(01\)00341-4](https://doi.org/10.1016/S0043-1354(01)00341-4)
- Springer, J. C., Kashinkunti, R., & Hong, Y. (2018a). Medium-Pressure UV/Chlorine Advanced Oxidation of Taste and Odor Compounds. *Journal AWWA*, 110(9), E16–E27. <https://doi.org/10.1002/awwa.1090>
- Springer, J. C., Kashinkunti, R., & Hong, Y. (2018b). Medium-Pressure UV/Chlorine Advanced Oxidation of Taste and Odor Compounds. *Journal AWWA*, 110(9), E16–E27. <https://doi.org/10.1002/awwa.1090>
- State of California. (2023). *Chemicals of Emerging Concern*. Department of Toxic Substances Control. <https://dtsc.ca.gov/emerging-chemicals-of-concern/>
- Tian, F.-X., Ye, W.-K., Xu, B., Hu, X.-J., Ma, S.-X., Lai, F., Gao, Y.-Q., Xing, H.-B., Xia, W.-H., & Wang, B. (2020). Comparison of UV-induced AOPs (UV/Cl₂, UV/NH₂Cl, UV/ClO₂ and UV/H₂O₂) in the degradation of iopamidol: Kinetics, energy requirements and DBPs-related toxicity in sequential disinfection processes. *Chemical Engineering Journal*, 398, 125570. <https://doi.org/10.1016/j.cej.2020.125570>
- Tojo, G., & Fernandez, M. (n.d.). *Oxidation of Alcohols to Aldehydes and Ketones*. Retrieved 8 March 2023, from <https://books-scholarsportal-info.ezproxy.library.yorku.ca/en/read?id=/ebooks/ebooks0/springer/2009-12-01/1/038725725X#page=11>
- United States Environmental Protection Agency. (1979). *Estimating Water Treatment Costs: Volume 2 Cost Curves Applicable to 1 to 200 MGD Treatment Plants*. EPA 815-R-05-013; EPA Office of Water.
- United States Environmental Protection Agency. (2015). *Technologies and Costs Document for the Final Long Term 2 Enhanced Surface Water Treatment Rule and Final Stage 2 Disinfectants and Disinfection Byproducts Rule*. EPA 815-R-05-013; EPA Office of Water.
- Verhoeven, S., Odegaard, C., & Hess, S. (n.d.). *Minimizing Collimated Beam Uncertainty*. 10.

Vlad, S., Anderson, W. B., Peldszus, S., & Huck, P. M. (2014). Removal of the cyanotoxin anatoxin-a by drinking water treatment processes: A review. *Journal of Water and Health*, 12(4), 601–617.

<https://doi.org/10.2166/wh.2014.018>

Wan, Q., Cao, R., Wen, G., Xu, X., Xia, Y., Wu, G., Li, Y., Wang, J., Lin, Y., & Huang, T. (2022). Sequential use of UV-LEDs irradiation and chlorine to disinfect waterborne fungal spores: Efficiency, mechanism and photoreactivation. *Journal of Hazardous Materials*, 423, 127102.

<https://doi.org/10.1016/j.jhazmat.2021.127102>

Wang, C., Moore, N., Bircher, K., Andrews, S., & Hofmann, R. (2019). Full-scale comparison of UV/H₂O₂ and UV/Cl₂ advanced oxidation: The degradation of micropollutant surrogates and the formation of disinfection byproducts. *Water Research*, 161, 448–458. <https://doi.org/10.1016/j.watres.2019.06.033>

Wang, C., Rosenfeldt, E., Li, Y., & Hofmann, R. (2020). External Standard Calibration Method To Measure the Hydroxyl Radical Scavenging Capacity of Water Samples. *Environmental Science & Technology*, 54(3), 1929–1937. <https://doi.org/10.1021/acs.est.9b06273>

Wang, W.-L., Wu, Q.-Y., Huang, N., Wang, T., & Hu, H.-Y. (n.d.). *Synergetic effect between UV and chlorine (UV/chlorine) on the degradation of CBZ: Influence factors and Radical Species*.

Water and Wastes Digest. (2018). Advanced Oxidation Process for 1,4-Dioxane Removal. *Water and Wastes Digest*.

Watts, M. J., Hofmann, R., & Rosenfeldt, E. J. (2012). Low-pressure UV/Cl² for advanced oxidation of taste and odor. *American Water Works Association. Journal*, 104(1), 47–48.

Weil, Ira., & Morris, J. Carrell. (1949). Kinetic Studies on the Chloramines. I. The Rates of Formation of Monochloramine, N-Chlormethylamine and N-Chlordimethylamine. *Journal of the American Chemical Society*, 71(5), 1664–1671. <https://doi.org/10.1021/ja01173a033>

World Health Organization. (2007). *pH in Drinking-water*. World Health Organization - Guidelines for Drinking-water Quality.

Xiujuan Kong, Jin Jiang, Jun Ma, Yi Yang, & Suyan Pang. (2018). Comparative investigation of X-ray contrast medium degradation by UV/chlorine and UV/H₂O₂. *Chemosphere*, *193*, 655–663.

Yin, R., Ling, L., & Shang, C. (2018). Wavelength-dependent chlorine photolysis and subsequent radical production using UV-LEDs as light sources. *Water Research*, *142*, 452–458.

<https://doi.org/10.1016/j.watres.2018.06.018>

Zhang, X., He, J., Xiao, S., & Yang, X. (2019). Elimination kinetics and detoxification mechanisms of microcystin-LR during UV/Chlorine process. *Chemosphere*, *214*, 702–709.

<https://doi.org/10.1016/j.chemosphere.2018.09.162>

Zhang, Z., Chuang, Y.-H., Szczuka, A., Ishida, K. P., Roback, S., Plumlee, M. H., & Mitch, W. A. (2019). Pilot-scale evaluation of oxidant speciation, 1,4-dioxane degradation and disinfection byproduct formation during UV/hydrogen peroxide, UV/free chlorine and UV/chloramines advanced oxidation process treatment for potable reuse. *Water Research*, *164*, 114939. <https://doi.org/10.1016/j.watres.2019.114939>

Zyara, A. M., Torvinen, E., Veijalainen, A.-M., & Heinonen-Tanski, H. (2016). The Effect of UV and Combined Chlorine/UV Treatment on Coliphages in Drinking Water Disinfection. *Water*, *8*(4), Article 4.

<https://doi.org/10.3390/w8040130>

Appendix A: UV Characterization Figures

Figure S. 1 and Figure S. 2 illustrate the intensity profiles of the 255 nm and 280 nm wavelengths, respectively, utilized in application of the external calibration method to UV/Cl. These intensity profiles were used to calculate the required time to achieve targeted UV doses using the method outlined in Chapter 2.5. Figure S. 3 illustrates the relative emission spectra of the wavelengths, highlighting the nominal wavelengths of 255 and 280 nm.

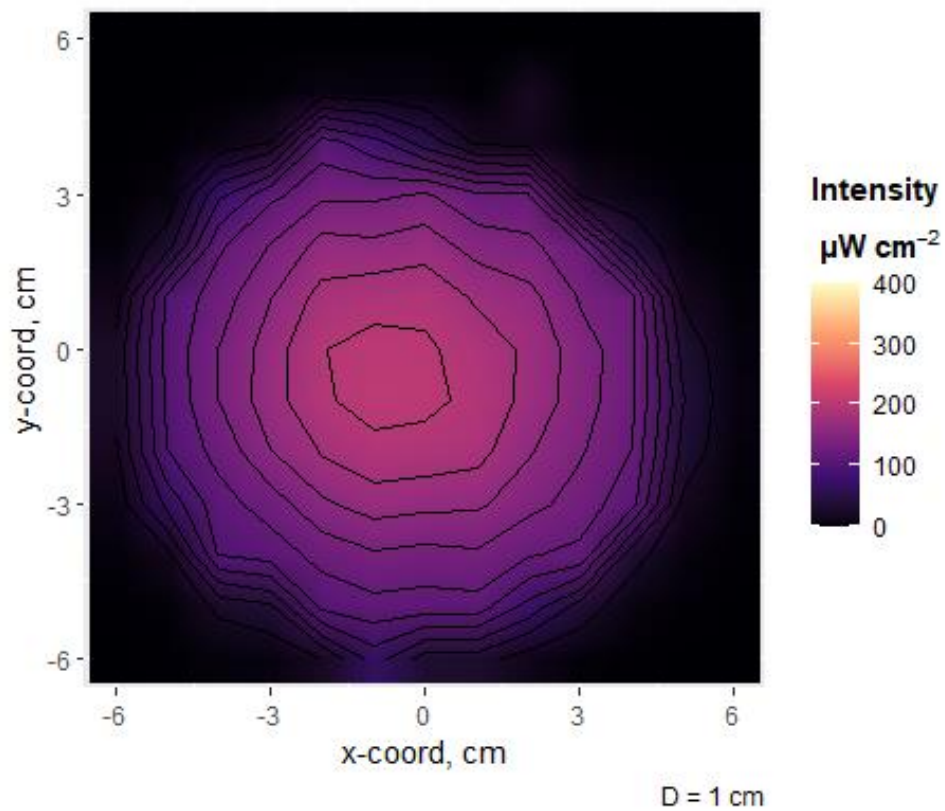


Figure S. 1: Intensity profile of the 255 nm wavelength used in experiments.

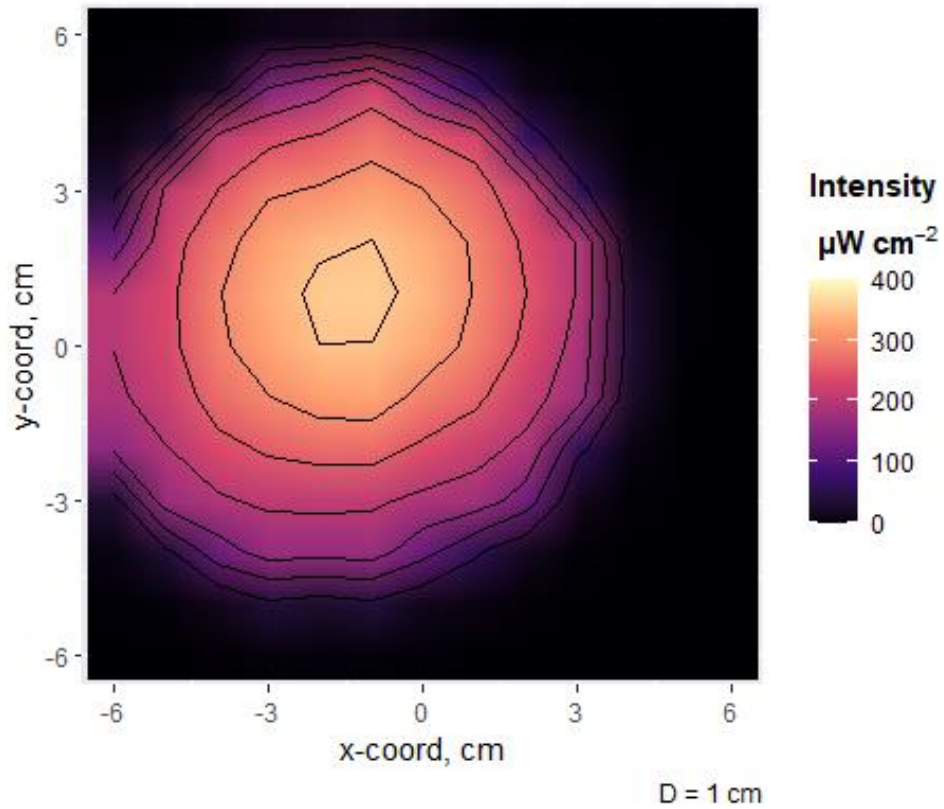


Figure S. 2: Intensity profile of the 280 nm wavelength used in experiments.

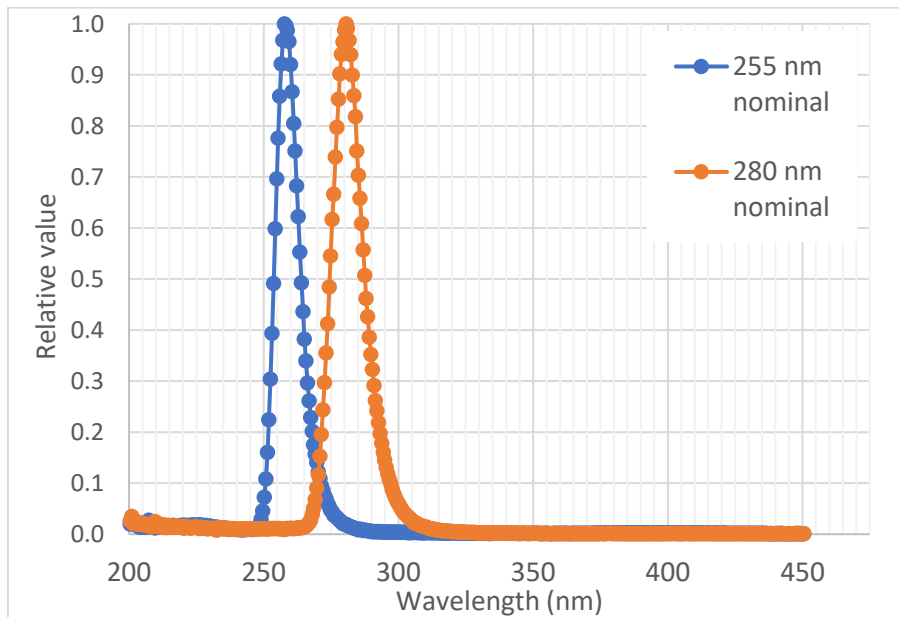


Figure S. 3: Relative emission spectra of UV LED wavelengths utilized in this study.

Appendix B: Fraction of HOCl/OCl⁻ Present in the Water Matrix

Figure S. 4 illustrates the fraction of HOCl and OCl⁻ at various pH. This figure is important in the determination of radical species present when utilizing free chlorine. HOCl is dominant at acidic pH and OCl⁻ is dominant at basic pH.

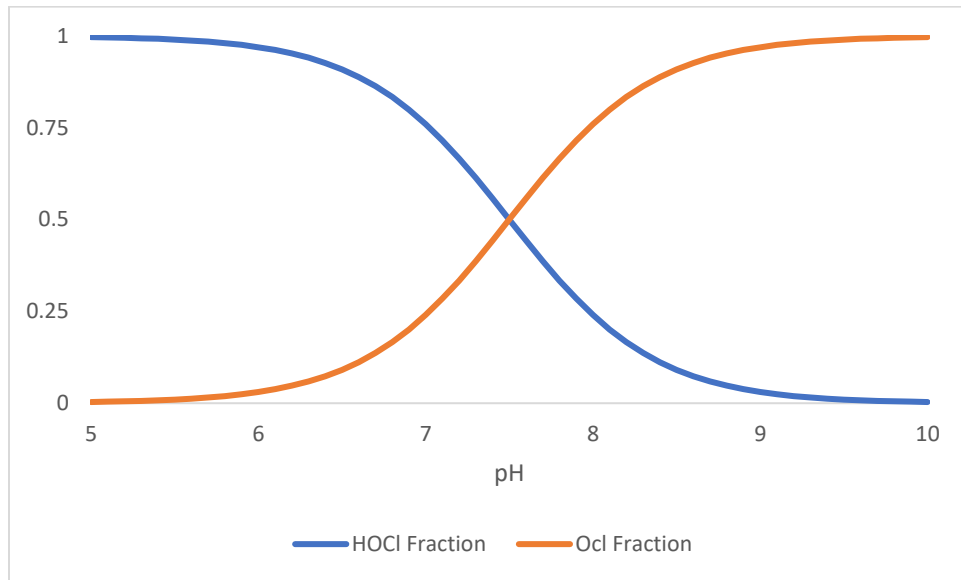


Figure S. 4: Illustration of the fraction of HOCl and OCl⁻ at various pH.

Appendix C: Methylene Blue Absorbance vs Concentration Calibration Curve

Figure S. 5 illustrates the calibration curve used to determine the concentration of methylene blue based on the absorbance reading at the dyes signature wavelength 664 nm. This curve was developed in the early summer of 2023 and validated in the winter of 2023.

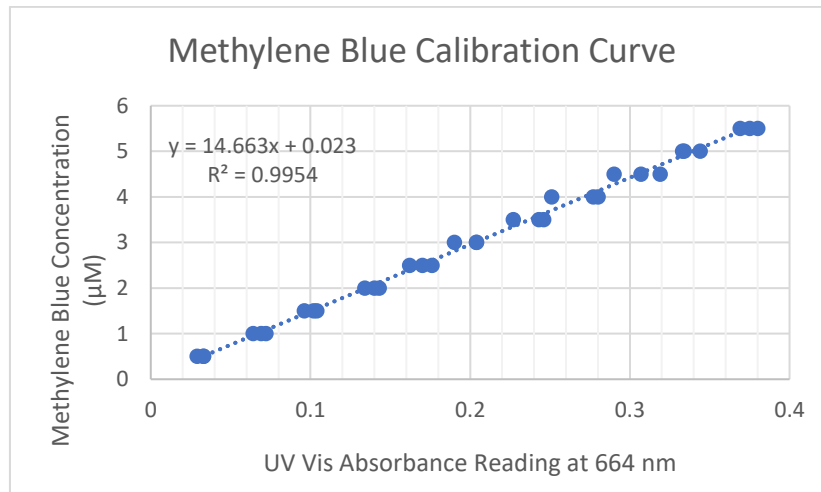


Figure S. 5: Methylene blue calibration curve.

Appendix D: Residual Free Chlorine Concentration of Treated Water Samples

To calculate the radical scavenging capacity of the treated water samples using the external calibration method, the same molar concentration of free chlorine was spiked in both treated and raw water samples. However, due to the residual free chlorine concentration in the treated water samples the concentration of free chlorine was higher than the targeted value. Figure S. 6 illustrates the residual concentration of free chlorine in the treated water samples collected from the surface water river source in southern Ontario over the time of when the experiments were conducted.

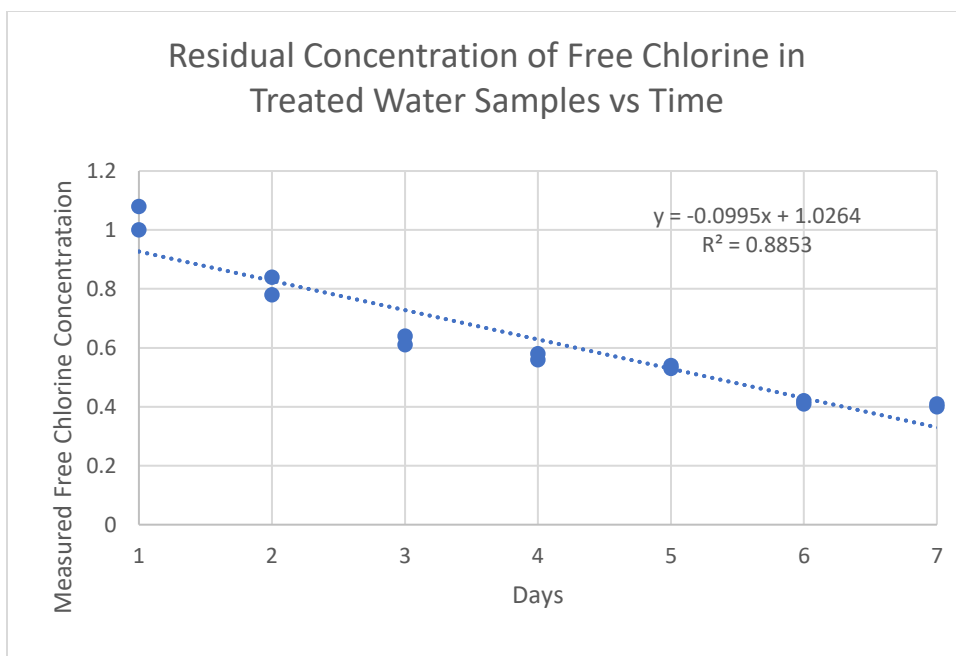


Figure S. 6: Residual concentration of free chlorine in treated water samples vs time.

Appendix E: Replicating Kwon et al., 2019

Figure S. 7 shows the of replication of the modelling results in Kwon et al., 2019. The exact same required doses were calculated for one log reduction of MC-LR which can conclude that the correct methodology was taken to predict required doses for two log reduction of MC-LR utilizing UV/H₂O₂ and UV/Cl.

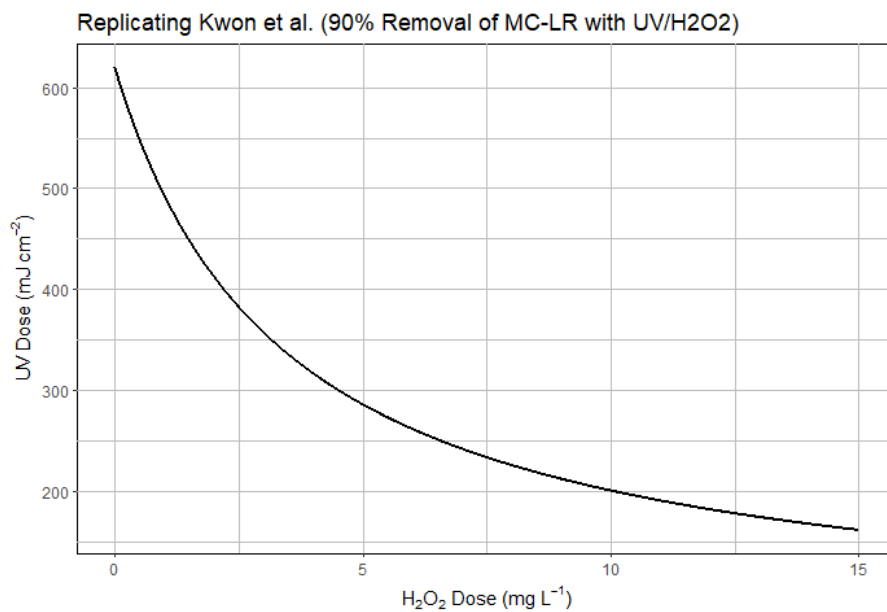


Figure S. 7: Replicating results of Kwon et al. 2019 with the exact same inputs in Equation 22. Results show the required UV and H₂O₂ doses to achieve 1-log reduction of MC-LR in a water matrix with a OH demand of $3 \times 10^4 \text{ s}^{-1}$.

Appendix F: Objective 1 RStudio Code

```
library(ggplot2)
library(tidyverse)
library(ggpubr)
library(dplyr)
library(patchwork)
library(ggpmisc)

# Manipulating H2O2 Data for figures
H2O2ExternalData <- read.csv("UVH2O2ExternalCalibrationMeanData.csv")
H2O2ExternalData <- H2O2ExternalData %>%
  mutate(Total_scavenging_capacity = (Total_scavenging_capacity/10000))

H2O2AllExternalData <- read.csv("UVH2O2ExternalCalibrationData.csv")
H2O2AllExternalData <- H2O2AllExternalData %>%
  mutate(Total_scavenging_capacity = (Total_scavenging_capacity/10000))

WangetalData <- read.csv("WangetalExternalCalibrationResults.csv")
WangetalData <- WangetalData %>%
  mutate(Scavenging_capacity = (Scavenging_capacity/10000))

H2O2RealWaterData <- read.csv("UVH2O2RealWaterSamplesExternalCalibrationData.csv")
H2O2RealWaterData <- H2O2RealWaterData %>%
  mutate(Scavenging_capacity = (Scavenging_capacity/10000))

#Manipulating Cl Data for Figures

#5mgL 500 mJ
```



```
UVCIExternalData5mg500mJ <- read.csv("UVCI5mgL500mJcm2ExternalCalibrationMeanData.csv")
```

```
UVCIExternalData5mg500mJ <- UVCIExternalData5mg500mJ %>%
```

```
  mutate(Total_scavenging_capacity = (Total_scavenging_capacity/10000))
```

```
UVCIExternalData5mg500mJ <- UVCIExternalData5mg500mJ %>%
```

```
  mutate(pH = factor(pH, levels = c("5", "7"), labels = c("pH 5", "pH 7")),
```

```
    Wavelength = factor(Wavelength, levels = c("255", "280"), labels = c("255 nm", "280 nm"))))
```

```
UVCIExternalAllData5mg500mJ <- read.csv("UVCI5mgL500mJcm2ExternalCalibrationData.csv")
```

```
UVCIExternalAllData5mg500mJ <- UVCIExternalAllData5mg500mJ %>%
```

```
  mutate(Total_scavenging_capacity = (Total_scavenging_capacity/10000))
```

```
UVCIExternalAllData5mg500mJ <- UVCIExternalAllData5mg500mJ %>%
```

```
  mutate(pH = factor(pH, levels = c("5", "7"), labels = c("pH 5", "pH 7")),
```

```
    Wavelength = factor(Wavelength, levels = c("255", "280"), labels = c("255 nm", "280 nm"))))
```

```
UVCIExternalAllData5mg500mJ %>%
```

```
  anova_test(Color_decay ~ Total_scavenging_capacity + pH + Wavelength + pH*Wavelength +  
Total_scavenging_capacity*pH + Total_scavenging_capacity*Wavelength +  
Total_scavenging_capacity*pH*Wavelength)
```

```
UVCIExternalData5mg500mJExtra <- read.csv("UVCI5mgL500mJcm2ExtraPoints.csv")
```

```
UVCIExternalData5mg500mJExtra <- UVCIExternalData5mg500mJExtra %>%
```

```
  mutate(Total_scavenging_capacity = (Total_scavenging_capacity/10000))
```

```
UVCIExternalData5mg500mJExtra <- UVCIExternalData5mg500mJExtra %>%
```

```
  mutate(pH = factor(pH, levels = c("5", "7"), labels = c("pH 5", "pH 7")),
```

```
    Wavelength = factor(Wavelength, levels = c("255", "280"), labels = c("255 nm", "280 nm"))))
```

```
#7mg 500 mJ
```

```
UVCIExternalData7mg500mJ <- read.csv("UVCI7mgL500mJcm2ExternalCalibrationMeanData.csv")
```

```

UVCIExternalData7mg500mJ <- UVCIExternalData7mg500mJ %>%
  mutate(Total_scavenging_capacity = (Total_scavenging_capacity/10000))
UVCIExternalData7mg500mJ <- UVCIExternalData7mg500mJ %>%
  mutate(pH = factor(pH, levels = c("5", "7"), labels = c("pH 5", "pH 7")),
         Wavelength = factor(Wavelength, levels = c("255", "280"), labels = c("255 nm", "280 nm")))

```

```

UVCIExternalAllData7mg500mJ <- read.csv("UVCI7mgL500mJcm2ExternalCalibrationData.csv")
UVCIExternalAllData7mg500mJ <- UVCIExternalAllData7mg500mJ %>%
  mutate(Total_scavenging_capacity = (Total_scavenging_capacity/10000))
UVCIExternalAllData7mg500mJ <- UVCIExternalAllData7mg500mJ %>%
  mutate(pH = factor(pH, levels = c("5", "7"), labels = c("pH 5", "pH 7")),
         Wavelength = factor(Wavelength, levels = c("255", "280"), labels = c("255 nm", "280 nm")))

```

```

model1 <- UVCIExternalAllData7mg500mJ %>%
  lm(Color_decay ~ Total_scavenging_capacity + pH + Wavelength + pH*Wavelength +
     Total_scavenging_capacity*pH + Total_scavenging_capacity*Wavelength +
     Total_scavenging_capacity*pH*Wavelength)

```

#5mg 1000 mJ

```

UVCIExternalData5mg1000mJ <- read.csv("UVCI5mgL1000mJcm2ExternalCalibrationMeanData.csv")
UVCIExternalData5mg1000mJ <- UVCIExternalData5mg1000mJ %>%
  mutate(Total_scavenging_capacity = (Total_scavenging_capacity/10000))
UVCIExternalData5mg1000mJ <- UVCIExternalData5mg1000mJ %>%
  mutate(pH = factor(pH, levels = c("5", "7"), labels = c("pH 5", "pH 7")),
         Wavelength = factor(Wavelength, levels = c("255", "280"), labels = c("255 nm", "280 nm")))

```

```

UVCIExternalAllData5mg1000mJ <- read.csv("UVCI5mgL1000mJcm2ExternalCalibrationData.csv")

```

```

UVCIExternalAllData5mg1000mJ <- UVCIExternalAllData5mg1000mJ %>%
  mutate(Total_scavenging_capacity = (Total_scavenging_capacity/10000))
UVCIExternalAllData5mg1000mJ <- UVCIExternalAllData5mg1000mJ %>%
  mutate(pH = factor(pH, levels = c("5", "7"), labels = c("pH 5", "pH 7")),
         Wavelength = factor(Wavelength, levels = c("255", "280"), labels = c("255 nm", "280 nm")))

UVCIExternalAllData5mg1000mJ %>%
  anova_test(Color_decay ~ Total_scavenging_capacity + pH + Wavelength + pH*Wavelength +
            Total_scavenging_capacity*pH + Total_scavenging_capacity*Wavelength +
            Total_scavenging_capacity*pH*Wavelength)

# 7 mg 1000 mJ

UVCIExternalData7mg1000mJ <- read.csv("UVCI7mgL1000mJcm2ExternalCalibrationMeanData.csv")
UVCIExternalData7mg1000mJ <- UVCIExternalData7mg1000mJ %>%
  mutate(Total_scavenging_capacity = (Total_scavenging_capacity/10000))
UVCIExternalData7mg1000mJ <- UVCIExternalData7mg1000mJ %>%
  mutate(pH = factor(pH, levels = c("5", "7"), labels = c("pH 5", "pH 7")),
         Wavelength = factor(Wavelength, levels = c("255", "280"), labels = c("255 nm", "280 nm")))

UVCIExternalAllData7mg1000mJ <- read.csv("UVCI7mgL1000mJcm2ExternalCalibrationData.csv")
UVCIExternalAllData7mg1000mJ <- UVCIExternalAllData7mg1000mJ %>%
  mutate(Total_scavenging_capacity = (Total_scavenging_capacity/10000))
UVCIExternalAllData7mg1000mJ <- UVCIExternalAllData7mg1000mJ %>%
  mutate(pH = factor(pH, levels = c("5", "7"), labels = c("pH 5", "pH 7")),
         Wavelength = factor(Wavelength, levels = c("255", "280"), labels = c("255 nm", "280 nm")))

UVCIExternalAllData7mg1000mJ %>%

```

```
anova_test(Color_decay ~ Total_scavenging_capacity + pH + Wavelength + pH*Wavelength +
Total_scavenging_capacity*pH + Total_scavenging_capacity*Wavelength +
Total_scavenging_capacity*pH*Wavelength)
```

```
#RCS
```

```
UVCIRCSData <- read.csv("UVCIRCS500mJcm2ExternalCalibrationMeanData.csv")
```

```
UVCIRCSData <- UVCIRCSData %>%
```

```
  mutate(Total_scavenging_capacity = (Total_scavenging_capacity/10000))
```

```
UVCIRCSData <- UVCIRCSData %>%
```

```
  mutate(pH = factor(pH, levels = c("5", "7"), labels = c("pH 5", "pH 7")),
```

```
         Wavelength = factor(Wavelength, levels = c("255", "280"), labels = c("255 nm", "280 nm"))))
```

```
UVCLRCSAllData <- read.csv("UVCLRCS500mJcm2ExternalCalibrationData.csv")
```

```
UVCLRCSAllData <- UVCLRCSAllData %>%
```

```
  mutate(Total_scavenging_capacity = (Total_scavenging_capacity/10000))
```

```
UVCLRCSAllData <- UVCLRCSAllData %>%
```

```
  mutate(pH = factor(pH, levels = c("5", "7"), labels = c("pH 5", "pH 7")),
```

```
         Wavelength = factor(Wavelength, levels = c("255", "280"), labels = c("255 nm", "280 nm"))))
```

```
# Dark experiments
```

```
UVCIDarkDataAll <- read.csv("UVCIDarkExperimentData.csv")
```

```
#UV CI Real Water
```

```
UVCIRRealWaterData <- read.csv("UVCIRRealWaterSamplesExternalCalibrationData.csv")
```

```
# x and y labs
```

```
x1 <- expression(Scavenging ~ Capacity ~ "(" * x10^4 ~ s^-1 * ")")
```

```
y1 <- expression(Methylene ~ Blue ~ Colour ~ Decay ~ Rate ~ "(" * s * ")")
```

```
y2 <- expression(Methylene ~ Blue ~ Log ~ Reduction)
```

```
x2 <- expression(Time ~ "(" * min * ")")
```

```

# UVH2O2 External Calibration Curve

tiff("UVH2O2ExternalCalibrationCurve.tiff", units = 'cm', width = 20, height = 10, res = 150)

ggplot()+

  geom_point(data = H2O2ExternalData, aes(x = Total_scavenging_capacity, y = Mean_color_decay,
  colour = "Experimental Data")) +

  geom_errorbar(data = H2O2ExternalData, aes(ymin = Mean_color_decay - STD, ymax =
  Mean_color_decay + STD, x = Total_scavenging_capacity), width = 0.4, colour = "Black") +

  geom_smooth(data = H2O2AllExternalData, method = "lm", aes(x = Total_scavenging_capacity, y =
  Color_decay), se = FALSE, colour = "black", linetype = 'dashed', size = 0.2) +

  stat_poly_eq(data = H2O2AllExternalData, method = "lm", aes(x = Total_scavenging_capacity, y =
  Color_decay, label = paste(stat(eq.label), stat(rr.label), sep = "*\\" ; \\"*")), size = 3, label.x.npc = "centre",
  label.y.npc = "top", colour = "black") +

  #geom_point(data = H2O2RealWaterData, aes(x = Scavenging_capacity, y = Color_decay, colour = "Lake
  Ontario Scavenging Capacity")) +

  geom_line(data = WangetalData, aes(x = Scavenging_capacity, y = Color_decay, colour = "Wang et al
  Results"), size = 0.2, linetype = "dashed") +

  scale_color_manual(values = c("Black", "Orange")) +

  labs(x = x1, y = y1, colour = "")+

  theme_bw()+

  theme(plot.title = element_text(face = "bold", size = 11, hjust = 0),
  axis.title.x = element_text(face = "bold", size = 11, vjust = 0.25),
  axis.title.y = element_text(face = "bold", size = 11, vjust = 0.25),
  axis.text.x = element_text(size = 11),
  axis.text.y = element_text(size = 11),
  strip.background = element_rect(fill = "white"),
  strip.text = element_text(size = 11),
  legend.text = element_text(size = 11),
  legend.position = NULL)

dev.off()

```

```
#UVCI 5mg/L 500mJ cm2 Calibration Curve
```

```
tiff("UVCI 5 mgL 500mJcm2 Calibration Curve.tiff", units = 'cm', width = 20, height = 10, res = 150)
```

```
ggplot()+
```

```
  geom_point(data = UVCIExternalData5mg500mJ, aes(x = Total_scavenging_capacity, y =  
Mean_color_decay, colour = "Experimental Data"), show.legend = FALSE) +
```

```
  geom_point(data = UVCIExternalData5mg500mJExtra, aes(x = Total_scavenging_capacity, y =  
Color_decay, colour = "Calculated from Equation"), show.legend = FALSE) +
```

```
  geom_errorbar(data = UVCIExternalData5mg500mJ, aes(ymin = Mean_color_decay - STD, ymax =  
Mean_color_decay + STD, x = Total_scavenging_capacity), width = 0.4, colour = "Black") +
```

```
  facet_grid( pH ~ Wavelength) +
```

```
  geom_smooth(data = UVCIExternalAllData5mg500mJ, method = "lm", aes(x =  
Total_scavenging_capacity, y = Color_decay), se = FALSE, colour = "black", linetype = 'dashed', size = 0.2)  
+
```

```
  stat_poly_eq(data = UVCIExternalAllData5mg500mJ, method = "lm", aes(x = Total_scavenging_capacity,  
y = Color_decay, label = paste(stat(eq.label), stat(rr.label), sep = "*\n ; \n*")), size = 2.4, label.x.npc =  
"centre", label.y.npc = "top", colour = "black") +
```

```
  scale_colour_manual(values = c("Grey", "Black")) +
```

```
  labs(x = x1, y = y1)+
```

```
  theme_bw()+
```

```
  theme(plot.title = element_text(face = "bold", size = 11, hjust = 0),
```

```
        axis.title.x = element_text(face = "bold", size = 11, vjust = 0.25),
```

```
        axis.title.y = element_text(face = "bold", size = 11, vjust = 0.25),
```

```
        axis.text.x = element_text(size = 11),
```

```
        axis.text.y = element_text(size = 11),
```

```
        strip.background = element_rect(fill = "white"),
```

```
        strip.text = element_text(size = 11),
```

```
        legend.text = element_text(size = 8),
```

```
        legend.position = "right")
```

```
dev.off()
```

```
#UVCI RCS Calibration Curve
```

```
tiff("UVCI RCS Calibration Curve.tiff", units ='cm', width = 20, height = 10, res = 150)

ggplot()+

  geom_point(data = UVCI RCSData, aes(x = Total_scavenging_capacity, y = Mean_color_decay,)) +

  geom_errorbar(data = UVCI RCSData, aes(ymin = Mean_color_decay - STD, ymax = Mean_color_decay +
STD, x = Total_scavenging_capacity), width = 0.4, colour = "Black") +

  facet_grid( pH ~ Wavelength) +

  geom_smooth(data = UVCI RCSAllData, method = "lm", aes(x = Total_scavenging_capacity, y =
Color_decay), se = FALSE, colour = "black", linetype = 'dashed', size = 0.2) +

  stat_poly_eq(data = UVCI RCSAllData, method = "lm", aes(x = Total_scavenging_capacity, y =
Color_decay, label = paste(stat(eq.label), stat(rr.label), sep = "*\\" ; \\"*")), size = 2.4, label.x.npc = "left",
label.y.npc = "bottom", parse = TRUE, colour = "black") +

  scale_color_manual(values = c("Black", "Blue", "Orange")) +

  labs(x = x1, y = y1)+

  theme_bw()+

  theme(plot.title = element_text(face = "bold", size = 11, hjust = 0),
        axis.title.x = element_text(face = "bold", size = 11, vjust = 0.25),
        axis.title.y = element_text(face = "bold", size = 11, vjust = 0.25),
        axis.text.x = element_text(size = 11),
        axis.text.y = element_text(size = 11),
        strip.background = element_rect(fill = "white"),
        strip.text = element_text(size = 11),
        legend.text = element_text(size = 8),
        legend.position = "right")

dev.off()
```

```
#UVCI 7mg/L 500mJ cm2 Calibration Curve
```

```
tiff("UVCI 7 mgL 500mJcm2 Calibration Curve.tiff", units ='cm', width = 20, height = 10, res = 150)
```

```

ggplot()+

  geom_point(data = UVCIExternalData7mg500mJ, aes(x = Total_scavenging_capacity, y =
Mean_color_decay,)) +

  geom_errorbar(data = UVCIExternalData7mg500mJ, aes(ymin = Mean_color_decay - STD, ymax =
Mean_color_decay + STD, x = Total_scavenging_capacity), width = 0.4, colour = "Black") +

  facet_grid( pH ~ Wavelength) +

  geom_smooth(data = UVCIExternalAllData7mg500mJ, method = "lm", aes(x =
Total_scavenging_capacity, y = Color_decay), se = FALSE, colour = "black", linetype = 'dashed', size = 0.2)
+

  stat_poly_eq(data = UVCIExternalAllData7mg500mJ, method = "lm", aes(x = Total_scavenging_capacity,
y = Color_decay, label = paste(stat(eq.label), stat(rr.label), sep = "*\ " ; "\ ")), size = 2.4, label.x.npc =
"left", label.y.npc = "bottom", colour = "black") +

  scale_color_manual(values = c("Black", "Blue", "Orange")) +

  labs(x = x1, y = y1)+

  theme_bw()+

  theme(plot.title = element_text(face = "bold", size = 11, hjust = 0),
        axis.title.x = element_text(face = "bold", size = 11, vjust = 0.25),
        axis.title.y = element_text(face = "bold", size = 11, vjust = 0.25),
        axis.text.x = element_text(size = 11),
        axis.text.y = element_text(size = 11),
        strip.background = element_rect(fill = "white"),
        strip.text = element_text(size = 11),
        legend.text = element_text(size = 8),
        legend.position = "right")

dev.off()

#UVCI 5mg/L 1000 mJ/cm2 calibration curve

tiff("UVCI 5 mgL 1000mJcm2 Calibration Curve.tiff", units = 'cm', width = 20, height = 10, res = 150)

ggplot()+

```



```

geom_point(data = UVCIExternalData5mg1000mJ, aes(x = Total_scavenging_capacity, y =
Mean_color_decay,)) +

geom_errorbar(data = UVCIExternalData5mg1000mJ, aes(ymin = Mean_color_decay - STD, ymax =
Mean_color_decay + STD, x = Total_scavenging_capacity), width = 0.4, colour = "Black") +

facet_grid( pH ~ Wavelength) +

geom_smooth(data = UVCIExternalAllData5mg1000mJ, method = "lm", aes(x =
Total_scavenging_capacity, y = Color_decay), se = FALSE, colour = "black", linetype = 'dashed', size = 0.2)
+

stat_poly_eq(data = UVCIExternalAllData5mg1000mJ, method = "lm", aes(x =
Total_scavenging_capacity, y = Color_decay, label = paste(stat(eq.label), stat(rr.label), sep = "*\" ; \"*\")),
size = 2.4, label.x.npc = "left", label.y.npc = "bottom", colour = "black") +

scale_color_manual(values = c("Black", "Blue", "Orange")) +

labs(x = x1, y = y1)+

theme_bw()+

theme(plot.title = element_text(face = "bold", size = 11, hjust = 0),
      axis.title.x = element_text(face = "bold", size = 11, vjust = 0.25),
      axis.title.y = element_text(face = "bold", size = 11, vjust = 0.25),
      axis.text.x = element_text(size = 11),
      axis.text.y = element_text(size = 11),
      strip.background = element_rect(fill = "white"),
      strip.text = element_text(size = 11),
      legend.text = element_text(size = 8),
      legend.position = "right")

dev.off()

#UVCI 7mg/L 1000mJ cm2 Calibration Curve

tiff("UVCI 7 mgL 1000mJcm2 Calibration Curve.tiff", units = 'cm', width = 20, height = 10, res = 150)

ggplot()+

geom_point(data = UVCIExternalData7mg1000mJ, aes(x = Total_scavenging_capacity, y =
Mean_color_decay,)) +

```

```

geom_errorbar(data = UVCIExternalData7mg1000mJ, aes(ymin = Mean_color_decay - STD, ymax =
Mean_color_decay + STD, x = Total_scavenging_capacity), width = 0.4, colour = "Black") +

facet_grid( pH ~ Wavelength) +

geom_smooth(data = UVCIExternalAllData7mg1000mJ, method = "lm", aes(x =
Total_scavenging_capacity, y = Color_decay), se = FALSE, colour = "black", linetype = 'dashed', size = 0.2)
+

stat_poly_eq(data = UVCIExternalAllData7mg1000mJ, method = "lm", aes(x =
Total_scavenging_capacity, y = Color_decay, label = paste(stat(eq.label), stat(rr.label), sep = "*\\" ; \\"*")),
size = 2.4, label.x.npc = "left", label.y.npc = "bottom", colour = "black") +

scale_color_manual(values = c("Black", "Blue", "Orange")) +

labs(x = x1, y = y1)+

theme_bw()+

theme(plot.title = element_text(face = "bold", size = 11, hjust = 0),
      axis.title.x = element_text(face = "bold", size = 11, vjust = 0.25),
      axis.title.y = element_text(face = "bold", size = 11, vjust = 0.25),
      axis.text.x = element_text(size = 11),
      axis.text.y = element_text(size = 11),
      strip.background = element_rect(fill = "white"),
      strip.text = element_text(size = 11),
      legend.text = element_text(size = 8),
      legend.position = "right")

dev.off()

# Degradation / log reduction figures

#5mgL 500 mJ

UVCIDegradationAllData5mg500mJ <- read.csv("UVCI5mgL500mJcm2DegradationData.csv")
UVCIDegradationAllData5mg500mJ <- UVCIDegradationAllData5mg500mJ %>%
mutate(Total_scavenging_capacity_summary = (Total_scavenging_capacity_summary/10000))

```

```

UVCIDegradationAllData5mg500mJ <- UVCIDegradationAllData5mg500mJ %>%
  mutate(pH_summary = factor(pH_summary, levels = c("5", "7"), labels = c("pH 5", "pH 7")),
         Wavelength_summary = factor(Wavelength_summary, levels = c("255", "280"), labels = c("255 nm",
"280 nm")))
#Plot

tiff("UVCIDegradationAllData5mg500mJcm2 Degradation Curve.tiff", units = 'cm', width = 20, height = 10, res = 150)

ggplot()+
  geom_point(data = UVCIDegradationAllData5mg500mJ, aes(x = Total_scavenging_capacity_summary, y
= Mean_log_reduction, color = Optimal)) +
  geom_errorbar(data = UVCIDegradationAllData5mg500mJ, aes(ymin = Mean_log_reduction -
Mean_log_reduction_STD, ymax = Mean_log_reduction + Mean_log_reduction_STD, x =
Total_scavenging_capacity_summary, color = Optimal), width = 0.4) +
  facet_grid( pH_summary ~ Wavelength_summary) +
  geom_smooth(data = UVCIDegradationAllData5mg500mJ, method = "lm", aes(x =
Total_scavenging_capacity_summary, y = Mean_log_reduction, color = Optimal), se = FALSE, linetype =
'dashed', size = 0.2) +
  stat_poly_eq(data = UVCIDegradationAllData5mg500mJ, method = "lm", aes(x =
Total_scavenging_capacity_summary, y = Mean_log_reduction, label = paste(stat(eq.label), stat(rr.label),
sep = "*\ " ; \ "*"")), size = 2.4, label.x.npc = "centre", label.y.npc = "top", colour = "black") +
  scale_color_manual(values = c("Dark Blue", "Dark Red")) +
  labs(x = x1, y = y2, color = "Legend")+
  theme_bw()+
  theme(plot.title = element_text(face = "bold", size = 11, hjust = 0),
        axis.title.x = element_text(face = "bold", size = 11, vjust = 0.25),
        axis.title.y = element_text(face = "bold", size = 11, vjust = 0.25),
        axis.text.x = element_text(size = 11),
        axis.text.y = element_text(size = 11),
        strip.background = element_rect(fill = "white"),
        strip.text = element_text(size = 11),
        legend.text = element_text(size = 8),
        legend.position = "right")

```

```

dev.off()

#7mg 500 mJ

UVCIDegradationAllData7mg500mJ <- read.csv("UVCI7mgL500mJcm2DegradationData.csv")
UVCIDegradationAllData7mg500mJ <- UVCIDegradationAllData7mg500mJ %>%
  mutate(Total_scavenging_capacity_summary = (Total_scavenging_capacity_summary/10000))
UVCIDegradationAllData7mg500mJ <- UVCIDegradationAllData7mg500mJ %>%
  mutate(pH_summary = factor(pH_summary, levels = c("5", "7"), labels = c("pH 5", "pH 7")),
         Wavelength_summary = factor(Wavelength_summary, levels = c("255", "280"), labels = c("255 nm",
"280 nm")))
#Plot

tiff("UVCI 7 mgL 500mJcm2 Degradation Curve.tiff", units = 'cm', width = 20, height = 10, res = 150)

ggplot()+
  geom_point(data = UVCIDegradationAllData7mg500mJ, aes(x = Total_scavenging_capacity_summary, y
= Mean_log_reduction, color = Optimal)) +
  geom_errorbar(data = UVCIDegradationAllData7mg500mJ, aes(ymin = Mean_log_reduction -
Mean_log_reduction_STD, ymax = Mean_log_reduction + Mean_log_reduction_STD, x =
Total_scavenging_capacity_summary, color = Optimal), width = 0.4) +
  facet_grid( pH_summary ~ Wavelength_summary) +
  geom_smooth(data = UVCIDegradationAllData7mg500mJ, method = "lm", aes(x =
Total_scavenging_capacity_summary, y = Mean_log_reduction, color = Optimal), se = FALSE, linetype =
'dashed', size = 0.2) +
  stat_poly_eq(data = UVCIDegradationAllData7mg500mJ, method = "lm", aes(x =
Total_scavenging_capacity_summary, y = Mean_log_reduction, label = paste(stat(eq.label), stat(rr.label),
sep = "*\\" ; \\"*")), size = 2.4, label.x.npc = "centre", label.y.npc = "top", colour = "black") +
  scale_color_manual(values = c("Dark Blue", "Dark Red")) +
  labs(x = x1, y = y2, color = "Legend")+
  theme_bw()+
  theme(plot.title = element_text(face = "bold", size = 11, hjust = 0),
        axis.title.x = element_text(face = "bold", size = 11, vjust = 0.25),

```

```

axis.title.y = element_text(face = "bold", size = 11, vjust = 0.25),
axis.text.x = element_text(size = 11),
axis.text.y = element_text(size = 11),
strip.background = element_rect(fill = "white"),
strip.text = element_text(size = 11),
legend.text = element_text(size = 8),
legend.position = "right")
dev.off()

#5mg 1000 mJ

UVCIDegradationAllData5mg1000mJ <- read.csv("UVCI5mgL1000mJcm2DegradationData.csv")
UVCIDegradationAllData5mg1000mJ <- UVCIDegradationAllData5mg1000mJ %>%
  mutate(Total_scavenging_capacity_summary = (Total_scavenging_capacity_summary/10000))
UVCIDegradationAllData5mg1000mJ <- UVCIDegradationAllData5mg1000mJ %>%
  mutate(pH_summary = factor(pH_summary, levels = c("5", "7"), labels = c("pH 5", "pH 7")),
         Wavelength_summary = factor(Wavelength_summary, levels = c("255", "280"), labels = c("255 nm",
"280 nm")))
#Plot

tiff("UVCI 5 mgL 1000mJcm2 Degradation Curve.tiff", units = 'cm', width = 20, height = 10, res = 150)
ggplot()+
  geom_point(data = UVCIDegradationAllData5mg1000mJ, aes(x = Total_scavenging_capacity_summary,
y = Mean_log_reduction, color = Optimal)) +
  geom_errorbar(data = UVCIDegradationAllData5mg1000mJ, aes(ymin = Mean_log_reduction -
Mean_log_reduction_STD, ymax = Mean_log_reduction + Mean_log_reduction_STD, x =
Total_scavenging_capacity_summary, color = Optimal), width = 0.4) +
  facet_grid( pH_summary ~ Wavelength_summary) +

```

```

geom_smooth(data = UVCIDegradationAllData5mg1000mJ, method = "lm", aes(x =
Total_scavenging_capacity_summary, y = Mean_log_reduction, color = Optimal), se = FALSE, linetype =
'dashed', size = 0.2) +

stat_poly_eq(data = UVCIDegradationAllData5mg1000mJ, method = "lm", aes(x =
Total_scavenging_capacity_summary, y = Mean_log_reduction, label = paste(stat(eq.label), stat(rr.label),
sep = "*\" ; \")"), size = 2.4, label.x.npc = "centre", label.y.npc = "top", colour = "black") +

scale_color_manual(values = c("Dark Blue", "Dark Red")) +

labs(x = x1, y = y2, color = "Legend")+

theme_bw()+

theme(plot.title = element_text(face = "bold", size = 11, hjust = 0),
      axis.title.x = element_text(face = "bold", size = 11, vjust = 0.25),
      axis.title.y = element_text(face = "bold", size = 11, vjust = 0.25),
      axis.text.x = element_text(size = 11),
      axis.text.y = element_text(size = 11),
      strip.background = element_rect(fill = "white"),
      strip.text = element_text(size = 11),
      legend.text = element_text(size = 8),
      legend.position = "right")

dev.off()

# 7 mg 1000 mJ

UVCIDegradationAllData7mg1000mJ <- read.csv("UVCI7mgL1000mJcm2DegradationData.csv")
UVCIDegradationAllData7mg1000mJ <- UVCIDegradationAllData7mg1000mJ %>%
  mutate(Total_scavenging_capacity_summary = (Total_scavenging_capacity_summary/10000))
UVCIDegradationAllData7mg1000mJ <- UVCIDegradationAllData7mg1000mJ %>%
  mutate(pH_summary = factor(pH_summary, levels = c("5", "7"), labels = c("pH 5", "pH 7")),
         Wavelength_summary = factor(Wavelength_summary, levels = c("255", "280"), labels = c("255 nm",
"280 nm")))

#Plot

```

```

tiff("UVCI 7 mgL 1000mJcm2 Degradation Curve.tiff", units = 'cm', width = 20, height = 10, res = 150)

ggplot()+

  geom_point(data = UVCIDegradationAllData7mg1000mJ, aes(x = Total_scavenging_capacity_summary,
y = Mean_log_reduction, color = Optimal)) +

  geom_errorbar(data = UVCIDegradationAllData7mg1000mJ, aes(ymin = Mean_log_reduction -
Mean_log_reduction_STD, ymax = Mean_log_reduction + Mean_log_reduction_STD, x =
Total_scavenging_capacity_summary, color = Optimal), width = 0.4) +

  facet_grid( pH_summary ~ Wavelength_summary) +

  geom_smooth(data = UVCIDegradationAllData7mg1000mJ, method = "lm", aes(x =
Total_scavenging_capacity_summary, y = Mean_log_reduction, color = Optimal), se = FALSE, linetype =
'dashed', size = 0.2) +

  stat_poly_eq(data = UVCIDegradationAllData7mg1000mJ, method = "lm", aes(x =
Total_scavenging_capacity_summary, y = Mean_log_reduction, label = paste(stat(eq.label), stat(rr.label),
sep = "*\\" ; \\"*")), size = 2.4, label.x.npc = "centre", label.y.npc = "top", colour = "black") +

  scale_color_manual(values = c("Dark Blue", "Dark Red")) +

  labs(x = x1, y = y2, color = "Legend")+

  theme_bw()+

  theme(plot.title = element_text(face = "bold", size = 11, hjust = 0),
        axis.title.x = element_text(face = "bold", size = 11, vjust = 0.25),
        axis.title.y = element_text(face = "bold", size = 11, vjust = 0.25),
        axis.text.x = element_text(size = 11),
        axis.text.y = element_text(size = 11),
        strip.background = element_rect(fill = "white"),
        strip.text = element_text(size = 11),
        legend.text = element_text(size = 8),
        legend.position = "right")

dev.off()

#RCS

UVCIDegradationAllDataRCS <- read.csv("UVCI RCS500mJcm2DegradationData.csv")

```

```

UVCIDegradationAllDataRCS <- UVCIDegradationAllDataRCS %>%
  mutate(Total_scavenging_capacity_summary = (Total_scavenging_capacity_summary/10000))
UVCIDegradationAllDataRCS <- UVCIDegradationAllDataRCS %>%
  mutate(pH_summary = factor(pH_summary, levels = c("5", "7"), labels = c("pH 5", "pH 7")),
         Wavelength_summary = factor(Wavelength_summary, levels = c("255", "280"), labels = c("255 nm",
"280 nm")))
#Plot

tiff("UVCI RCS Degradation Curve.tiff", units = 'cm', width = 20, height = 10, res = 150)

ggplot()+
  geom_point(data = UVCIDegradationAllDataRCS, aes(x = Total_scavenging_capacity_summary, y =
Mean_log_reduction, color = Optimal)) +
  geom_errorbar(data = UVCIDegradationAllDataRCS, aes(ymin = Mean_log_reduction -
Mean_log_reduction_STD, ymax = Mean_log_reduction + Mean_log_reduction_STD, x =
Total_scavenging_capacity_summary, color = Optimal), width = 0.4) +
  facet_grid( pH_summary ~ Wavelength_summary) +
  geom_smooth(data = UVCIDegradationAllDataRCS, method = "lm", aes(x =
Total_scavenging_capacity_summary, y = Mean_log_reduction, color = Optimal), se = FALSE, linetype =
'dashed', size = 0.2) +
  stat_poly_eq(data = UVCIDegradationAllDataRCS, method = "lm", aes(x =
Total_scavenging_capacity_summary, y = Mean_log_reduction, label = paste(stat(eq.label), stat(rr.label),
sep = "*\\" ; \\"*")), size = 2.4, label.x.npc = "centre", label.y.npc = "top", colour = "black") +
  scale_color_manual(values = c("Dark Blue", "Dark Red")) +
  labs(x = x1, y = y2, color = "Legend")+
  theme_bw()+
  theme(plot.title = element_text(face = "bold", size = 11, hjust = 0),
        axis.title.x = element_text(face = "bold", size = 11, vjust = 0.25),
        axis.title.y = element_text(face = "bold", size = 11, vjust = 0.25),
        axis.text.x = element_text(size = 11),
        axis.text.y = element_text(size = 11),
        strip.background = element_rect(fill = "white"),
        strip.text = element_text(size = 11),

```



```

    legend.text = element_text(size = 8),
    legend.position = "right")
dev.off()

# Real Water Samples

#UVCI 7mg/L 500mJ cm2 Calibration Curve with real water samples

UVCIRealWaterData7mgL500mJcm2 <- UVCIRealWaterData %>%
  filter(RCS == "No")
UVCIRealWaterData7mgL500mJcm2 <- UVCIRealWaterData7mgL500mJcm2 %>%
  mutate(Total_scavenging_capacity = Total_scavenging_capacity/10000,
         pH = factor(pH, levels = c("5", "7"), labels = c("pH 5", "pH 7")),
         Wavelength = factor(Wavelength, levels = c("255", "280"), labels = c("255 nm", "280 nm")))

tiff("UVCI Real Water Samples Calibration Curve.tiff", units='cm', width = 20, height = 10, res = 150)
ggplot()+
  geom_point(data = UVCIExternalData7mg500mJ, aes(x = Total_scavenging_capacity, y =
Mean_color_decay), size = 1.5) +
  geom_errorbar(data = UVCIExternalData7mg500mJ, aes(ymin = Mean_color_decay - STD, ymax =
Mean_color_decay + STD, x = Total_scavenging_capacity), width = 1, colour = "Black") +
  geom_point(data = UVCIRealWaterData7mgL500mJcm2, aes(x = Total_scavenging_capacity, y =
Color_decay, colour = Raw_Treated)) +
  facet_grid( pH ~ Wavelength) +
  geom_smooth(data = UVCIExternalAllData7mg500mJ, method = "lm", aes(x =
Total_scavenging_capacity, y = Color_decay), se = FALSE, colour = "black", linetype = 'dashed', size = 0.2)
+
  #stat_poly_eq(data = UVCIExternalAllData7mg500mJ, method = "lm", aes(x =
Total_scavenging_capacity, y = Color_decay, label = paste(stat(eq.label), stat(rr.label), sep = "*\\" ; \\"*")),
size = 2.4, label.x.npc = "left", label.y.npc = "bottom", colour = "black") +

```

```

scale_color_manual(values = c("Orange", "Blue")) +
labs(x = x1, y = y1, colour = "Legend")+
theme_bw()+
theme(plot.title = element_text(face = "bold", size = 11, hjust = 0),
      axis.title.x = element_text(face = "bold", size = 11, vjust = 0.25),
      axis.title.y = element_text(face = "bold", size = 11, vjust = 0.25),
      axis.text.x = element_text(size = 11),
      axis.text.y = element_text(size = 11),
      strip.background = element_rect(fill = "white"),
      strip.text = element_text(size = 11),
      legend.text = element_text(size = 8),
      legend.position = "right")
dev.off()

#UVCI RCS Calibration Curve with real water samples

UVCIRealWaterDataRCS <- UVCIRealWaterData %>%
  filter(RCS == "Yes")
UVCIRealWaterDataRCS <- UVCIRealWaterDataRCS %>%
  mutate(Total_scavenging_capacity = Total_scavenging_capacity/10000,
         pH = factor(pH, levels = c("5", "7"), labels = c("pH 5", "pH 7")),
         Wavelength = factor(Wavelength, levels = c("255", "280"), labels = c("255 nm", "280 nm")))

tiff("UVCI RCS Real Water Samples Calibration Curve.tiff", units = 'cm', width = 20, height = 10, res = 150)
ggplot()+
  geom_point(data = UVCIRCSData, aes(x = Total_scavenging_capacity, y = Mean_color_decay), size = 1.5)
+
  geom_errorbar(data = UVCIRCSData, aes(ymin = Mean_color_decay - STD, ymax = Mean_color_decay +
STD, x = Total_scavenging_capacity), width = 1, colour = "Black") +

```

```

geom_point(data = UVCIRealWaterDataRCS, aes(x = Total_scavenging_capacity, y = Color_decay, colour
= Raw_Treated)) +

facet_grid( pH ~ Wavelength) +

geom_smooth(data = UVCLRCSAllData, method = "lm", aes(x = Total_scavenging_capacity, y =
Color_decay), se = FALSE, colour = "black", linetype = 'dashed', size = 0.2) +

#stat_poly_eq(data = UVCLRCSAllData, method = "lm", aes(x = Total_scavenging_capacity, y =
Color_decay, label = paste(stat(eq.label), stat(rr.label), sep = "*\\" ; \\"*")), size = 2.4, label.x.npc = "left",
label.y.npc = "bottom", colour = "black") +

scale_color_manual(values = c("Orange", "Blue")) +

labs(x = x1, y = y1, colour = "Legend")+

theme_bw()+

theme(plot.title = element_text(face = "bold", size = 11, hjust = 0),
      axis.title.x = element_text(face = "bold", size = 11, vjust = 0.25),
      axis.title.y = element_text(face = "bold", size = 11, vjust = 0.25),
      axis.text.x = element_text(size = 11),
      axis.text.y = element_text(size = 11),
      strip.background = element_rect(fill = "white"),
      strip.text = element_text(size = 11),
      legend.text = element_text(size = 8),
      legend.position = "right")

dev.off()

# Real Water Samples Log reduction

UVCIRealWaterDegradationData <- read.csv("UVCIRealWaterSamplesDegradationData.csv")
UVCIRealWaterDegradationData <- UVCIRealWaterDegradationData %>%
  filter(RCS == "No")
UVCIRealWaterDegradationData <- UVCIRealWaterDegradationData %>%
  mutate(pH = factor(pH, levels = c("5", "7"), labels = c("pH 5", "pH 7")),
         Wavelength = factor(Wavelength, levels = c("255", "280"), labels = c("255 nm", "280 nm")))

```

```

tiff("UVCI Real Water Samples Degradation.tiff", units = 'cm', width = 20, height = 10, res = 150)

ggplot() +

  geom_bar(data = UVCIRealWaterDegradationData, stat = "identity", aes(y = Mean_log_reduction, x =
Raw_Treated, fill = Raw_Treated), show.legend = FALSE) +

  geom_errorbar(data = UVCIRealWaterDegradationData, aes(ymin = Mean_log_reduction -
Log_reduction_STD, ymax = Mean_log_reduction + Log_reduction_STD, x = Raw_Treated), colour = "Dark
Red", width = 0.3, size = 0.5) +

  facet_grid(pH ~ Wavelength)+

  scale_fill_manual(values = c("Black", "Dark Grey")) +

  labs(y = y2, x = NULL) +

theme_bw()+

  theme(plot.title = element_text(face = "bold", size = 11, hjust = 0),
        axis.title.x = element_text(face = "bold", size = 11, vjust = 0.25),
        axis.title.y = element_text(face = "bold", size = 11, vjust = 0.25),
        axis.text.x = element_text(size = 11),
        axis.text.y = element_text(size = 11),
        strip.background = element_rect(fill = "white"),
        strip.text = element_text(size = 11),
        legend.text = element_text(size = 8),
        legend.position = "right")

dev.off()

UVCIRealWaterDegradationDataRCS <- read.csv("UVCIRealWaterSamplesDegradationData.csv")
UVCIRealWaterDegradationDataRCS <- UVCIRealWaterDegradationDataRCS %>%
  filter(RCS == "Yes")
UVCIRealWaterDegradationDataRCS <- UVCIRealWaterDegradationDataRCS %>%
  mutate(pH = factor(pH, levels = c("5", "7"), labels = c("pH 5", "pH 7")),
        Wavelength = factor(Wavelength, levels = c("255", "280"), labels = c("255 nm", "280 nm")))

```

```

tiff("UVCI RCS Real Water Samples Degradation.tiff", units = 'cm', width = 20, height = 10, res = 150)

ggplot() +

  geom_bar(data = UVCIRealWaterDegradationDataRCS, stat = "identity", aes(y = Mean_log_reduction, x
= Raw_Treated, fill = Raw_Treated), show.legend = FALSE) +

  geom_errorbar(data = UVCIRealWaterDegradationDataRCS, aes(ymin = Mean_log_reduction -
Log_reduction_STD, ymax = Mean_log_reduction + Log_reduction_STD, x = Raw_Treated), colour = "Dark
Red", width = 0.3, size = 0.5) +

  facet_grid(pH ~ Wavelength)+

  scale_fill_manual(values = c("Black", "Dark Grey")) +

  labs(y = y2, x = NULL) +

  theme_bw()+

  theme(plot.title = element_text(face = "bold", size = 11, hjust = 0),
        axis.title.x = element_text(face = "bold", size = 11, vjust = 0.25),
        axis.title.y = element_text(face = "bold", size = 11, vjust = 0.25),
        axis.text.x = element_text(size = 11),
        axis.text.y = element_text(size = 11),
        strip.background = element_rect(fill = "white"),
        strip.text = element_text(size = 11),
        legend.text = element_text(size = 8),
        legend.position = "right")

dev.off()

# Dark experiments

UVCIDarkData <- read.csv("UVCIDarkExperimentDataSummary.csv")

UVCIDarkData <- UVCIDarkData %>%

  mutate(pH = factor(pH, levels = c("5", "7"), labels = c("pH 5", "pH 7")),
        HOCl = factor(HOCl, levels = c("5", "7"), labels = c("5 mg/L", "7 mg/L")))

UVCIDarkData5mgL <- UVCIDarkData %>%

  filter(HOCl == "5 mg/L")

```

```

UVCIDarkDataAll <- UVCIDarkDataAll %>%
  mutate(pH = factor(pH, levels = c("5", "7"), labels = c("pH 5", "pH 7")),
         HOCl = factor(HOCl, levels = c("5", "7"), labels = c("5 mg/L", "7 mg/L")))

UVCIDarkDataAll0 <- UVCIDarkDataAll %>%
  filter(TBA == "No" & NB == "No")

UVCIDarkDataAll0 %>%
  anova_test(Log_reduction ~ Time + pH + HOCl + Time*HOCl + Time*pH + pH*HOCl + Time*HOCl*pH)

tiff("Dark Experiments.tiff", units = 'cm', width = 20, height = 10, res = 150)

ggplot() +
  geom_point(data = UVCIDarkData, aes(y = Mean_log_reduction, x = Time_summary), colour = "Black")
+
  geom_errorbar(data = UVCIDarkData, aes(ymin = Mean_log_reduction - Mean_log_reduction_STD,
    ymax = Mean_log_reduction + Mean_log_reduction_STD, x = Time_summary), colour = "Black", width =
    0.3,) +
  geom_smooth(data = UVCIDarkDataAll, method = "lm", aes(x = Time, y = Log_reduction), se = FALSE,
    colour = "black", linetype = 'dashed', size = 0.2) +
  stat_poly_eq(data = UVCIDarkDataAll, method = "lm", aes(x = Time, y = Log_reduction, label =
    paste(stat(eq.label), stat(rr.label), sep = "*\ " ; "\ ")), size = 2.4, label.x.npc = "centre", label.y.npc =
    "bottom", colour = "black") +
  facet_grid(pH ~ HOCl)+
  labs(y = y2, x = x2) +
  theme_bw()+
  theme(plot.title = element_text(face = "bold", size = 11, hjust = 0),
        axis.title.x = element_text(face = "bold", size = 11, vjust = 0.25),
        axis.title.y = element_text(face = "bold", size = 11, vjust = 0.25),
        axis.text.x = element_text(size = 11),
        axis.text.y = element_text(size = 11),

```

```

strip.background = element_rect(fill = "white"),
strip.text = element_text(size = 11),
legend.text = element_text(size = 8),
legend.position = "right")
dev.off()

# Percent contribution

percentMBdegradation <- read.csv("UVCIPercentContribution.csv")
percentMBdegradation <- percentMBdegradation %>%
  mutate(pH = factor(pH, levels = c("5", "7"), labels = c("pH 5", "pH 7")),
         Wavelength = factor(Wavelength, levels = c("255", "280"), labels = c("255 nm", "280 nm")))
y3 <- expression(Percentage ~ of ~ Total ~ First ~ Order ~ Rate ~ Constant ~ "(" * s^-1 * ")")

tiff("Percent MB Degradation.tiff", units = 'cm', width = 20, height = 10, res = 150)

ggplot()+
  geom_col(data = percentMBdegradation, aes (x = pH, y = Percent_contribution, fill = Component),
  colour = "black")+
  scale_fill_brewer(palette = "Spectral")+
  labs(x = NULL, y = y3 )+
  theme_bw()+
  theme(plot.title = element_text(face = "bold", size = 11, hjust = 0),
        axis.title.x = element_text(face = "bold", size = 11, vjust = 0.25),
        axis.title.y = element_text(face = "bold", size = 11, vjust = 0.25),
        axis.text.x = element_text(size = 11, angle = 0),
        axis.text.y = element_text(size = 11),
        strip.background = element_rect(fill = "white"),
        strip.text = element_text(size = 11),
        legend.text = element_text(size = 11),

```

```
    legend.title = element_blank()+  
  facet_wrap(~Wavelength)  
dev.off()
```


Appendix G: Objective 2 RStudio Code

```
library(ggplot2)
library(tidyverse)
library(ggpubr)
library(ggrepel)
install.packages("installr")
library(installr)
updateR()

EH2O2 <- 18.7
phiOH <- 1.0
OHRSC1 <- 3*10^4
OHRSC2 <- 8*10^4
kohH2O2 <- 2.7*10^7
kOH <- 11*10^9
H2O2 <- seq(2.9*10^-5, 7.35*10^-4, by = 0.0000001)
U <- 471
phim <- 0.0610
Em <- 12445
H2O2_mgL <- H2O2 * 1000 * 34.0147
H2O2_kgm <- H2O2_mgL * 0.001

Ki1 = kOH * ((EH2O2 * H2O2 * phiOH * log(10))/(U * (OHRSC1 + kohH2O2 * H2O2)))
Ki2 = kOH * ((EH2O2 * H2O2 * phiOH * log(10))/(U * (OHRSC2 + kohH2O2 * H2O2)))
kd <- 3.71

Ha <- (log(100))/((Ki1+kd))
Hb <- (log(100))/((Ki2+kd))
```

```
H1 <- Ha*1000
```

```
H2 <- Hb*1000
```

```
x1 <- expression(H[2]*O[2]* ~ Dose ~ "(" * mg ~ L^-1 * ")")
```

```
y1 <- expression(UV ~ Dose ~ "(" * mJ ~ cm^-2 * ")")
```

```
tiff("Required Doses UVH2O2.tiff", units = 'cm', width = 20, height = 15, res = 300)
ggplot(data = NULL, aes(x = H2O2_mgL)) +
  geom_line(aes(y = H1, group = 1L, colour = "Low OH Demand"), size = 1) +
  geom_line(aes(y = H2, group = 1L, colour = "High OH Demand"), size = 1) +
  scale_color_manual(values = c("Light Blue", "Green")) +
  scale_x_continuous(breaks = c(0, 5, 10, 15, 20, 25), labels = c(0, 5, 10, 15, 20, 25)) +
  xlab(x1)+
  ylab(y1) +
  theme(panel.background = element_rect(fill = "White", colour = "white", siz =0.5,
    linetype = "solid", color = "black"),
    panel.grid.minor = element_line(size = 0.01, colour = "grey"),
    panel.grid.major = element_line(colour = "grey", size = 0.01)) +
  labs(title = "Required UV and Oxidant Doses for 99% Removal of MC-LR with UV/H2O2",
    colour = "Legend")+
  theme(legend.justification = c("right", "top"),
    legend.key = element_rect(fill =NA))
dev.off()
```

```
plot1
```

```
l <- 0.1
```

```

a <- 0.01
WF <- (1-10^(-a*I))/(a*I*log(10))
n <- 0.30
EED1 = (((2.78*10^-7)*(10*H1/WF))/(I*n))+10.62*H2O2_kgm)
EED2 = (((2.78*10^-7)*(10*H2/WF))/(I*n))+10.62*H2O2_kgm)

table1<- data.frame(H1, H2O2_mgL, EED1)
table2 <- data.frame(H2, H2O2_mgL, EED2)

optimum1 <- min(EED1)
optimum2 <- min(EED2)

tiff("Optimum UV and Oxidant Doses UVH2O2.tif", units='cm', width = 20, height = 15, res = 300)
ggplot(data = NULL, aes(x = H2O2_mgL)) +
  geom_line(aes(y = H1, group =1L, colour = "Low RSC"), linetype = "solid", size = 1) +
  geom_line(aes(y = H2, group =1L, colour = "High RSC"), size = 1) +
  geom_point(aes(x = 2.4, y = 776, colour = "Min EED")) +
  geom_point(aes(x = 1, y = 1130, colour = "Min EED")) +
  scale_color_manual(values = c("Light Blue", "Green", "Black")) +
  guides(color = guide_legend(override.aes = list(linetype = c(1, 1, 0)))) +
  geom_text_repel(aes(x = 2.4, y = 776, label = "(2.4 mg/L, 776 mJ/cm^2)")) +
  geom_text_repel(aes(x = 1, y = 1130, label = "(1 mg/L, 1130 mJ/cm^2)")) +
  scale_x_continuous(breaks = c(0, 5, 10, 15, 20, 25), labels = c(0, 5, 10, 15, 20, 25)) +
  xlab(x1)+
  ylab(y1) +
  theme(panel.background = element_rect(fill = "White", colour = "white", siz =0.5,
    linetype = "solid", color = "black"),
    panel.grid.minor = element_line(size = 0.01, colour = "grey"),
    panel.grid.major = element_line(colour = "grey", size = 0.01)) +

```

```

labs(title = "Optimum UV and Oxidant Doses for 99% Removal of MC-LR with UV/H2O2",
      colour = "Legend",
      shape = "Legend")+
theme(legend.justification = c("right", "top"),
      legend.key = element_rect(fill = NA))
dev.off()
library(ggplot2)
library(tidyverse)
library(ggpubr)
library(ggrepel)

EHOCl <- 80
phiOH <- 1.0
phiCl <- 0.28
OHRSC1 <- 3*10^4
OHRSC2 <- 8*10^4
CIRSC <- 1.14*10^4
kohHOCl <- 2*10^9
kClHOCl <- 3*10^9
kOH <- 11*10^9
kCl <- 2.25*10^10
HOCl <- seq(1.9*10^-5, 1.9*10^-4, by = 0.0000001)
U <- 471
phim <- 0.0610
Em <- 12445
HOCl_mgL <- HOCl * 1000 * 52.46
HOCl_kgm <- HOCl_mgL * 0.001

```

```
Ki1 = KOH * ((EHOCl * HOCl * phiOH * log(10))/(U * (OHRSC1 + kohHOCl * HOCl))) + kCl * ((EHOCl * HOCl * phiCl * log(10))/(U * (ClRSC + kClHOCl * HOCl)))
```

```
Ki2 = KOH * ((EHOCl * HOCl * phiOH * log(10))/(U * (OHRSC2 + kohHOCl * HOCl))) + kCl * ((EHOCl * HOCl * phiCl * log(10))/(U * (ClRSC + kClHOCl * HOCl)))
```

```
kd <- 3.71
```

```
Ha <- (log(100))/((Ki1+kd))
```

```
Hb <- (log(100))/((Ki2+kd))
```

```
H1 <- Ha*1000
```

```
H2 <- Hb*1000
```

```
x1 <- expression(HOCl * ~ Dose ~ "(" * mg ~ L^-1 * ")")
```

```
y1 <- expression(UV ~ Dose ~ "(" * mJ ~ cm^-2 * ")")
```

```
tiff("Required Doses UVCl.tiff", units = 'cm', width = 20, height = 15, res = 300)
```

```
ggplot(data = NULL, aes(x = HOCl_mgL)) +
```

```
  geom_line(aes(y = H1, group = 1L, colour = "Low OH Demand"), size = 1) +
```

```
  geom_line(aes(y = H2, group = 1L, colour = "High OH Demand"), size = 1) +
```

```
  scale_color_manual(values = c("Light Blue", "Green")) +
```

```
  scale_x_continuous(breaks = c(0, 2, 4, 6, 8, 10), labels = c(0, 2, 4, 6, 8, 10)) +
```

```
  xlab(x1)+
```

```
  ylab(y1) +
```

```
  theme(panel.background = element_rect(fill = "White", colour = "white", siz =0.5,
```

```
        linetype = "solid", color = "black"),
```

```
        panel.grid.minor = element_line(size = 0.01, colour = "grey"),
```

```
        panel.grid.major = element_line(colour = "grey", size = 0.01)) +
```

```
  labs(title = "Required UV and Oxidant Doses for 99% Removal of MC-LR with UV/Cl",
```

```
        colour = "Legend")+
```

```

theme(legend.justification = c("right", "top"),
      legend.key = element_rect(fill =NA))
dev.off()

plot1

l <- 0.1
a <- 0.04
WF <- (1-10^(-a*l))/(a*l*log(10))
n <- 0.30
EED1 = (((2.78*10^-7)*(10*H1/WF))/(l*n))+3.38*HOCl_kgm)
EED2 = (((2.78*10^-7)*(10*H2/WF))/(l*n))+3.38*HOCl_kgm

table1<- data.frame(H1, HOCl_mgL, EED1)
table2 <- data.frame(H2, HOCl_mgL, EED2)

optimum1 <- min(EED1)
optimum2 <- min(EED2)

tiff("Optimum Doses UVCl.tiff", units ='cm', width = 20, height = 15, res = 300)
ggplot(data = NULL, aes(x = HOCl_mgL)) +
  geom_line(aes(y = H1, group =1L, colour = "Low RSC"), size = 1) +
  geom_line(aes(y = H2, group =1L, colour = "High RSC"), size = 1) +
  geom_point(aes(x = 2.40, y = 820, colour = "Min EED")) +
  geom_point(aes(x = 1.86, y = 772, colour = "Min EED")) +
  scale_color_manual(values = c("Light Blue", "Green", "Black")) +
  guides(color = guide_legend(override.aes = list(linetype = c(1, 1, 0)))) +
  geom_text_repel(aes(x = 1.86, y = 772, label = "(1.86 mg/L, 772 mJ/cm^2)")) +

```

```

geom_text_repel(aes(x = 2.40, y = 820, label = "(2.40 mg/L, 820 mJ/cm^2)")) +
scale_x_continuous(breaks = c(0, 2, 4, 6, 8, 10), labels = c(0, 2, 4, 6, 8, 10)) +
xlab(x1)+
ylab(y1) +
theme(panel.background = element_rect(fill = "White", colour = "white", siz =0.5,
linetype = "solid", color = "black"),
panel.grid.minor = element_line(size = 0.01, colour = "grey"),
panel.grid.major = element_line(colour = "grey", size = 0.01)) +
labs(title = "Optimum UV and Oxidant Doses for 99% Removal of MC-LR with UV/Cl (pH = 7)",
colour = "Legend")+
theme(legend.justification = c("right", "top"),
legend.key =element_rect(fill =NA))
dev.off()

```

```
##### pH 5
```

```

EHOCl <- 50
phiOH <- 1.4
phiCl <- 0.8
OHRSC1 <- 3*10^4
OHRSC2 <- 8*10^4
ClRSC <- 1.14*10^4
kohHOCl <- 2*10^9
kClHOCl <- 3*10^9
kOH <- 11*10^9
kCl <- 2.25*10^10
HOCl <- seq(1.9*10^-5, 1.9*10^-4, by = 0.0000001)

```

```

U <- 471
phim <- 0.0610
Em <- 12445
HOCl_mgL <- HOCl * 1000 * 52.46
HOCl_kgm <- HOCl_mgL * 0.001

Ki1 = kOH * ((EHOCl * HOCl * phiOH * log(10))/(U * (OHRSC1 + kohHOCl * HOCl))) + kCl * ((EHOCl * HOCl
* phiCl * log(10))/(U * (ClRSC + kClHOCl * HOCl)))

Ki2 = kOH * ((EHOCl * HOCl * phiOH * log(10))/(U * (OHRSC2 + kohHOCl * HOCl))) + kCl * ((EHOCl * HOCl
* phiCl * log(10))/(U * (ClRSC + kClHOCl * HOCl)))

kd <- 3.71

Ha <- (log(100))/((Ki1+kd))
Hb <- (log(100))/((Ki2+kd))
H1 <- Ha*1000
H2 <- Hb*1000

x1 <- expression(HOCl ~ Dose ~ "(" * mg ~ L^-1 * ")")
y1 <- expression(UV ~ Dose ~ "(" * mJ ~ cm^-2 * ")")

l <- 0.1
a <- 0.04
WF <- (1-10^(-a*l))/(a*l*log(10))
n <- 0.30
EED1 = (((2.78*10^-7)*(10*H1/WF))/(l*n))+3.38*HOCl_kgm
EED2 = (((2.78*10^-7)*(10*H2/WF))/(l*n))+3.38*HOCl_kgm

table1<- data.frame(H1, HOCl_mgL, EED1)
table2 <- data.frame(H2, HOCl_mgL, EED2)

```



```

optimum1 <- min(EED1)
optimum2 <- min(EED2)

tiff("Optimum Doses UVCl ph5.tiff", units = 'cm', width = 20, height = 15, res = 300)
ggplot(data = NULL, aes(x = HOCl_mgL)) +
  geom_line(aes(y = H1, group = 1L, colour = "Low RSC"), size = 1) +
  geom_line(aes(y = H2, group = 1L, colour = "High RSC"), size = 1) +
  geom_point(aes(x = 2.08, y = 770, colour = "Min EED")) +
  geom_point(aes(x = 1.72, y = 730, colour = "Min EED")) +
  scale_color_manual(values = c("Light Blue", "Green", "Black")) +
  guides(color = guide_legend(override.aes = list(linetype = c(1, 1, 0)))) +
  geom_text_repel(aes(x = 1.72, y = 730, label = "(1.72 mg/L, 730 mJ/cm^2)")) +
  geom_text_repel(aes(x = 2.08, y = 770, label = "(2.08 mg/L, 770 mJ/cm^2)")) +
  scale_x_continuous(breaks = c(0, 2, 4, 6, 8, 10), labels = c(0, 2, 4, 6, 8, 10)) +
  xlab(x1)+
  ylab(y1) +
  theme(panel.background = element_rect(fill = "White", colour = "white", siz =0.5,
    linetype = "solid", color = "black"),
    panel.grid.minor = element_line(size = 0.01, colour = "grey"),
    panel.grid.major = element_line(colour = "grey", size = 0.01)) +
  labs(title = "Optimum UV and Oxidant Doses for 99% Removal of MC-LR with UV/Cl (pH = 5) ",
    colour = "Legend")+
  theme(legend.justification = c("right", "top"),
    legend.key =element_rect(fill =NA))
dev.off()

```

Appendix H: Objective 3 RStudio Code

```
library(tidyverse)
library(ggsci)
library(RColorBrewer)

#UV/CI

UVCI_data <- read.csv("Unit cost data_UVCI.csv") %>%
  mutate(Cl_dose = factor(Cl_dose, levels = c("1.86", "2.4"), labels = c("1.86 mg/L", "2.4 mg/L")))

data_cap_UVCI <- UVCI_data %>%
  filter(Type == "Direct_cap")

data_OM_UVCI <- UVCI_data %>%
  filter(Type == "OM")

# mutate(Short_cost = (Cost/52)*8, Short_upper = (Cost_upper/52)*8, Short_lower =
(Cost_lower/52)*8)

tiff("Unit_cost_curve_UVCI_capital.tif", units = 'cm', width = 20, height = 15, res = 300)

ggplot(data = data_cap_UVCI, aes(x = Design_flow_mld))+
  geom_line(aes(y = Cost/1000000), size = 1.5)+
  geom_line(aes(y = Cost_upper/1000000), colour = "red", alpha = 0.75, linetype = 'dashed', size = 0.75)+
  geom_line(aes(y = Cost_lower/1000000), colour = "green", alpha = 0.75, linetype = 'dashed', size =
0.75)+
```

```

facet_wrap(~Radical_scavenging_capacity)+
# xlim(0,80)+
ylim(0, 1750) +
labs(x = 'Design flow rate (MLD)', y = 'Direct capital cost (MCAD)', title = NULL)+
theme_bw()+
theme(plot.title = element_text(face = "bold", size = 20, hjust = 0),
      axis.title.x = element_text(face = "bold", size = 20, vjust = 0.25),
      axis.title.y = element_text(face = "bold", size = 20, vjust = 0.25),
      axis.text.x = element_text(size = 20, angle = 90),
      axis.text.y = element_text(size = 20),
      strip.background = element_rect(fill = "white"),
      strip.text = element_text(size = 20),
      legend.position = "none")
dev.off()

tiff("Unit_cost_curve_UVCI_OMI.tif", units='cm', width = 20, height = 15, res = 300)
ggplot(data = data_OM_UVCI)+
  geom_line(aes(x = Design_flow_mld, y = Cost/1000000), size = 1.5)+
  geom_line(aes(x = Design_flow_mld, y = Cost_upper/1000000), colour = "Red", alpha = 1, linetype =
'dashed', size = 1)+
  geom_line(aes(x = Design_flow_mld, y = Cost_lower/1000000), colour = "Green", alpha = 1, linetype =
'dashed', size = 1)+
  labs(x = 'Design flow rate (MLD)', y = 'O&M cost (MCAD)',)+
  theme_bw()+
  theme(plot.title = element_text(face = "bold", size = 20, hjust = 0.5),
        axis.title.x = element_text(face = "bold", size = 20, vjust = 0.25),
        axis.title.y = element_text(face = "bold", size = 20, vjust = 0.25),
        axis.text.x = element_text(size = 20, angle = 90),
        axis.text.y = element_text(size = 20),

```

```

strip.background = element_rect(fill = "white"),
strip.text = element_text(size = 20),
legend.position = "none")+
facet_wrap(~Radical_scavenging_capacity)+
#xlim(0, 80)+
ylim(0, 55)
dev.off()

#Seasonal
tiff("Unit_cost_curve_UVCI_OM_seasonal.tif", units = 'cm', width = 20, height = 15, res = 300)
ggplot(data = data_OM_UVCI)+
  geom_line(aes(x = Design_flow_mld, y = Cost/1000000/2), size = 1.5)+
  geom_line(aes(x = Design_flow_mld, y = Cost_upper/1000000/2), colour = "Red", alpha = 1, linetype =
'dashed', size = 1)+
  geom_line(aes(x = Design_flow_mld, y = Cost_lower/1000000/2), colour = "Green", alpha = 1, linetype
= 'dashed', size = 1)+
  labs(x = 'Design flow rate (MLD)', y = 'O&M cost (MCAD)',)+
  theme_bw()+
  theme(plot.title = element_text(face = "bold", size = 20, hjust = 0.5),
        axis.title.x = element_text(face = "bold", size = 20, vjust = 0.25),
        axis.title.y = element_text(face = "bold", size = 20, vjust = 0.25),
        axis.text.x = element_text(size = 20, angle = 90),
        axis.text.y = element_text(size = 20),
        strip.background = element_rect(fill = "white"),
        strip.text = element_text(size = 20),
        legend.position = "none")+
  facet_wrap(~Radical_scavenging_capacity)+
  #xlim(0, 80)+
  ylim(0, 30)

```

```

#UVH2O2
UVH2O2_data <- read.csv("Unit cost data_UVH2O2.csv") %>%
  mutate(H2O2_dose = factor(H2O2_dose, levels = c("1", "2.4"),
    labels = c("1 mg/L", "2.4 mg/L")))

data_cap_UVH2O2 <- UVH2O2_data %>%
  filter(Type == "Direct_cap", Source == "USEPA_2003")

data_cap_UVH2O2_Plumlee <- UVH2O2_data %>%
  filter(Type == "Direct_cap", Source == "Plumlee_2014")

#data_small_cap_UVH2O2 <- data_cap_UVH2O2 %>%
# filter(Size == "Small")

#data_large_cap_UVH2O2 <- data_cap_UVH2O2 %>%
# filter(Size == "Large")

data_OM_UVH2O2 <- UVH2O2_data %>%
  filter(Type == "OM", Source == "USEPA_2003")

#data_small_OM_UVH2O2 <- data_OM_UVH2O2 %>%
# filter(Size == "Small")

#data_large_OM_UVH2O2 <- data_OM_UVH2O2 %>%
# filter(Size == "Large")

```

```

#data_OM_UVH2O2_USEPA1 <- UVH2O2_data %>%
# filter(Type == "OM", Source == "USEPA_2003", H2O2_dose == "5 mg/L")

data_OM_UVH2O2_Plumlee <- UVH2O2_data %>%
  filter(Type == "OM", Source == "Plumlee_2014")

DWRG_UVH2O2 <-UVH2O2_data

Real_cost <- read.csv("Real_costs.csv")

tiff("Cost_curve_UVH2O2_Cap_LowOH Demand.tif", units ='cm', width = 20, height = 15, res = 300)
ggplot()+
  geom_line(data = subset(data_cap_UVH2O2, Radical_scavenging_capacity == "Low RSC"),aes(x =
Design_flow_mlpd, y =CAD_cost), size = 1.5)+
  geom_line(data = subset(data_cap_UVH2O2, Radical_scavenging_capacity == "Low RSC"),aes(x =
Design_flow_mlpd, y = CAD_cost_upper),colour = "Red", alpha = 0.75, linetype = 'dashed', size = 0.75)+
  geom_line(data = subset(data_cap_UVH2O2, Radical_scavenging_capacity == "Low RSC"),aes(x =
Design_flow_mlpd, y = CAD_cost_lower), colour = "Green", alpha = 0.75, linetype = 'dashed', size =
0.75)+
  geom_point(data = subset(Real_cost, Source == "A"),aes(x = Capacity, y = Cost_2023_MCAD), colour =
"#A73030FF", shape = 15, size = 5)+
  geom_point(data = subset(Real_cost, Source == "B"),aes(x = Capacity, y = Cost_2023_MCAD), colour =
"#3B3B3BFF", shape = 16, size = 5)+
  geom_point(data = subset(Real_cost, Source == "C"),aes(x = Capacity, y = Cost_2023_MCAD), colour =
"#A73030FF", shape = 17, size = 5)+
  geom_point(data = subset(Real_cost, Source == "D"),aes(x = Capacity, y = Cost_2023_MCAD), colour =
"#A73030FF", shape = 18, size = 5)+
  #geom_point(data = subset(Real_cost, Source == "E"),aes(x = Capacity, y = Cost_2023_MCAD), colour =
"#A73030FF", shape = 19, size = 5)+
  geom_point(data = subset(Real_cost, Source == "F"),aes(x = Capacity, y = Cost_2023_MCAD), colour =
"#3B3B3BFF", shape = 3, size = 5)+

```

```

geom_point(data = subset(Real_cost, Source == "G"),aes(x = Capacity, y = Cost_2023_MCAD), colour =
"#3B3B3BFF", shape = 4, size = 5)+

geom_point(data = subset(Real_cost, Source == "H"),aes(x = Capacity, y = Cost_2023_MCAD), colour =
"#3B3B3BFF", shape = 5, size = 5)+

labs(x = 'Design flow rate (MLD)', y = 'Direct capital cost (MCAD)', title = "Low RSC UV/H2O2 Capital
Costs")+

ylim(0,300)+

xlim(0,305)+

theme_bw()+

theme(plot.title = element_text(face = "bold", size = 20, hjust = 0),
      axis.title.x = element_text(face = "bold", size = 20, vjust = 0.25),
      axis.title.y = element_text(face = "bold", size = 20, vjust = 0.25),
      axis.text.x = element_text(size = 20, angle = 90),
      axis.text.y = element_text(size = 20),
      strip.background = element_rect(fill = "white"),
      strip.text = element_text(size = 20),
      legend.position = "none")

dev.off()

tiff("Cost_curve_UVH2O2_Cap_HighOH Demand.tif", units = 'cm', width = 20, height = 15, res = 300)

ggplot()+

  geom_line(data = subset(data_cap_UVH2O2, Radical_scavenging_capacity == "High RSC"),aes(x =
Design_flow_mlpd, y = CAD_cost), size = 1.5)+

  geom_line(data = subset(data_cap_UVH2O2, Radical_scavenging_capacity == "High RSC"),aes(x =
Design_flow_mlpd, y = CAD_cost_upper),colour = "Red", alpha = 0.75, linetype = 'dashed', size = 0.75)+

  geom_line(data = subset(data_cap_UVH2O2, Radical_scavenging_capacity == "High RSC"),aes(x =
Design_flow_mlpd, y = CAD_cost_lower), colour = "Green", alpha = 0.75, linetype = 'dashed', size =
0.75)+

  geom_point(data = subset(Real_cost, Source == "A"),aes(x = Capacity, y = Cost_2023_MCAD), colour =
"#A73030FF", shape = 15, size = 5)+

  geom_point(data = subset(Real_cost, Source == "B"),aes(x = Capacity, y = Cost_2023_MCAD), colour =
"#3B3B3BFF", shape = 16, size = 5)+

```

```

geom_point(data = subset(Real_cost, Source == "C"),aes(x = Capacity, y = Cost_2023_MCAD), colour =
"#A73030FF", shape = 17, size = 5)+

geom_point(data = subset(Real_cost, Source == "D"),aes(x = Capacity, y = Cost_2023_MCAD), colour =
"#A73030FF", shape = 18, size = 5)+

geom_point(data = subset(Real_cost, Source == "F"),aes(x = Capacity, y = Cost_2023_MCAD), colour =
"#3B3B3BFF", shape = 3, size = 5)+

geom_point(data = subset(Real_cost, Source == "G"),aes(x = Capacity, y = Cost_2023_MCAD), colour =
"#3B3B3BFF", shape = 4, size = 5)+

geom_point(data = subset(Real_cost, Source == "H"),aes(x = Capacity, y = Cost_2023_MCAD), colour =
"#3B3B3BFF", shape = 5, size = 5)+

labs(x = 'Design flow rate (MLD)', y = 'Direct capital cost (MCAD)', title = "High RSC UV/H2O2 Capital
Costs")+

ylim(0,500)+

xlim(0,305)+

theme_bw()+

theme(plot.title = element_text(face = "bold", size = 20, hjust = 0),
      axis.title.x = element_text(face = "bold", size = 20, vjust = 0.25),
      axis.title.y = element_text(face = "bold", size = 20, vjust = 0.25),
      axis.text.x = element_text(size = 20, angle = 90),
      axis.text.y = element_text(size = 20),
      strip.background = element_rect(fill = "white"),
      strip.text = element_text(size = 20),
      legend.position = "none")

dev.off()

tiff("Cost_curve_UVH2O2_Cap_Facet.tif", units = 'cm', width = 20, height = 15, res = 300)

ggplot()+

geom_line(data = subset(data_cap_UVH2O2),aes(x = Design_flow_mlpd, y = CAD_cost), size = 1.5)+

geom_line(data = subset(data_cap_UVH2O2),aes(x = Design_flow_mlpd, y = CAD_cost_upper),colour =
"Red", alpha = 0.75, linetype = 'dashed', size = 0.75)+

geom_line(data = subset(data_cap_UVH2O2),aes(x = Design_flow_mlpd, y = CAD_cost_lower), colour =
"Green", alpha = 0.75, linetype = 'dashed', size = 0.75)+

```



```

facet_wrap(~Radical_scavenging_capacity) +
labs(x = 'Design flow rate (MLD)', y = 'Direct capital cost (MCAD)')+
theme_bw()+
theme(plot.title = element_text(face = "bold", size = 20, hjust = 0),
      axis.title.x = element_text(face = "bold", size = 20, vjust = 0.25),
      axis.title.y = element_text(face = "bold", size = 20, vjust = 0.25),
      axis.text.x = element_text(size = 20, angle = 90),
      axis.text.y = element_text(size = 20),
      strip.background = element_rect(fill = "white"),
      strip.text = element_text(size = 20),
      legend.position = "none")
dev.off()

tiff("Cost_curve_UVH2O2_OM_Facet.tif", units = 'cm', width = 20, height = 15, res = 300)

ggplot()+
  geom_line(data = subset(data_OM_UVH2O2),aes(x = Design_flow_mlpd, y = CAD_cost), size = 1.5)+
  geom_line(data = subset(data_OM_UVH2O2),aes(x = Design_flow_mlpd, y = CAD_cost_upper),colour =
"Red", alpha = 0.75, linetype = 'dashed', size = 0.75)+
  geom_line(data = subset(data_OM_UVH2O2),aes(x = Design_flow_mlpd, y = CAD_cost_lower), colour =
"Green", alpha = 0.75, linetype = 'dashed', size = 0.75)+
  facet_wrap(~Radical_scavenging_capacity) +
  labs(x = 'Design flow rate (MLD)', y = 'OM cost (MCAD)')+
  theme_bw()+
  theme(plot.title = element_text(face = "bold", size = 20, hjust = 0),
        axis.title.x = element_text(face = "bold", size = 20, vjust = 0.25),
        axis.title.y = element_text(face = "bold", size = 20, vjust = 0.25),
        axis.text.x = element_text(size = 20, angle = 90),
        axis.text.y = element_text(size = 20),
        strip.background = element_rect(fill = "white"),

```

```

strip.text = element_text(size = 20),
legend.position = "none")
dev.off()

tiff("Cost_curve_UVH2O2_OM_all.tif", units = 'cm', width = 22, height = 15, res = 300)

ggplot()+

  geom_line(data = subset(data_OM_UVH2O2, Source == "USEPA_2003"), aes(x = Design_flow_mlpd, y =
Short_cost), colour = "#E31837", size = 1.5)+

  geom_line(data = subset(data_OM_UVH2O2, Source == "USEPA_2003"), aes(x = Design_flow_mlpd, y =
Short_upper), colour = "#E31837", alpha = 0.75, linetype = 'dashed', size = 1)+

  geom_line(data = subset(data_OM_UVH2O2, Source == "USEPA_2003"), aes(x = Design_flow_mlpd, y =
Short_lower), colour = "#E31837", alpha = 0.75, linetype = 'dashed', size = 1)+

  geom_line(data = subset(data_OM_UVH2O2, Source == "USEPA_2003"), aes(x = Design_flow_mlpd, y =
Cost), colour = "#264578", size = 1.5)+

  geom_line(data = subset(data_OM_UVH2O2, Source == "USEPA_2003"), aes(x = Design_flow_mlpd, y =
Cost_upper), colour = "#264578", alpha = 1, linetype = 'dashed', size = 1)+

  geom_line(data = subset(data_OM_UVH2O2, Source == "USEPA_2003"), aes(x = Design_flow_mlpd, y =
Cost_lower), colour = "#264578", alpha = 1, linetype = 'dashed', size = 1)+

  labs(x = 'Design flow rate (MLD)', y = 'OM cost (MUSD)', title = 'Hydrogen peroxide dose')+

  theme_bw()+

  theme(plot.title = element_text(face = "bold", size = 20, hjust = 0.5),
        axis.title.x = element_text(face = "bold", size = 20, vjust = 0.25),
        axis.title.y = element_text(face = "bold", size = 20, vjust = 0.25),
        axis.text.x = element_text(size = 20, angle = 90),
        axis.text.y = element_text(size = 20),
        strip.background = element_rect(fill = "white"),
        strip.text = element_text(size = 20),
        legend.position = "none")+

  facet_wrap(~H2O2_dose)

dev.off()

```

```

tiff("Cost_curve_UVH2O2_OM_USEPA1.tif", units = 'cm', width = 7, height = 10, res = 150)

ggplot()+

  geom_line(data = data_OM_UVH2O2_USEPA1, aes(x = Design_flow_mgd, y = Cost), colour =
"#3B3B3BFF", size = 0.5)+

  geom_line(data = data_OM_UVH2O2_USEPA1, aes(x = Design_flow_mgd, y = Cost_upper), colour =
"#3B3B3BFF", alpha = 0.75, linetype = 'dashed', size = 0.5)+

  geom_line(data = data_OM_UVH2O2_USEPA1, aes(x = Design_flow_mgd, y = Cost_lower), colour =
"#3B3B3BFF", alpha = 0.75, linetype = 'dashed', size = 0.5)+

  labs(x = 'Design flow rate (MGD)', y = NULL, title = "A")+

  ylim(0,6)+

  xlim(0,80)+

  theme_bw()+

  theme(plot.title = element_text(face = "bold", size = 11, hjust = 0),
        axis.title.x = element_text(face = "bold", size = 11, vjust = 0.25),
        axis.title.y = element_text(face = "bold", size = 11, vjust = 0.25),
        axis.text.x = element_text(size = 11, angle = 90),
        axis.text.y = element_text(size = 11),
        strip.background = element_rect(fill = "white"),
        strip.text = element_text(size = 11),
        legend.position = "none")

dev.off()

```

```

tiff("Cost_curve_UVH2O2_OM_Plumlee.tif", units = 'cm', width = 7, height = 10, res = 150)

ggplot()+

  geom_line(data = data_OM_UVH2O2_Plumlee, aes(x = Design_flow_mgd, y = Cost), colour =
"#0073C2FF", size = 0.5)+

  geom_line(data = data_OM_UVH2O2_Plumlee, aes(x = Design_flow_mgd, y = Cost_upper), colour =
"#0073C2FF", alpha = 0.75, linetype = 'dashed', size = 0.5)+

  geom_line(data = data_OM_UVH2O2_Plumlee, aes(x = Design_flow_mgd, y = Cost_lower), colour =
"#0073C2FF", alpha = 0.75, linetype = 'dashed', size = 0.5)+

```

```

labs(x = 'Design flow rate (MGD)', y = NULL, title = "B")+
ylim(0,6)+
xlim(0,80)+
theme_bw()+
theme(plot.title = element_text(face = "bold", size = 11, hjust = 0),
      axis.title.x = element_text(face = "bold", size = 11, vjust = 0.25),
      axis.title.y = element_text(face = "bold", size = 11, vjust = 0.25),
      axis.text.x = element_text(size = 11, angle = 90),
      axis.text.y = element_text(size = 11),
      strip.background = element_rect(fill = "white"),
      strip.text = element_text(size = 11),
      legend.position = "none")
dev.off()

#seasonal

tiff("Cost_curve_UVH2O2_OM_Facet_seasonal.tif", units = 'cm', width = 20, height = 15, res = 300)
ggplot()+
  geom_line(data = subset(data_OM_UVH2O2), aes(x = Design_flow_mlpd, y = CAD_cost/2), size = 1.5)+
  geom_line(data = subset(data_OM_UVH2O2), aes(x = Design_flow_mlpd, y = CAD_cost_upper/2), colour
= "Red", alpha = 0.75, linetype = 'dashed', size = 0.75)+
  geom_line(data = subset(data_OM_UVH2O2), aes(x = Design_flow_mlpd, y = CAD_cost_lower/2), colour
= "Green", alpha = 0.75, linetype = 'dashed', size = 0.75)+
  facet_wrap(~Radical_scavenging_capacity) +
  labs(x = 'Design flow rate (MLD)', y = 'OM cost (MCAD)')+
  theme_bw()+
  theme(plot.title = element_text(face = "bold", size = 20, hjust = 0),
        axis.title.x = element_text(face = "bold", size = 20, vjust = 0.25),
        axis.title.y = element_text(face = "bold", size = 20, vjust = 0.25),

```

```

axis.text.x = element_text(size = 20, angle = 90),
axis.text.y = element_text(size = 20),
strip.background = element_rect(fill = "white"),
strip.text = element_text(size = 20),
legend.position = "none") +
ylim(0,30)
dev.off()
library(tidyverse)
library(ggsci)
library(RColorBrewer)

#Capital costs - UV/H2O2

percent_data_cap_UVH2O2 <- read.csv("TEA_percent_cap_UVH2O2.csv") %>%
mutate(H2O2_dose_factor = factor(H2O2_dose, levels = c("1", "2.4"),
labels = c("1 mg/L", "2.4 mg/L"))) %>%
mutate(Percent = Value*100) %>%
mutate(Flow_factor = factor(Design_flow, levels = c(0.091, 0.18, 0.27, 0.36,
0.68, 1, 1.2, 2, 3.5, 7,
10, 16, 17, 21, 22, 41, 52,
76, 200, 210, 288, 389, 430))) %>%
mutate(Element_factor = factor(Element, levels = c("UV", "H2O2"),
labels = c("UV equipment", "H2O2 storage and dosing")))

tiff("Percent_UVH2O2_capital.tif", units = 'cm', width = 20, height = 10, res = 150)
ggplot()+

```

```

geom_col(data = percent_data_cap_UVH2O2, aes (x = Flow_factor, y = Percent, fill = Element_factor),
colour = "black")+
scale_fill_brewer(palette = "Spectral")+
labs(x = "Design flow rate (MGD)", y = "Percentage of total capital cost")+
theme_bw()+
theme(plot.title = element_text(face = "bold", size = 11, hjust = 0),
      axis.title.x = element_text(face = "bold", size = 11, vjust = 0.25),
      axis.title.y = element_text(face = "bold", size = 11, vjust = 0.25),
      axis.text.x = element_text(size = 11, angle = 45),
      axis.text.y = element_text(size = 11),
      strip.background = element_rect(fill = "white"),
      strip.text = element_text(size = 11),
      legend.text = element_text(size = 11),
      legend.title = element_blank()+
      facet_wrap(~Radical_scavenging_capacity)
dev.off()

```

#OM costs - UVH2O2

```

percent_data_UVH2O2_OM <-read.csv("TEA_percent_OM_UVH2O2.csv") %>%
mutate(H2O2_dose_factor = factor(H2O2_dose, levels = c("1", "2.4"),
      labels = c("1 mg/L", "2.4 mg/L"))) %>%
mutate(Percent = Value*100) %>%
mutate(Flow_factor = factor(Design_flow, levels = c(0.34, 0.68, 1.02, 1.36,
      2.57, 3.79, 4.54, 7.57, 13.25, 26.5,
      64.35, 83.27, 287.66, 794.85, 1627.55))) %>%

```

```

mutate(Element_factor = factor(Element, levels = c("Oxidant", "Quenching", "Parts", "Energy",
"Labour"),
      labels = c("Oxidant", "Quenching (HOCl)", "Maintenance", "Energy", "Labour")))

tiff("percent_UVH2O2_OM_col_rev.tif", units = 'cm', width = 20, height = 10, res = 150)

ggplot()+

  geom_col(data = percent_data_UVH2O2_OM, aes (x = Flow_factor, y = Value, fill = Element_factor),
  colour = "black")+

  scale_fill_manual(values = c("Oxidant" = "red", "Quenching (HOCl)" = "orange", "Maintenance" =
"beige", "Energy" = "yellow", "Labour" = "blue")) +

  labs(x = "Design flow rate (MGD)", y = "Percentage of total O&M cost")+

  theme_bw()+

  theme(plot.title = element_text(face = "bold", size = 11, hjust = 0.5),
        axis.title.x = element_text(face = "bold", size = 11, vjust = 0.25),
        axis.title.y = element_text(face = "bold", size = 11, vjust = 0.25),
        axis.text.x = element_text(size = 11, angle = 90),
        axis.text.y = element_text(size = 11),
        strip.background = element_rect(fill = "white"),
        strip.text = element_text(size = 11),
        legend.text = element_text(size = 11),
        legend.position = "bottom",
        legend.title = element_blank()+

  facet_wrap(~Radical_scavenging_capacity)

dev.off()

#Capital costs - UV/Cl

percent_data_cap_UVCl <-read.csv("TEA_percent_cap_UVCl.csv") %>%

```

```

mutate(Flow_factor = factor(Design_flow, levels = c(0.34, 0.68, 1.02, 1.36,
          2.57, 3.79, 4.54, 7.57, 13.25, 26.5,
          64.35, 83.27, 287.66, 794.85, 1627.55))) %>%
mutate(Element_factor = factor(Element, levels = c("UV", "Cl"),
          labels = c("UV equipment", "NaOCl storage and dosing")))

tiff("Percent_UVCl_capital.tif", units = 'cm', width = 20, height = 10, res = 150)
ggplot()+
  geom_col(data = percent_data_cap_UVCl, aes (x = Flow_factor, y = Value, fill = Element_factor), colour
= "black")+
  scale_fill_brewer(palette = "Spectral")+
  labs(x = "Design flow rate (MGD)", y = "Percentage of total capital cost")+
  theme_bw()+
  theme(plot.title = element_text(face = "bold", size = 11, hjust = 0),
        axis.title.x = element_text(face = "bold", size = 11, vjust = 0.25),
        axis.title.y = element_text(face = "bold", size = 11, vjust = 0.25),
        axis.text.x = element_text(size = 11, angle = 45),
        axis.text.y = element_text(size = 11),
        strip.background = element_rect(fill = "white"),
        strip.text = element_text(size = 11),
        legend.text = element_text(size = 11),
        legend.title = element_blank()+
  facet_wrap(~Radical_scavenging_capacity)
dev.off()

```

#OM costs - UVCl


```

percent_data_UVCl_OM <-read.csv("TEA_percent_OM_UVCl.csv") %>%

mutate(Flow_factor = factor(Design_flow, levels = c(0.34, 0.68, 1.02, 1.36,
          2.57, 3.79, 4.54, 7.57, 13.25, 26.5,
          64.35, 83.27, 287.66, 794.85, 1627.55))) %>%

mutate(Element_factor = factor(Element, levels = c("Oxidant", "Energy", "Labour", "Maintenance"),
          labels = c("Oxidant", "Energy", "Labour", "Maintenance")))

tiff("percent_UVCl_OM_col_rev.tif", units = 'cm', width = 20, height = 10, res = 150)

ggplot()+

  geom_col(data = percent_data_UVCl_OM, aes (x = Flow_factor, y = Value, fill = Element_factor), colour
= "black")+

  scale_fill_manual(values = c("Oxidant" = "red", "Maintenance" = "beige", "Energy" = "yellow", "Labour"
= "blue" )) +

  labs(x = "Design flow rate (MGD)", y = "Percentage of total O&M cost",)+

  theme_bw()+

  theme(plot.title = element_text(face = "bold", size = 11, hjust = 0.5),
        axis.title.x = element_text(face = "bold", size = 11, vjust = 0.25),
        axis.title.y = element_text(face = "bold", size = 11, vjust = 0.25),
        axis.text.x = element_text(size = 11, angle = 90),
        axis.text.y = element_text(size = 11),
        strip.background = element_rect(fill = "white"),
        strip.text = element_text(size = 11),
        legend.text = element_text(size = 11),
        legend.position = "bottom",
        legend.title = element_blank()+

  facet_wrap(~Radical_scavenging_capacity)

```

```

dev.off()

#OM costs - UVCl - pH

percent_data_UVCl_OM <-read.csv("TEA_percent_OM_UVCl_pH.csv") %>%

mutate(Flow_factor = factor(Design_flow, levels = c(0.34, 0.68, 1.02, 1.36,
          2.57, 3.79, 4.54, 7.57, 13.25, 26.5,
          64.35, 83.27, 287.66, 794.85, 1627.55))) %>%

mutate(Element_factor = factor(Element, levels = c("Oxidant", "Energy", "Labour", "Maintenance", "pH
Adjustment"),
          labels = c("Oxidant", "Energy", "Labour", "Maintenance", "pH Adjustment")))

tiff("percent_UVCl_OM_col_pH_rev.tif", units = 'cm', width = 20, height = 10, res = 150)

ggplot()+

geom_col(data = percent_data_UVCl_OM, aes (x = Flow_factor, y = Value, fill = Element_factor), colour
= "black")+

scale_fill_manual(values = c("Oxidant" = "red", "Maintenance" = "beige", "Energy" = "yellow", "Labour"
= "blue", "pH Adjustment" = "purple")) +

labs(x = "Design flow rate (MGD)", y = "Percentage of total O&M cost",)+

theme_bw()+

theme(plot.title = element_text(face = "bold", size = 11, hjust = 0.5),
axis.title.x = element_text(face = "bold", size = 11, vjust = 0.25),
axis.title.y = element_text(face = "bold", size = 11, vjust = 0.25),
axis.text.x = element_text(size = 11, angle = 90),
axis.text.y = element_text(size = 11),
strip.background = element_rect(fill = "white"),
strip.text = element_text(size = 11),
legend.text = element_text(size = 11),

```

```

    legend.position = "bottom",
    legend.title = element_blank()+
  facet_wrap(~Radical_scavenging_capacity)
dev.off()

#UV/Cl

UVCl_data <-read.csv("Unit cost data_UVCl_pHAdjustment.csv") %>%
  mutate(Cl_dose = factor(Cl_dose, levels = c("1.", "2.4"), labels = c("1.72 mg/L", "2.08 mg/L")))

# mutate(Short_cost = (Cost/52)*8, Short_upper = (Cost_upper/52)*8, Short_lower =
(Cost_lower/52)*8)

tiff("Unit_cost_curve_UVCl_OM_pH5.tif", units = 'cm', width = 20, height = 15, res = 300)
ggplot(data = UVCl_data)+
  geom_line(aes(x = Design_flow_mld, y = Cost/1000000), size = 1.5)+
  geom_line(aes(x = Design_flow_mld, y = Cost_upper/1000000), colour = "Red", alpha = 1, linetype =
'dashed', size = 1)+
  geom_line(aes(x = Design_flow_mld, y = Cost_lower/1000000), colour = "Green", alpha = 1, linetype =
'dashed', size = 1)+
  labs(x = 'Design flow rate (MLD)', y = 'O&M cost (MCAD)',)+
  theme_bw()+
  theme(plot.title = element_text(face = "bold", size = 20, hjust = 0.5),
        axis.title.x = element_text(face = "bold", size = 20, vjust = 0.25),
        axis.title.y = element_text(face = "bold", size = 20, vjust = 0.25),
        axis.text.x = element_text(size = 20, angle = 90),
        axis.text.y = element_text(size = 20),
        strip.background = element_rect(fill = "white"),

```

```

strip.text = element_text(size = 20),
legend.position = "none")+
facet_wrap(~Radical_scavenging_capacity)+
#xlim(0, 80)+
ylim(0, 55)
dev.off()

#seasonal
tiff("Unit_cost_curve_UVCI_OM_pH5_seasonal.tif", units = 'cm', width = 20, height = 15, res = 300)
ggplot(data = UVCI_data)+
geom_line(aes(x = Design_flow_mld, y = Cost/1000000/2), size = 1.5)+
geom_line(aes(x = Design_flow_mld, y = Cost_upper/1000000/2), colour = "Red", alpha = 1, linetype =
'dashed', size = 1)+
geom_line(aes(x = Design_flow_mld, y = Cost_lower/1000000/2), colour = "Green", alpha = 1, linetype
= 'dashed', size = 1)+
labs(x = 'Design flow rate (MLD)', y = 'O&M cost (MCAD)',)+
theme_bw()+
theme(plot.title = element_text(face = "bold", size = 20, hjust = 0.5),
axis.title.x = element_text(face = "bold", size = 20, vjust = 0.25),
axis.title.y = element_text(face = "bold", size = 20, vjust = 0.25),
axis.text.x = element_text(size = 20, angle = 90),
axis.text.y = element_text(size = 20),
strip.background = element_rect(fill = "white"),
strip.text = element_text(size = 20),
legend.position = "none")+
facet_wrap(~Radical_scavenging_capacity)+
#xlim(0, 80)+
ylim(0, 30)
dev.off()

```

```

#UVH2O2
UVH2O2_data <- read.csv("Unit cost data_UVH2O2.csv") %>%
  mutate(H2O2_dose = factor(H2O2_dose, levels = c("1", "2.4"),
    labels = c("1 mg/L", "2.4 mg/L")))
#mutate(Size = factor(ifelse(Design_flow_mgd>=1, "Large", "Small")))

data_cap_UVH2O2 <- UVH2O2_data %>%
  filter(Type == "Direct_cap", Source == "USEPA_2003")

data_cap_UVH2O2_Plumlee <- UVH2O2_data %>%
  filter(Type == "Direct_cap", Source == "Plumlee_2014")

#data_small_cap_UVH2O2 <- data_cap_UVH2O2 %>%
# filter(Size == "Small")

#data_large_cap_UVH2O2 <- data_cap_UVH2O2 %>%
# filter(Size == "Large")

data_OM_UVH2O2 <- UVH2O2_data %>%
  filter(Type == "OM", Source == "USEPA_2003")

#data_small_OM_UVH2O2 <- data_OM_UVH2O2 %>%
# filter(Size == "Small")

#data_large_OM_UVH2O2 <- data_OM_UVH2O2 %>%
# filter(Size == "Large")

```

```

#data_OM_UVH2O2_USEPA1 <- UVH2O2_data %>%
# filter(Type == "OM", Source == "USEPA_2003", H2O2_dose == "5 mg/L")

data_OM_UVH2O2_Plumlee <- UVH2O2_data %>%
  filter(Type == "OM", Source == "Plumlee_2014")

DWRG_UVH2O2 <-UVH2O2_data

Real_cost <- read.csv("Real_costs.csv")

tiff("Cost_curve_UVH2O2_Cap_LowOH Demand.tif", units ='cm', width = 20, height = 15, res = 300)
ggplot()+
  geom_line(data = subset(data_cap_UVH2O2, Radical_scavenging_capacity == "Low RSC"),aes(x =
Design_flow_mlpd, y =CAD_cost), size = 1.5)+
  geom_line(data = subset(data_cap_UVH2O2, Radical_scavenging_capacity == "Low RSC"),aes(x =
Design_flow_mlpd, y = CAD_cost_upper),colour = "Red", alpha = 0.75, linetype = 'dashed', size = 0.75)+
  geom_line(data = subset(data_cap_UVH2O2, Radical_scavenging_capacity == "Low RSC"),aes(x =
Design_flow_mlpd, y = CAD_cost_lower), colour = "Green", alpha = 0.75, linetype = 'dashed', size =
0.75)+
  geom_point(data = subset(Real_cost, Source == "A"),aes(x = Capacity, y = Cost_2023_MCAD), colour =
"#A73030FF", shape = 15, size = 5)+
  geom_point(data = subset(Real_cost, Source == "B"),aes(x = Capacity, y = Cost_2023_MCAD), colour =
"#3B3B3BFF", shape = 16, size = 5)+
  geom_point(data = subset(Real_cost, Source == "C"),aes(x = Capacity, y = Cost_2023_MCAD), colour =
"#A73030FF", shape = 17, size = 5)+
  geom_point(data = subset(Real_cost, Source == "D"),aes(x = Capacity, y = Cost_2023_MCAD), colour =
"#A73030FF", shape = 18, size = 5)+
  #geom_point(data = subset(Real_cost, Source == "E"),aes(x = Capacity, y = Cost_2023_MCAD), colour =
"#A73030FF", shape = 19, size = 5)+
  geom_point(data = subset(Real_cost, Source == "F"),aes(x = Capacity, y = Cost_2023_MCAD), colour =
"#3B3B3BFF", shape = 3, size = 5)+

```

```

geom_point(data = subset(Real_cost, Source == "G"),aes(x = Capacity, y = Cost_2023_MCAD), colour =
"#3B3B3BFF", shape = 4, size = 5)+

geom_point(data = subset(Real_cost, Source == "H"),aes(x = Capacity, y = Cost_2023_MCAD), colour =
"#3B3B3BFF", shape = 5, size = 5)+

labs(x = 'Design flow rate (MLD)', y = 'Direct capital cost (MCAD)', title = "Low RSC UV/H2O2 Capital
Costs")+

ylim(0,300)+

xlim(0,305)+

theme_bw()+

theme(plot.title = element_text(face = "bold", size = 20, hjust = 0),
      axis.title.x = element_text(face = "bold", size = 20, vjust = 0.25),
      axis.title.y = element_text(face = "bold", size = 20, vjust = 0.25),
      axis.text.x = element_text(size = 20, angle = 90),
      axis.text.y = element_text(size = 20),
      strip.background = element_rect(fill = "white"),
      strip.text = element_text(size = 20),
      legend.position = "none")

dev.off()

tiff("Cost_curve_UVH2O2_Cap_HighOH Demand.tif", units = 'cm', width = 20, height = 15, res = 300)

ggplot()+

  geom_line(data = subset(data_cap_UVH2O2, Radical_scavenging_capacity == "High RSC"),aes(x =
Design_flow_mlpd, y = CAD_cost), size = 1.5)+

  geom_line(data = subset(data_cap_UVH2O2, Radical_scavenging_capacity == "High RSC"),aes(x =
Design_flow_mlpd, y = CAD_cost_upper),colour = "Red", alpha = 0.75, linetype = 'dashed', size = 0.75)+

  geom_line(data = subset(data_cap_UVH2O2, Radical_scavenging_capacity == "High RSC"),aes(x =
Design_flow_mlpd, y = CAD_cost_lower), colour = "Green", alpha = 0.75, linetype = 'dashed', size =
0.75)+

  geom_point(data = subset(Real_cost, Source == "A"),aes(x = Capacity, y = Cost_2023_MCAD), colour =
"#A73030FF", shape = 15, size = 5)+

  geom_point(data = subset(Real_cost, Source == "B"),aes(x = Capacity, y = Cost_2023_MCAD), colour =
"#3B3B3BFF", shape = 16, size = 5)+

```

```

geom_point(data = subset(Real_cost, Source == "C"),aes(x = Capacity, y = Cost_2023_MCAD), colour =
"#A73030FF", shape = 17, size = 5)+

geom_point(data = subset(Real_cost, Source == "D"),aes(x = Capacity, y = Cost_2023_MCAD), colour =
"#A73030FF", shape = 18, size = 5)+

geom_point(data = subset(Real_cost, Source == "F"),aes(x = Capacity, y = Cost_2023_MCAD), colour =
"#3B3B3BFF", shape = 3, size = 5)+

geom_point(data = subset(Real_cost, Source == "G"),aes(x = Capacity, y = Cost_2023_MCAD), colour =
"#3B3B3BFF", shape = 4, size = 5)+

geom_point(data = subset(Real_cost, Source == "H"),aes(x = Capacity, y = Cost_2023_MCAD), colour =
"#3B3B3BFF", shape = 5, size = 5)+

labs(x = 'Design flow rate (MLD)', y = 'Direct capital cost (MCAD)', title = "High RSC UV/H2O2 Capital
Costs")+

ylim(0,500)+

xlim(0,305)+

theme_bw()+

theme(plot.title = element_text(face = "bold", size = 20, hjust = 0),
      axis.title.x = element_text(face = "bold", size = 20, vjust = 0.25),
      axis.title.y = element_text(face = "bold", size = 20, vjust = 0.25),
      axis.text.x = element_text(size = 20, angle = 90),
      axis.text.y = element_text(size = 20),
      strip.background = element_rect(fill = "white"),
      strip.text = element_text(size = 20),
      legend.position = "none")

dev.off()

tiff("Cost_curve_UVH2O2_Cap_Facet.tif", units = 'cm', width = 20, height = 15, res = 300)

ggplot()+

geom_line(data = subset(data_cap_UVH2O2),aes(x = Design_flow_mlpd, y = CAD_cost), size = 1.5)+

geom_line(data = subset(data_cap_UVH2O2),aes(x = Design_flow_mlpd, y = CAD_cost_upper),colour =
"Red", alpha = 0.75, linetype = 'dashed', size = 0.75)+

geom_line(data = subset(data_cap_UVH2O2),aes(x = Design_flow_mlpd, y = CAD_cost_lower), colour =
"Green", alpha = 0.75, linetype = 'dashed', size = 0.75)+

```



```

facet_wrap(~Radical_scavenging_capacity) +
labs(x = 'Design flow rate (MLD)', y = 'Direct capital cost (MCAD)')+
theme_bw()+
theme(plot.title = element_text(face = "bold", size = 20, hjust = 0),
      axis.title.x = element_text(face = "bold", size = 20, vjust = 0.25),
      axis.title.y = element_text(face = "bold", size = 20, vjust = 0.25),
      axis.text.x = element_text(size = 20, angle = 90),
      axis.text.y = element_text(size = 20),
      strip.background = element_rect(fill = "white"),
      strip.text = element_text(size = 20),
      legend.position = "none")
dev.off()

tiff("Cost_curve_UVH2O2_OM_Facet.tif", units = 'cm', width = 20, height = 15, res = 300)

ggplot()+
  geom_line(data = subset(data_OM_UVH2O2),aes(x = Design_flow_mlpd, y = CAD_cost), size = 1.5)+
  geom_line(data = subset(data_OM_UVH2O2),aes(x = Design_flow_mlpd, y = CAD_cost_upper),colour =
"Red", alpha = 0.75, linetype = 'dashed', size = 0.75)+
  geom_line(data = subset(data_OM_UVH2O2),aes(x = Design_flow_mlpd, y = CAD_cost_lower), colour =
"Green", alpha = 0.75, linetype = 'dashed', size = 0.75)+
  facet_wrap(~Radical_scavenging_capacity) +
  labs(x = 'Design flow rate (MLD)', y = 'OM cost (MCAD)')+
  theme_bw()+
  theme(plot.title = element_text(face = "bold", size = 20, hjust = 0),
        axis.title.x = element_text(face = "bold", size = 20, vjust = 0.25),
        axis.title.y = element_text(face = "bold", size = 20, vjust = 0.25),
        axis.text.x = element_text(size = 20, angle = 90),
        axis.text.y = element_text(size = 20),
        strip.background = element_rect(fill = "white"),

```

```

strip.text = element_text(size = 20),
legend.position = "none")
dev.off()

tiff("Cost_curve_UVH2O2_OM_all.tif", units = 'cm', width = 22, height = 15, res = 300)

ggplot()+

  geom_line(data = subset(data_OM_UVH2O2, Source == "USEPA_2003"), aes(x = Design_flow_mlpd, y =
Short_cost), colour = "#E31837", size = 1.5)+

  geom_line(data = subset(data_OM_UVH2O2, Source == "USEPA_2003"), aes(x = Design_flow_mlpd, y =
Short_upper), colour = "#E31837", alpha = 0.75, linetype = 'dashed', size = 1)+

  geom_line(data = subset(data_OM_UVH2O2, Source == "USEPA_2003"), aes(x = Design_flow_mlpd, y =
Short_lower), colour = "#E31837", alpha = 0.75, linetype = 'dashed', size = 1)+

  geom_line(data = subset(data_OM_UVH2O2, Source == "USEPA_2003"), aes(x = Design_flow_mlpd, y =
Cost), colour = "#264578", size = 1.5)+

  geom_line(data = subset(data_OM_UVH2O2, Source == "USEPA_2003"), aes(x = Design_flow_mlpd, y =
Cost_upper), colour = "#264578", alpha = 1, linetype = 'dashed', size = 1)+

  geom_line(data = subset(data_OM_UVH2O2, Source == "USEPA_2003"), aes(x = Design_flow_mlpd, y =
Cost_lower), colour = "#264578", alpha = 1, linetype = 'dashed', size = 1)+

  labs(x = 'Design flow rate (MLD)', y = 'OM cost (MUSD)', title = 'Hydrogen peroxide dose')+

  theme_bw()+

  theme(plot.title = element_text(face = "bold", size = 20, hjust = 0.5),
        axis.title.x = element_text(face = "bold", size = 20, vjust = 0.25),
        axis.title.y = element_text(face = "bold", size = 20, vjust = 0.25),
        axis.text.x = element_text(size = 20, angle = 90),
        axis.text.y = element_text(size = 20),
        strip.background = element_rect(fill = "white"),
        strip.text = element_text(size = 20),
        legend.position = "none")+

  facet_wrap(~H2O2_dose)

dev.off()

```

```

tiff("Cost_curve_UVH2O2_OM_USEPA1.tif", units = 'cm', width = 7, height = 10, res = 150)

ggplot()+

  geom_line(data = data_OM_UVH2O2_USEPA1, aes(x = Design_flow_mgd, y = Cost), colour =
"#3B3B3BFF", size = 0.5)+

  geom_line(data = data_OM_UVH2O2_USEPA1, aes(x = Design_flow_mgd, y = Cost_upper),colour =
"#3B3B3BFF", alpha = 0.75, linetype = 'dashed', size = 0.5)+

  geom_line(data = data_OM_UVH2O2_USEPA1, aes(x = Design_flow_mgd, y = Cost_lower), colour =
"#3B3B3BFF", alpha = 0.75, linetype = 'dashed', size = 0.5)+

  labs(x = 'Design flow rate (MGD)', y = NULL, title = "A")+

  ylim(0,6)+

  xlim(0,80)+

  theme_bw()+

  theme(plot.title = element_text(face = "bold", size = 11, hjust = 0),
        axis.title.x = element_text(face = "bold", size = 11, vjust = 0.25),
        axis.title.y = element_text(face = "bold", size = 11, vjust = 0.25),
        axis.text.x = element_text(size = 11, angle = 90),
        axis.text.y = element_text(size = 11),
        strip.background = element_rect(fill = "white"),
        strip.text = element_text(size = 11),
        legend.position = "none")

dev.off()

```

```

tiff("Cost_curve_UVH2O2_OM_Plumlee.tif", units = 'cm', width = 7, height = 10, res = 150)

ggplot()+

  geom_line(data = data_OM_UVH2O2_Plumlee, aes(x = Design_flow_mgd, y = Cost), colour =
"#0073C2FF", size = 0.5)+

  geom_line(data = data_OM_UVH2O2_Plumlee, aes(x = Design_flow_mgd, y = Cost_upper),colour =
"#0073C2FF", alpha = 0.75, linetype = 'dashed', size = 0.5)+

  geom_line(data = data_OM_UVH2O2_Plumlee, aes(x = Design_flow_mgd, y = Cost_lower), colour =
"#0073C2FF", alpha = 0.75, linetype = 'dashed', size = 0.5)+

  labs(x = 'Design flow rate (MGD)', y = NULL, title = "B")+

```

```
ylim(0,6)+
xlim(0,80)+
theme_bw()+
theme(plot.title = element_text(face = "bold", size = 11, hjust = 0),
      axis.title.x = element_text(face = "bold", size = 11, vjust = 0.25),
      axis.title.y = element_text(face = "bold", size = 11, vjust = 0.25),
      axis.text.x = element_text(size = 11, angle = 90),
      axis.text.y = element_text(size = 11),
      strip.background = element_rect(fill = "white"),
      strip.text = element_text(size = 11),
      legend.position = "none")
dev.off()
```